

การสังเคราะห์เชิงเคมีไฟฟ้าของ 1,3-โพรเพนไดออลจากกลีเซอรอลดิบจากการผลิตไบโอดีเซล



นายคังกรม์ คงเจาะ

ศูนย์วิจัยทรัพยากร

วิทยานิพนธ์นี้เป็นส่วนหนึ่งของการศึกษาตามหลักสูตรปริญญาวิทยาศาสตรดุษฎีบัณฑิต

สาขาวิชาเคมีเทคนิค ภาควิชาเคมีเทคนิค

คณะวิทยาศาสตร์ จุฬาลงกรณ์มหาวิทยาลัย

ปีการศึกษา 2552

ลิขสิทธิ์ของจุฬาลงกรณ์มหาวิทยาลัย

ELECTROCHEMICAL SYNTHESIS OF 1,3-PROPANEDIOL FROM CRUDE
GLYCEROL FROM BIODIESEL PRODUCTION



Mr. Sangkorn Kongjao

A Dissertation Submitted in Partial Fulfillment of the Requirements
for the Degree of Doctor of Philosophy Program in Chemical Technology

Department of Chemical Technology

Faculty of Science

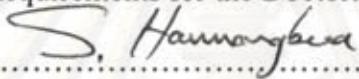
Chulalongkorn University

Academic Year 2009

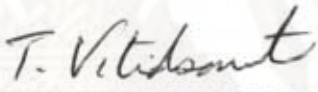
Copyright of Chulalongkorn University

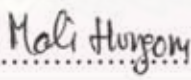
Thesis Title ELECTROCHEMICAL SYNTHESIS OF 1,3-
PROPANEDIOL FROM CRUDE GLYCEROL FROM
BIODIESEL PRODUCTION
By Mr. Sangkorn Kongjao
Field of Study Chemical Technology
Thesis Advisor Associate Professor Mali Hunsom, Ph.D., Dr. de L'INPT
Thesis Co-Advisor Professor Somsak Damronglerd, Dr.Ing.

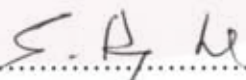
Accepted by the Faculty of Science, Chulalongkorn University in Partial
Fulfillment of the Requirements for the Doctoral Degree


..... Dean of the Faculty of Science
(Professor Supot Hannongbua, Dr. rer.nat.)

THESIS COMMITTEE



..... Chairman
(Associate Professor Tharapong Vitidsant, Dr.de L'INPT)


..... Thesis Advisor
(Associate Professor Mali Hunsom, Ph.D., Dr. de L'INPT)


..... Thesis Co-Advisor
(Professor Somsak Damronglerd, Dr.Ing.)


..... Examiner
(Associate Professor Kejvalee Pruksathorn, Dr.de L'INPT)


..... External Examiner
(Assistant Professor Kanda Wongwailikhit, Ph.D.)


..... External Examiner
(Mr.Thawat Chatchupong, Ph.D.)

ดั่งกรม คงเจาะ: การสังเคราะห์เชิงเคมีไฟฟ้าของ 1,3-โพรเพนไดออลจากกลีเซอรอล
 ดิบจากการผลิตไบโอดีเซล (ELECTROCHEMICAL SYNTHESIS OF 1,3-
 PROPANEDIOL FROM CRUDE GLYCEROL FROM BIODIESEL
 PRODUCTION) อ. ที่ปรึกษาวิทยานิพนธ์หลัก: รศ.ดร.มะลิ หุ่นสม, อ. ที่ปรึกษา
 วิทยานิพนธ์ร่วม: ศ.ดร.สมศักดิ์ ดำรงค์เลิศ, 150 หน้า.

งานวิจัยนี้ศึกษาภาวะที่เหมาะสมในการสังเคราะห์ 1,3-โพรเพนไดออลจากกลีเซอรอล
 ดิบจากกระบวนการผลิตไบโอดีเซลโดยเทคนิคทางเคมีไฟฟ้าโดยงานวิจัยแบ่งออกเป็น 3 ส่วน
 ส่วนที่หนึ่งเป็นการสังเคราะห์ 1,3-โพรเพนไดออลจากสารละลายกลีเซอรอลด้วยเทคนิคทาง
 เคมีไฟฟ้า พบว่าที่กระแสไฟฟ้าเท่ากับ 4.5 แอมแปร์ ความเป็นกรด-เบสเริ่มต้นเท่ากับ 1 เมื่อ
 ปรับด้วยกรดซัลฟูริกเข้มข้น ความเข้มข้นของโซเดียมคลอไรด์เท่ากับ 2.93 กรัมต่อลิตร และค่า
 ประจุไฟฟ้าเท่ากับ 100 แอมแปร์ชั่วโมงต่อลิตร โดยใช้โลหะแพลทินัมเป็นขั้วไฟฟ้าสามารถ
 สังเคราะห์ 1,3-โพรเพนไดออลจากสารละลายกลีเซอรอลและกลีเซอรอลดิบได้ร้อยละ 40.81
 และ 4.76 ตามลำดับ ส่วนที่สองเป็นการเพิ่มความบริสุทธิ์ของกลีเซอรอลดิบจากกระบวนการ
 ผลิตไบโอดีเซลในภาวะกรดด้วยกระบวนการทางเคมี พบว่าที่ค่าความเป็นกรด-เบสเท่ากับ 2.2
 เมื่อปรับด้วยกรดฟอสฟอริกเข้มข้น 1.19 โมลต่อลิตร แล้วนำชั้นของกลีเซอรอลมาสกัดด้วย
 เฮกเซน ปรับสภาพความเป็นกรด-เบสเท่ากับ 7 ด้วยโพแทสเซียมไฮดรอกไซด์เข้มข้น 12.50
 โมลต่อลิตร และสกัดด้วยเอทานอล ตามลำดับ ได้กลีเซอรอลดิบที่มีความบริสุทธิ์สูงสุดร้อยละ
 97.92 และมีการปนเปื้อนของแฉะ สารอินทรีย์ที่ไม่ใช่กลีเซอรอล และ น้ำ ร้อยละ 0.01 0.79
 และ 1.28 ตามลำดับ ส่วนที่สามเป็นการสังเคราะห์ 1,3-โพรเพนไดออลจากกลีเซอรอลดิบที่
 ผ่านการทำให้บริสุทธิ์ พบว่าที่กระแสไฟฟ้าเท่ากับ 6 แอมแปร์ ความเป็นกรด-เบสเริ่มต้นเท่ากับ
 1 และค่าประจุไฟฟ้าเท่ากับ 184.61 แอมแปร์ชั่วโมงต่อลิตร โดยใช้โลหะแพลทินัมเป็นขั้วไฟฟ้า
 สามารถสังเคราะห์ 1,3-โพรเพนไดออลร้อยละ 26.31

ภาควิชา.....เคมีเทคนิค.....ลายมือชื่อนิสิต.....
 สาขาวิชา.....เคมีเทคนิค.....ลายมือชื่อ อ.ที่ปรึกษาวิทยานิพนธ์หลัก.....
 ปีการศึกษา.....2552.....ลายมือชื่อ อ.ที่ปรึกษาวิทยานิพนธ์ร่วม.....

#4973848923: MAJOR CHEMICAL TECHNOLOGY

KEYWORDS : ELECTROCHEMICAL REFORMING/ CRUDE GLYCEROL/
1,3-PROPANEDIOL/ BIODIESEL/ PURIFICATION

SANGKORN KONGJAO: ELECTROCHEMICAL SYNTHESIS OF 1,3-PROPANEDIOL FROM CRUDE GLYCEROL FROM BIODIESEL PRODUCTION. THESIS ADVISOR: ASSOC.PROF. MALI HUNSOM, Ph.D, Dr.de L'INPT, THESIS CO-ADVISOR: PROF. SOMSAK DAMRONGLERD, Dr.Ing., 150 pp.

This work was carried out to evaluate the optimum conditions for synthesis of 1,3-propanediol from crude glycerol by an electrochemical technique. The experiment of glycerol reforming was separated into three parts. The first part was studied the glycerol reforming from synthetic and purified crude glycerol to 1,3-propanediol by the electrochemical technique. It was found that the optimum conditions; applied current intensity of 4.5 A, an initial pH of 1 set by H_2SO_4 , 2.93 g/l NaCl, electrical charge of 100 Ah/l with Pt electrode; provided the yield of 1,3-propanediol by using synthetic and crude glycerol of 40.81% and 4.76%, respectively. For the second part, the purification of crude glycerol from biodiesel plant under strong acid conditions by using the chemical process was observed. The pH of crude glycerol was adjusted to 2.2 by 1.19 M H_3PO_4 and extracted glycerol-rich layer solution with $n-C_6H_{14}$. After that, glycerol-rich layer neutralized with 12.50 M KOH and extracted with excess C_2H_5OH could provide the purity of glycerol around 97.92 % with low contaminant levels ash, matter organic non glycerol and water around 0.01, 0.79 and 1.28% w/w, respectively. As studied in the final part of the purified crude glycerol reforming to 1,3-propanediol, the optimum conditions of applied current intensity of 6 A, an initial pH of 1, and an electrical charge of 184.61 Ah/l with Pt electrode could provide the yield of 1,3-propanediol about 26.31%.

Department: Chemical Technology.....

Student's Signature *Sangkorn Kongjao*

Field of Study: Chemical Technology.....

Advisor's Signature *Mali Hunsom*

Academic Year 2009.....

Co-Advisor's Signature *Somsak Damronglerd*

ACKNOWLEDGEMENTS

I would like to express my heartfelt gratitude and appreciation to my advisor Assoc.Prof.Dr. Mali Hunsom, and my co-advisor Prof.Dr. Somsak Damronglerd, for their kind supervision, invaluable guidance and constant encouragement.

Acknowledgements are also sincerely grateful to Assoc.Prof.Dr. Tharapong Vitidsant for serving as chairman and to Assoc.Prof.Dr. Kejvalee Pruksathorn, Asst.Prof.Dr. Kanda Wongwailikhit and Dr. Thawach Chatchupong as member of examiner of the thesis committee.

I would like to thank the Center for Petroleum, Petrochemicals and Advanced Materials (NCE-PPAM) and Graduate School Chulalongkorn University for financial support to this project, and the Bangchak Petroleum Co., Ltd., for samples and materials. Also, I wish to express my grateful appreciation to Department of Chemical Technology, Faculty of Science, Chulalongkorn University, Bangkok, Thailand.

I would like to thank NANOTEC, A Center of NSTDA, Thailand and Department of Environmental Science, Faculty of Science, Chulalongkorn University by supplying us with an analytical apparatus of GC/MS and HPLC, respectively.

A very special thank you is conducted to my family and my friends for their endless encouragement, love and care.

ศูนย์วิทยทรัพยากร
จุฬาลงกรณ์มหาวิทยาลัย

CONTENTS

	Page
ABSTRACT IN THAI	iv
ABSTRACT IN ENGLISH	v
ACKNOWLEDGEMENTS	vi
CONTENTS	vii
LIST OF TABLES	xi
LIST OF FIGURES AND SCHEMES	xii
LIST OF ABBREVIATIONS	xx
CHAPTER	
I. INTRODUCTION	1
1.1 Background.....	1
1.2 Objectives of dissertation.....	2
1.3 Scope of dissertation.....	2
II. THEORY AND LITERATURE REVIEW	3
2.1 Renewable energy resource.....	3
2.2 Biodiesel production process and by-product.....	4
2.2.1 Biodiesel.....	4
2.2.2 Transesterification.....	5
2.2.3 Process flow chart.....	7
2.2.4 By-product from biodiesel production plant.....	8
2.3 Glycerol.....	9
2.3.1 Glycerol and source of formation.....	9
2.3.2 Application of glycerol.....	11
2.3.4 Value-added products of glycerol.....	13
2.4 1,3-propanediol.....	16
2.4.1 1,3-propanediol based on acrolein.....	17
2.4.2 1,3-propanediol process based on ethyleneoxide.....	18
2.4.3 1,3-propanediol process based on fermentation of glycerol.....	18
2.4.4 1,3-propanediol process based on hydrogenolysis reaction of	

	Page
glycerol.....	20
2.5 Fundamentals of electrochemical.....	21
2.5.1 The nature of electrode reactions.....	22
2.5.2 Half-cell reaction.....	23
2.5.3 Standard electrode potential (E°).....	23
2.5.4 Potential of an electrochemical cell.....	24
2.5.5 Reference electrode.....	24
2.5.6 Nernst equation.....	25
2.5.7 Thermodynamics of electrochemical reactions.....	26
2.5.8 Faraday's law.....	27
2.5.9 Tafel Plots.....	28
2.5.10 Electrode kinetics and mass transport phenomena.....	30
2.5.11 Cyclic voltammetry.....	33
2.6 Application of electrochemical technology for organic reforming.....	35
2.7 Electrochemical synthesis.....	37
2.7.1 Main reactions of organic electrochemistry.....	38
2.7.2 Reaction mechanisms, kinetics and thermodynamics.....	39
2.7.3 Electron transfer mechanism.....	39
2.7.4 Electrochemical reforming of alkane compounds.....	40
2.7.5 Electrochemical reforming of alkene compounds.....	41
2.7.6 Electrochemical reforming of alcohol and ester compounds.....	42
2.7.7 Electrochemical reforming of amine compounds.....	42
2.7.8 Electrochemical reforming of aromatic compounds.....	43
2.7.9 Electrochemical reforming of sulfur and selenium compounds...	44
2.7.10 Electrochemical reforming of functional group at cathode electrode.....	44
2.8 Literature reviews.....	45
III. METHODOLOGY	50
3.1 Experimental set up of polarization curve.....	50
3.2 Electrochemical reactor.....	52

	Page
3.3 Chemical substances.....	52
3.4 Experimental set up of glycerol reforming.....	53
3.4.1 Electrochemical reforming of synthetic glycerol.....	53
3.4.2 Purification of crude glycerol from biodiesel plant.....	54
3.4.3 Electrochemical reforming for purified crude glycerol.....	57
3.5 The characterization.....	57
3.5.1 High performance liquid chromatography.....	57
3.5.2 Fourier transforms infrared spectroscopy.....	58
3.5.3 Gas chromatograph and mass spectrometry	58
IV. RESULTS AND DISCUSSION.....	60
4.1 Electrochemical reforming of synthetic glycerol.....	60
4.1.1 Current density-potential curve.....	60
4.1.2 Effect of parameters on synthetic glycerol reforming.....	65
- Effect of anode type.....	68
- Effect of acid type.....	70
- Effect of current intensity.....	72
- Effect of pH.....	73
- Effect of type of additive.....	75
- Effect of concentration of NaCl.....	77
4.1.3 Mechanisms of synthetic glycerol reforming to 1,3-propanediol...	82
4.1.4 Preliminary study of electrochemical reforming of crude glycerol	91
4.2 Purification of crude glycerol from biodiesel plant.....	93
4.2.1 Characteristics of the original crude glycerol from waste used-oil biodiesel plant.....	93
4.2.2 Composition and characteristics of the purified crude glycerol followed route I.....	96
4.2.3 Composition and characteristics of the purified crude glycerol followed route II.....	102
4.2.4 Characteristics of the purified crude glycerol.....	103
4.3 Electrochemical reforming of purified crude glycerol.....	109

	Page
4.3.1 Current density potential curve.....	109
4.3.2 Effect of parameter on purified crude glycerol reforming.....	110
- Effect of current intensity.....	110
- Effect of concentration of NaCl.....	113
4.3.3 Mechanisms of purified crude glycerol reforming to 1,3-propanediol.....	115
4.4 Comparison of yield of 1,3-propanediol from synthetic glycerol solution, crude glycerol and purified crude glycerol by electrochemical technique.....	123
4.5 Comparison of concentration and production yield of 1,3-propanediol between this work and some previous works.....	123
V. CONCLUSIONS AND RECOMMENDATIONS.....	125
REFERENCES.....	127
APPENDICES.....	135
APPENDIX A.....	136
APPENDIX B.....	139
APPENDIX C.....	142
APPENDIX D.....	145
BIOGRAPHY.....	150

LIST OF TABLES

Table	Page
Table 2.1 Raw materials for biodiesel production and their physical and chemical properties.....	5
Table 2.2 Product derived from glycerol with some previous researches....	14
Table 2.3 Synthesis of 1,3-propanediol by <i>K. Pneumoniae</i> and <i>C. Butyicum</i> ..	18
Table 2.4 Glycerol hydrogenolysis to 1,3-propanediol with various supported metal catalysts.....	21
Table 4.1 Characteristics of crude glycerol, commercial glycerol, and purified crude glycerol compared with The BS standard.....	95
Table 4.2 The contents of glycerol, ash, water, and MONG in purified crude glycerol obtained after base neutralization and extraction.....	101
Table 4.3 Comparison of purified crude glycerol properties obtained from this work with other works.....	108
Table 4.4 Comparison of concentration and production yield of 1,3-propanediol between this work and some previous works.....	124
Table C.1 List of compounds generated from glycerol reforming by the electrochemical technique under strong acidic conditions.....	1 4 2

LIST OF FIGURES AND SCHEMES

Figure and Scheme	Page
Figure 2.1 Simplified process flow of catalyzed biodiesel production.....	8
Figure 2.2 Comparison of saponification and transesterification.....	10
Figure 2.3 Application of refined glycerol.....	11
Figure 2.4 Chemical substances produced from glycerol.....	16
Figure 2.5 Industrial 1,3-propanediol processes.....	17
Figure 2.6 Anaerobic metabolism pathways of glycerol fermentation.....	20
Figure 2.7 Schematic of a simple electrode reaction.....	22
Figure 2.8 Reference electrodes SCE (a) and Ag/AgCl (b).....	25
Figure 2.9 Tafel-plot diagrams for the cathodic and anodic process.....	30
Figure 2.10 General scheme of a faradic process.....	31
Figure 2.11 Schematic representation of a concentration profile of a species reacting on the electrode surface.....	32
Figure 2.12 The oxidation - reduction peaks from cyclic voltammogram.....	33
Figure 2.13 Cyclic voltammogram showing reduction and oxidation peaks of one reaction.....	34
Figure 2.14 Cyclic voltammogram showing reduction and oxidation peaks of many reactions.....	35
Figure 2.15 Principal reactions of organic electrochemistry.....	38
Figure 2.16 The dissociative electron transfer or Savéant's Theory.....	39
Figure 2.17 Passage from the stepwise to the concerted mechanism upon decreasing the driving force.....	40
Figure 2.18 Electrochemical reforming of alkane compounds.....	41
Figure 2.19 Electrochemical reforming of alkene compounds.....	41
Figure 2.20 Electrochemical reforming of alcohol compounds.....	42
Figure 2.21 Electrochemical reforming of ester compounds.....	42
Figure 2.22 Electrochemical reforming of amine compounds.....	43
Figure 2.23 Electrochemical reforming of aromatic compounds with nucleophilic.....	43
Figure 2.24 Electrochemical reforming of aromatic compounds.....	44

Figure and Scheme	Page
Figure 2.25 Electrochemical reforming of sulfur and selenium compounds....	44
Figure 2.26 Electrochemical reduction of alkene compounds.....	45
Figure 2.27 Electrochemical reduction of nitroaromatic compounds.....	45
Figure 3.1 Schematic diagram of apparatus for current density-potential studies.....	51
Figure 3.2 Schematic diagram of experiment set up.....	52
Figure 3.3 Schematic diagram of the chemical treatment of crude glycerol obtained from biodiesel production.....	55
Figure 3.4 High performance liquid chromatography (HPLC).....	57
Figure 3.5 Fourier Transform Infrared spectroscopy (FTIR).....	58
Figure 3.6 Gas chromatograph and mass spectrometry (GC/MS).....	59
Figure 4.1 Current density-potential curves of solvent solution (water) at different pH with Pt electrode at constant stirring rate of 400 rpm and scan rate of 5 mV/s with Ag/AgCl reference electrode.....	61
Figure 4.2 Current density-potential curves of synthetic glycerol solution pH 2, 4 and 6 (a) and synthetic glycerol solution 8, 10 and 12 (b) with Pt electrode at constant stirring rate of 400 rpm and scan rate of 5 mV/s with Ag/AgCl reference electrode.....	63
Figure 4.3 Representative HPLC chromatograms of solutions at pH 12 (a, b), pH 10 (c, d), pH 8 (e, f), pH 6 (g, h), pH 4 (i, j) and pH 2 (k, l), before (a, c, e, g, i, k), and after (b, d, f, h, j, l) running the polarization curve.....	64
Figure 4.4 The yield of 1,2-propanediol and 1,3-propanediol obtained from synthetic glycerol solution at various pH by the cyclic voltametry..	65
Figure 4.5 Evaluation of the normalized concentration (a) and glycerol reforming (b) as a function of electrical charges in the presence of different electrodes by using synthetic glycerol solution at the concentration of 46.2 g/l, pH of 2 and current intensity of 1 A.....	66
Figure 4.6 Plot of rate constant of pseudo-first-order kinetics of glycerol reforming as a function of type of anode by using synthetic	

Figure and Scheme	Page
glycerol solution at the concentration of 46.2 g/l and pH of 2.....	68
Figure 4.7 The yield of 1,3-propanediol as a function of electrical charges in the presence of different electrodes by using synthetic glycerol solution at the concentration of 46.2 g/l, pH of 2 and current intensity of 1 A.....	69
Figure 4.8 Evaluation of the normalized concentration (a), glycerol reforming (b) and yield of 1,3-propanediol (c) as a function of electrical charges with different acid types by using synthetic glycerol solution at the concentration of 46.2 g/l, pH of 2 and current density of 3 A with Pt electrode.....	70
Figure 4.9 Evaluation of the normalized concentration (a) and glycerol reforming (b) as a function of electrical charges at an applied current intensity of 3 - 5 A by using synthetic glycerol solution at the concentration of 46.2 g/l and pH of 2 with Pt electrode.....	71
Figure 4.10 Plot of rate constant of pseudo-first-order kinetics of glycerol reforming as a function of current intensity by using synthetic glycerol solution at the concentration of 46.2 g/l and pH of 2 with Pt electrode.....	72
Figure 4.11 The yield of 1,3-propanediol as a function of electrical charges at an applied current intensity of 3 - 5 A by using synthetic glycerol solution at the concentration of 46.2 g/l and pH of 2 with Pt electrode.....	72
Figure 4.12 Evaluation of the normalized concentration (a) and glycerol reforming (b) as a function of electrical charges at different initial electrolyte pH values by using synthetic glycerol solution at the concentration of 46.2 g/l and current intensity of 4.5 A with Pt electrode.....	74
Figure 4.13 Plot of rate constant of pseudo-first-order kinetics of glycerol reforming as different initial electrolyte pH values by using synthetic glycerol solution at the concentration of 46.2 g/l and	

Figure and Scheme	Page
current intensity of 4.5 A with Pt electrode.....	74
Figure 4.14 The yield of 1,3-propanediol as a function of electrical charges at different initial electrolyte pH values by using synthetic glycerol solution at the concentration of 46.2 g/l and current intensity of 4.5 A with Pt electrode.....	75
Figure 4.15 Evaluation of the normalized concentration (a) and glycerol reforming (b) at different types of additive by using synthetic glycerol solution at the concentration of 46.2 g/l, current intensity of 4.5 A and pH of 1 with Pt electrode.....	76
Figure 4.16 The yield of 1,3-propanediol as a function of electrical charges at different types of additive by using synthetic glycerol solution at the concentration of 46.2 g/l, current intensity of 4.5 A and pH of 1 with Pt electrode.....	77
Figure 4.17 Evaluation of the normalized concentration (a) and glycerol reforming (b) as a function of electrical charges at different initial concentrations of NaCl at an applied current intensity of 4.5 A by using synthetic glycerol solution at the concentration of 46.2 g/l and pH of 1 with Pt electrode.....	78
Figure 4.18 Plot of rate constant of pseudo-first-order kinetics of glycerol reforming as different concentrations of NaCl by using synthetic glycerol solution at the concentration of 46.2 g/l and current intensity of 4.5 A with Pt electrode.....	81
Figure 4.19 The yield of 1,3-propanediol as a function of electrical charges at different initial concentrations of NaCl at an applied current intensity of 4.5 A by using synthetic glycerol solution at the concentration of 46.2 g/l and pH of 1 with Pt electrode.....	82
Figure 4.20 Representative GC/MS spectra of glycerol solution at pH of 1 in the absence of NaCl (a) and the presence of NaCl (b) before supplying electricity.....	84
Figure 4.21 Representative GC/MS spectra of glycerol solution at pH of 1 in	

Figure and Scheme	Page
the absence of NaCl (a) and the presence of NaCl (b) obtained after electrolysis by employing the current intensity of 4.5 A with Pt electrode at the electrical charge of 100 Ah/l.....	85
Figure 4.22 Quantity of various compounds generated from glycerol reforming by electrochemical as a function of electrical charge in the absence of NaCl at an applied current intensity of 4.5 A by using synthetic glycerol solution pH of 1 with Pt electrode.....	86
Figure 4.23 Quantity of various compounds generated from glycerol reforming by electrochemical as a function of electrical charge in the presence of NaCl at an applied current intensity of 4.5 A by using synthetic glycerol solution pH of 1 with Pt electrode.....	87
Scheme 4.1 Possible reaction pathways of synthetic glycerol reforming to 1,3-propanediol and value-added compounds by electrochemical technique.....	90
Figure 4.24 Evaluation of the normalized concentration (a) and glycerol reforming (b) as a function of electrical charges by using different glycerol sources including synthetic glycerol solution and crude glycerol solution.....	91
Figure 4.25 The yield of 1,3-propanediol as a function of electrical charges by using different glycerol sources including synthetic glycerol solution and crude glycerol solution.....	92
Figure 4.26 Representative GC/MS chromatogram of crude glycerol obtained from the waste used-oil biodiesel production plant.....	92
Figure 4.27 Representative FTIR spectra of commercial glycerol (a) and crude glycerol from biodiesel production plant (b).....	94
Figure 4.28 Weight fraction of the four distinct layers, free fatty acid layer ($\bar{\text{r}}$), char and soap layer (£), glycerol-rich layer (r) and alkaline-catalyst layer (\times) obtained from the H_2SO_4 (---) and H_3PO_4 (—) acidification stage of crude glycerol purification at different pH values.....	97

Figure and Scheme	Page
Figure 4.29 Weight fraction of glycerol (w), ash (ϵ), water (r), and MONG (\bar{I}) contents in glycerol-rich layer obtained from the H_3PO_4 (a) and H_2SO_4 (b) acidification stages of glycerol at different pH values.....	98
Figure 4.30 Representative FTIR spectra of the crude glycerol (a), a commercial glycerol (b) and purified crude glycerol with the H_3PO_4 (a') and H_2SO_4 (b') performed at a pH of 1.0 (c), 2.2 (d), 3.5 (e) and 6.0 (f).....	100
Figure 4.31 The neutralized glycerol-rich layer with NaOH (a) and KOH (b) after leaving for 5 h.....	102
Figure 4.32 Representation of commercial glycerol (a), crude glycerol (b) and purified crude glycerol with H_2SO_4 (c) and H_3PO_4 (d) at pH of 1, purified crude with H_3PO_4 at pH of 2.2 after neutralization with NaOH (e) and KOH (f) and extraction with $n-C_6H_{14}$ (g) and purified crude glycerol with H_3PO_4 at pH of 2.2 after extraction with $n-C_6H_{14}$, neutralization with KOH, and extraction with C_2H_5OH (h).....	103
Figure 4.33 Representative FTIR spectra of commercial glycerol (a), crude glycerol (b) and purified crude glycerol (c).....	105
Figure 4.34 Representative ^{13}C -NMR spectrums of commercial glycerol (a), crude glycerol (b) and purified crude glycerol (c).....	105
Figure 4.35 Representative GC/MS spectrums of commercial glycerol (a), the crude glycerol (b) and purified crude glycerol (c).....	106
Figure 4.36 Current density-potential curves of the purified crude glycerol (x), synthetic glycerol (y) and the crude glycerol solution (z) at pH of 1 by using the Pt electrodes with a constant magnetic stirring rate of 400 rpm. The scan rate was 5 mV/s with Ag/AgCl reference electrode.....	110
Figure 4.37 Evaluation of the normalized concentration (a) and glycerol reforming (b) as a function of electrical charges at different	

Figure and Scheme	Page
applied current intensities by using purified crude glycerol solution at the concentration of 46.2 g/l and pH of 1 with Pt electrode.....	111
Figure 4.38 Plot of rate constant of pseudo-first-order kinetics of glycerol reforming as a function of current intensity by using purified crude glycerol solution at the concentration of 46.2 g/l and pH of 2 with Pt electrode.....	112
Figure 4.39 The yield of 1,3-propanediol as a function of electrical charges at different applied current intensities by using purified crude glycerol solution at the concentration of 46.2 g/l and pH of 1 with Pt electrode.....	112
Figure 4.40 Evaluation of the normalized concentration (a) and glycerol reforming (b) as a function of electrical charges at different concentrations of NaCl by using purified crude glycerol solution at the concentration of 46.2 g/l, current intensity of 6 A and pH of 1 with Pt electrode.....	113
Figure 4.41 Plot of rate constant of pseudo-first-order kinetics of glycerol reforming as a function of different concentration of NaCl by using purified crude glycerol solution at the concentration of 46.2 g/l, current intensity of 6 A and pH of 1 with Pt electrode.....	115
Figure 4.42 The yield of 1,3-propanediol as a function of electrical charges at different concentrations of NaCl by using current intensity of 6 A and initial pH of 1 with Pt electrode.....	116
Figure 4.43 Representative GC/MS spectra of purified crude glycerol solution at pH of 1 in the absence of NaCl (a) and the presence of NaCl (b) before supplying electricity.....	117
Figure 4.44 Representative GC-MS spectra of purified crude glycerol solution at pH of 1 in the absence of NaCl (a) and the presence of NaCl (b) obtained after electrolysis by employing the current intensity of 6 A by using Pt electrode at the electrical	

Figure and Scheme	Page
charge of 184.61 Ah/l.....	118
Figure 4.45 Quantity of various compounds generated from purified crude glycerol reforming by electrochemical as a function of electrical charge in the absence of NaCl at an applied current intensity of 6 A by using purified crude glycerol solution pH of 1 with Pt electrode.....	119
Scheme 4.2 Possible reaction pathways of purified crude glycerol reforming to 1,3-propanediol and value-added compounds by electrochemical technique.....	122
Figure D.1 Glycerol reforming to 1-hydroxly-2- propanone (acetol), acrylaldehyde (acrolein) and pronene in acid solution.....	145
Figure D.2 Glycerol reforming to 1-hydroxly-2- propanone and acrylaldehyde in acid solution within applied electricity.....	146
Figure D.3 Glycerol reforming to formaldehyde, acetaldehyde and ethylene glycol in acid solution within applied electricity.....	146
Figure D.4 Glycerol reforming to 2,3-dihydroxyl-propanal in acid solution within applied electricity.....	147
Figure D.5 Glycerol reforming to propanal and 2-propenol (allyl alcohol) in acid solution within applied electricity.....	147
Figure D.6 1-hydroxyl-2-propanone reforming to 1,2-propanediol and 2-ethyl-4-methanol-1,3-dioxolane in acid solution within applied electricity.....	148
Figure D.7 1-hydroxyl-2-propanone reforming to acetaldehyde and acetic acid and propanoic acid in acid solution within applied electricity..	148
Figure D.8 Acrylaldehyde reforming to propene and 1,3-propanediol in acid solution within applied elect.....	149
Figure D.9 Glycerol reforming with formaldehyde to 5-hydroxy-1,3-dioxolane in acid solution within applied electricit.....	149
Figure D.10 Glycerol reforming to glycidol in acid solution within applied electricity.....	149

LIST OF ABBREVIATIONS

a	Constant values for a particular species or stoichiometric constant
a_i	Activity of species i
A	Transfer coefficient
A_e	Electrode area (square meter, m^2)
$A\zeta$	Alkalinity of the sample (milliequivalent per 100 gram, meq./100 g)
A^2	Mass of the as-received test specimen (gram, g)
b	Constant values for a particular species or stoichiometric constant
$B\zeta$	Mass of the oven-dried specimen (gram, g)
C	Charge passed (coulomb, C)
C'	Reactant concentration
C_b	Bulk concentration of selected species (mole per cubic meter, mol/m^3)
C_i	Concentration of species i
C_s	Surface concentration of selected species (mole per cubic meter, mol/m^3)
$[C_3H_5(OH)_3]_i$	Initial concentration of glycerol (milligram per liter, mg/l)
$[C_3H_5(OH)_3]_t$	Concentration of glycerol at particular time t (milligram per liter, mg/l)
D_i	Diffusion coefficient (square meter per second, m^2/s)
D_{R-X}	Diving force (pascal, Pa)
E	Electrode potential (volt, V)
E^0	Standard electrode potential (volt, V)
E_{anode}^0	Anodic potential (volt, V)
$E_{cathode}^0$	Cathodic potential (volt, V)
DE°	Difference in the standard potentials of two half-cell reactions (volt, V)
F	Faraday's constant (96,484 coulomb per mole, 96,484 C/mol)
DG°	Standard Gibbs free energy change in a chemical process (kilojoule per mole, kJ/mol)
i	Current intensity (ampere, A)
j_o	Term of exchange current density (ampere per square meter, A/m^2)
j	Current density (ampere per square meter, A/m^2)

J_i	Flux of species i at distance from the surface (mole per second-square meter, $\text{mol/s}\cdot\text{m}^2$)
k_{app}	Apparent rate constant of the glycerol reforming
$k_{C_3H_5(OH)_3}$	Real rate constant
k_{obs}	Observe rate constant of the glycerol reforming
k_m	Mass transfer coefficient (meter per second, m/s)
k'	Rate constant at the equilibrium potential (per second, s^{-1})
K	Equilibrium constant for the overall reaction
m	Mass of the substance altered at an electrode (gram, g)
m_A	Mass of species A
M	Molarity (mole per liter, mol/l)
M_w	Molecular mass of the substance (gram per mole, g/mol)
n	Number of electrons in unit
$n\mathcal{C}$	Amount of substance altered (mole, mol)
N	Number of moles
O_x	Oxidized form of involved species
P	Static pressure (pascal, Pa)
Q	Total electric charge passed through the substance (coulomb, C)
r	Rate of chemical reaction ($\frac{dN}{dt}$) (mole per gram-second, $\text{mol/g}\cdot\text{s}$)
R	Universal gas constant as 8.3145 (joule per mole-kelvin, $\text{J/mol}\cdot\text{K}$)
R_{ed}	Reduced form of involved species
S	Entropy (kilojoule per kelvin-mole, $\text{kJ/K}\cdot\text{mol}$)
t	Electrolysis time (hour, h)
T	Absolute temperature (kelvin, K)
$T\mathcal{C}$	The water equivalent of the Karl Fisher reagent (milligram H_2O per milliliter, $\text{mgH}_2\text{O/ml}$)
μ_i	Charge of species i
U	Internal energy (kilojoule per mole, kJ/mol)
u_i	Velocity of which a volume element in solution moves along the axis (meter per second, m/s)

V	Electrolyte volume (liter, l)
V_R	Volume of reactor (liter, l)
V_C	Volume of Karl Fisher reagent used for the titration (milliliter, ml)
$w_{electrical}$	Electrical work (kilojoule per mole, kJ/mol)
α	Reaction order relating to the adsorbed hydroxyl radicals concentration
α'	Transfer coefficient
β	Charge transfer coefficient for oxidation step
g_i	Activity coefficients of species
δ	Thickness of the Nernst diffusion layer
h	Over potential (volt, V)
h_{gly}	Glycerol reforming (mg glycerol/C)
f	Potential gradient

CHAPTER I

INTRODUCTION

1.1 Background

Owing to the energy crisis in the world, the alternative fuel such as biodiesel has been widely used instead of fossil fuel. Biodiesel is an alternative diesel fuel made from renewable biological sources such as vegetable oils and animal fats by using the reaction known as “Transesterification” in the presence of acidic or alkaline catalysts. Currently, the capacity of biodiesel production in our country has increased sharply from less than 2.1×10^6 liters/day in 2008 to an expected 6.4×10^6 liters/day in 2012 (Biodiesel, 2009). During the biodiesel production process, oils or fats (triglycerides) are mixed with methyl alcohol and alkaline catalysts to produce esters of free fatty acids or biodiesel. The by-product from biodiesel production process is glycerol. In general, the production of 100 kilograms biodiesel yields approximately 10 kilograms of crude glycerol. Increasing the biodiesel production would be raised higher amount of crude glycerol. Crude glycerol has been purified by distillation, which is used in both food and pharmaceutical industries. However, distillation process is costly and uneconomic. To make the value-added glycerol and to reduce the crude glycerol surplus in the environment, many processes have been developed to reform glycerol to other valuable forms such as blending with biomass, producing a solid fuel or using as a raw material to produce other valuable compounds such as ethanediol, 1,2-propanediol, 1,3-propanediol, dihydroxyacetone, glyceraldehydes and glyceric acid.

One interesting compound that can be produced from glycerol is 1,3-propanediol because it has numerous applications in polymers, cosmetics, foods, lubricants, and medicine industries. Typically, 1,3-propanediol is produced from various methods such as chemical hydration of acrolein, hydroformylation of ethylene oxide and biotechnological method of glucose and sucrose. Besides, the fermentation of glycerol with bacterial strains is effective to produce 1,3-propanediol. This process provides a good yield of 1,3-propanediol but it is a two-step reaction and the reaction rate is very low in aqueous solution. By the direct hydrogenolysis of glycerol to 1,3-propanediol, it is particularly interesting because it is one-step reaction and can be

carried out in organic solvents. But this reaction proceeded under high temperature and pressure, though the yield of 1,3-propanediol remained very low.

To eliminate the drawbacks of the previous techniques, the synthesis of 1,3-propanediol by electrochemical technique is of interest because of its fast reaction rate, versatility, simplicity and easy in operation.

1.2 Objectives of dissertation

1. To study the feasibility synthetic glycerol reforming to 1,3-propanediol by electrochemical technique
2. To investigate the effect of parameters on crude glycerol from biodiesel production reforming to 1,3-propanediol by electrochemical technique
3. To study the kinetic of glycerol reforming and mechanism of glycerol reforming to 1,3-propanediol by electrochemical technique

1.3 Scope of dissertation

1. Synthesize 1,3-propanediol from synthetic glycerol solution by electrochemical technique and study the mechanism of 1,3-propanediol synthesis
2. Synthesize 1,3-propanediol from crude glycerol solution by electrochemical technique
3. Purification procedure of crude glycerol by using the chemical and physical treatments
4. Synthesize 1,3-propanediol from purified crude glycerol solution by electrochemical technique and study the mechanism of 1,3-propanediol synthesis

CHAPTER II

THEORY AND LITERATURE REVIEW

2.1 Renewable energy resource

The global energy consumption is increasing at a huge rate compared to the population growth ([International Energy Outlook, 2009](#)). In recent years, total worldwide energy consumption was derived from the combustion of fossil fuels by means of oil, coal and natural gas of about 80-90% of the energy supply. However, these available resources are limited and fast depleted. Moreover, a higher combustion of fossil fuels has increased the concentration of carbon dioxide in atmosphere, which can trap solar energy on the earth atmosphere led to the formation of global warming.

According to the environmental worries and the consumption of non-renewable energy resources, the development of alternative resources of energy has been raised. Various alternative fuels such as biomass and biofuels (ethanol and biodiesel) are the solution to those problems. As its technical feasibility, economic competition, environmental acceptance and reduce the energy and global warming crisis.

One environmental benefit of replacing fossil fuels with biomass is that the energy obtained from biomass does not increase the global warming. However, biomass is not suitable for using as energy directly due to its high moisture content and low calorific value. To eradicate the aforementioned problems, biodiesel that gains advantage over biomass in terms of high calorific value is interesting.

Biodiesel (methyl esters) is the most promising sources for the substitution of the fossil fuels. It can be directly used in most diesel engines without any requiring extensive engine modification. Biodiesel has high potential as liquid transportation fuel and has been interested in worldwide because of its environmental benefits such as minimal emission of particular matter, carbon monoxide, sulfur, polyaromatics, hydrocarbons, smoke and noise compared with the regular diesel fuel ([Zullaikah et al., 2005](#)). In addition, burning of vegetable-oil based fuel does not contribute to the

net atmospheric CO₂ level because this fuel is made from agricultural materials which are produced via photosynthetic carbon fixation. (National Biodiesel Board, 2009).

2.2 Biodiesel production process

2.2.1 Raw material

These raw materials for biodiesel production usually contain free fatty acids, phospholipids, water, odorants and other impurities, so it cannot be directly used as a fuel in combustion engine because they had a higher viscosity compared with the public acceptance of standard fuel. The high viscosity of raw materials can be reduced by the chemical modification, transesterification, pyrolysis and emulsification.

Table 2.1 shows the raw materials of biodiesel and their physical and chemical properties. It is found that the physical and chemical properties of biodiesel change with kinds of raw material. The vegetable oils including edible and non-edible oils are very suitable to be used as raw materials to produce biodiesel because the properties of biodiesel produced from vegetable oils are similar to the properties of diesel fuel (Gui et al., 2008 and Patil and Deng, 2009). However, the edible and non-edible oils have some problems. For example, the edible oils are the competition with the edible oil market leading to the increase in cost of edible oils and biodiesel (Kansedo et al., 2009). The non-edible oils have a higher content of free fatty acids and required multiple chemical steps, which will be increased the production cost of biodiesel (Haas, 2005). The waste cooking oils are a suitable raw material for biodiesel production because its usage significantly reduces the cost of biodiesel production and increased the value-added waste cooking oils. On the other hand, the quality of waste cooking oils depends significantly upon the physical and chemical properties and content of fresh cooking oil and it had contaminated with lots of undesired impurity such as water and free fatty acids (Leung and Guo, 2006).

Table 2.1. Raw materials for biodiesel production and their physical and chemical properties (Leung et al., 2010).

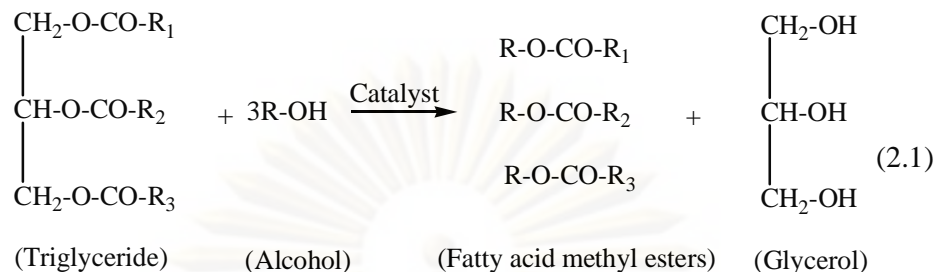
Type of oil	Species	Main chemical composition (fatty acid composition)	Density (g/cm ³)	Flash point (°C)	Kinematic viscosity (cst, at 40°C)	Acid value (mgKOH/g)	Heating value (MJ/kg)	
Edible oil	Soybean	C _{16:0} , C _{18:1} , C _{18:2}	0.91	254	32.9	0.2	39.6	
	Repressed Sunflower	C _{16:0} , C _{18:0} , C _{18:1}	0.91	246	35.1	2.92	39.7	
	Palm	C _{16:0} , C _{18:0} , C _{18:1}	0.92	274	32.6	-	39.6	
	Peanut	C _{16:0} , C _{18:0} , C _{18:1} , C _{18:2} , C _{20:0} , C _{22:0}	0.90	271	22.72	3	39.8	
	Camelina	C _{16:0} , C _{18:0} , C _{18:1} , C _{18:2} , C _{18:3} , C _{20:0} , C _{20:1} , C _{20:3}	0.91	-	-	0.76	42.2	
	Corn	C _{16:0} , C _{18:0} , C _{18:1} , C _{18:2} , C _{18:3}	0.91	277	34.9 ^a	-	39.5	
	Canola	C _{16:0} , C _{18:0} , C _{18:1} , C _{18:2} , C _{18:3}	-	-	38.2	0.4	-	
	Cotton	C _{16:0} , C _{18:0} , C _{18:1} , C _{18:2}	0.91	234	18.2	-	39.5	
	Pumpkin	C _{16:0} , C _{18:0} , C _{18:1} , C _{18:2}	0.92	>234	35.6	0.55	39	
	Non-edible oil	Jatropha curcas	C _{16:0} , C _{16:1} , C _{18:0} , C _{18:1} , C _{18:2}	0.92	225	29.4	28	38.5
		Pongamina Pinnata	C _{16:0} , C _{18:0} , C _{18:1} , C _{18:2} , C _{18:3}	0.91	205	27.8	5.06	34
		Sea mango	C _{16:0} , C _{18:0} , C _{18:1} , C _{18:2}	0.92	-	29.6	0.24	40.86
Palanga		C _{16:0} , C _{18:0} , C _{18:1} , C _{18:2}	0.90	221	72.0	44	39.25	
Tallow		C _{14:0} , C _{16:0} , C _{16:1} , C _{17:0} , C _{18:0} , C _{18:1} , C _{18:2}	0.92	-	-	-	40.05	
Nile tilapia		C _{16:0} , C _{18:1} , C _{20:5} , C _{22:6} , other acids	0.91	-	32.1 ^b	2.81	-	
Poultry		C _{16:0} , C _{16:1} , C _{18:0} , C _{18:1} , C _{18:2} , C _{18:3}	0.9	-	-	-	39.4	
Others	Used cooking oil	Depends on fresh cooking oil	0.9	-	44.7	2.5	-	

^a Kinematic viscosity at 38 °C (mm²/s)

^b Kinematic viscosity at 37 °C (mm²/s)

2.2.2 Transesterification (Srivastava and Prasad, 2000)

The transesterification or alcoholysis process is the reaction that an alcohol (like methanol) reacts with the triglyceride contained oils in renewable feedstock to form fatty acid alkyl esters (biodiesel) and glycerol or glycerine. The reaction requires heat and a homogenous strong base catalyst such as sodium hydroxide or potassium hydroxide. The simplified transesterification reaction is shown below.

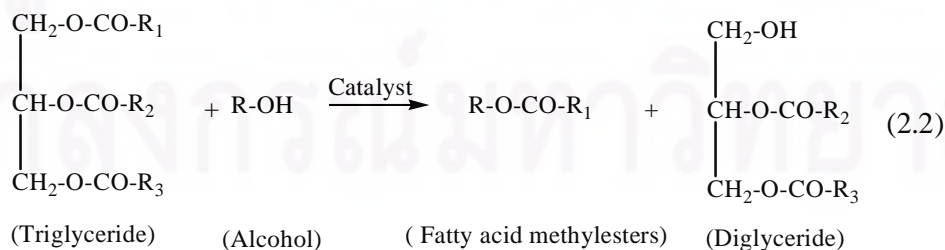


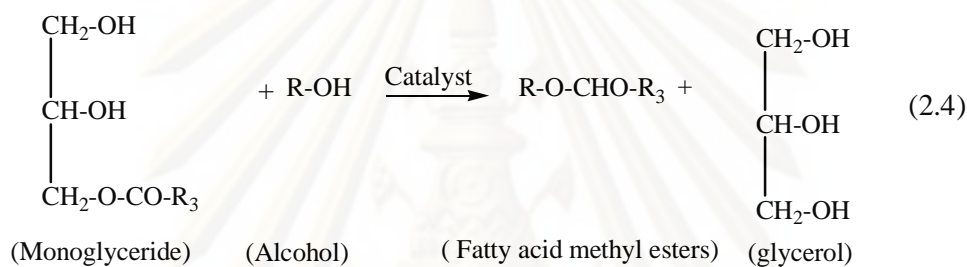
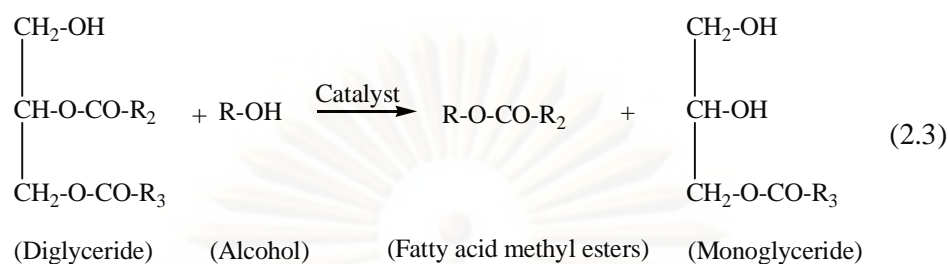
Where R_1 , R_2 , and R_3 are long chains of carbons and hydrogen atoms, sometimes called fatty acid chains.

Transesterification of triglycerides produces a mixture of fatty acid methyl esters and glycerol. After settling overnight, the product mixture separates into two layers: fatty acid methyl esters with excess methanol layer in the upper layer with glycerol and excess base catalyst layer in the lower layer (Leung and Guo, 2006).

The reaction mechanism for alkali-catalyzed transesterification is three reactions (2.2)-(2.4). Firstly, the anion of the alcohol (methoxide ion) reacts with the carbonyl carbon atom of the triglyceride molecule to form di-glycerides. Secondly, the di-glyceride intermediate reacts with an alcohol to produce mono-glycerides. Finally, the mono-glycerides react with excess alcohol to form fatty acid methyl esters and glycerol. The mono- and di-glycerides are the intermediates in this process.

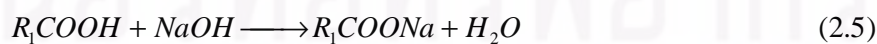
These steps of reactions are reversible and a little excess of alcohol is used to shift the equilibrium towards the formation of esters. In the presence of excess alcohol, the forward reaction is pseudo-first order reaction and the reverse reaction is found to be second order reaction. It is also observed that the transesterification is faster by alkali catalyst (Ma and Hanna, 1999).





2.2.3 Process flow chart

Figure 2.1 shows a simplified flow chart of biodiesel production process catalyzed by the alkali catalyst. In the process, the vegetable oils or some food-grade animal fats contain small amounts of water and 2.5%wt of free fatty acid (FFA) is directly used in the production step. If the renewable feedstock has free fatty acid content over 2.5%wt, it must be necessary pretreatment with strong acid such as sulfuric acid or phosphoric acid to convert free fatty acid to triglyceride because the utilized alkali catalyst can be reacted with the free fatty acid to form soap and water (saponification reaction) as reaction (2.5)



This reaction is undesirable because it provides a lower yield of biodiesel production and inhibits the separation of fatty acid methyl esters from glycerol.

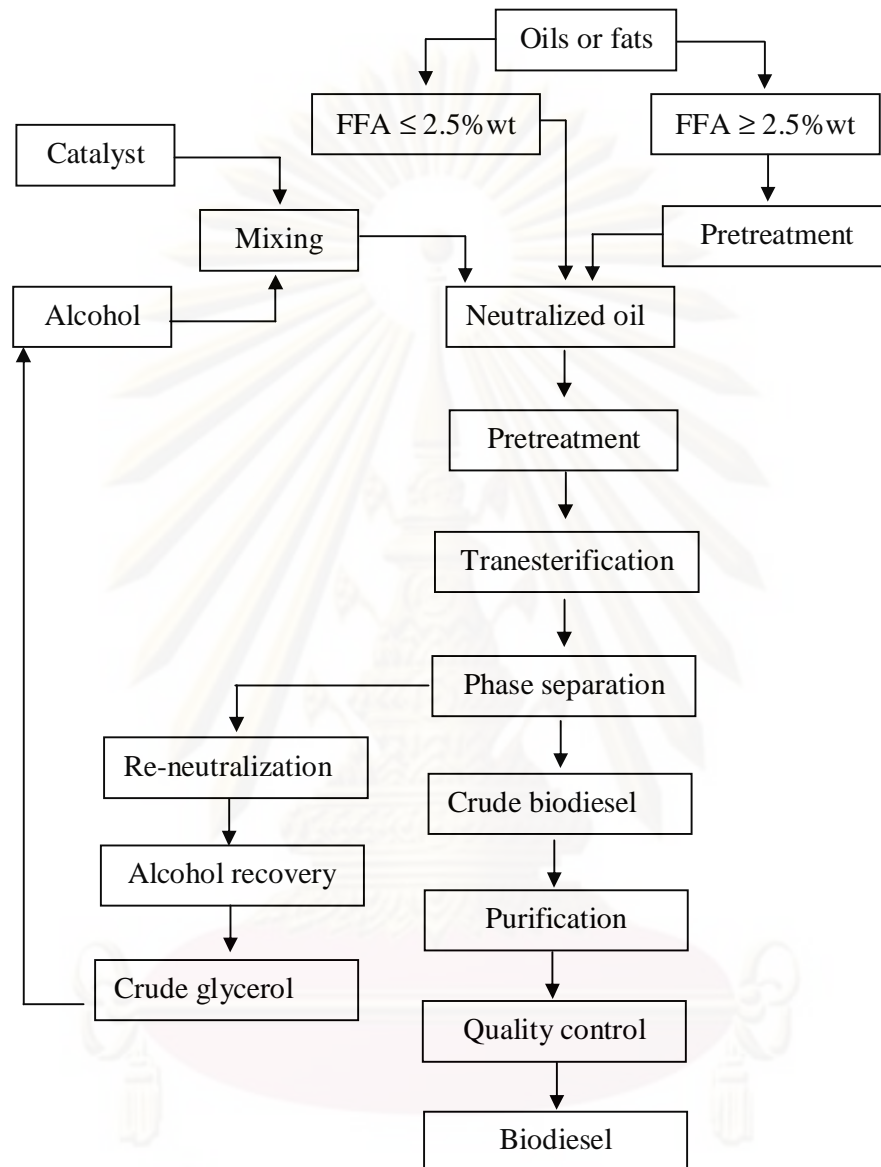


Figure 2.1. Simplified process flow of catalyzed biodiesel production (Leung et al., 2010).

2.2.4 By-product from biodiesel production plant

A major by-product from biodiesel production plant is glycerol in which is contaminated with an unreacted catalyst, alcohol and residual raw material during the transesterification step. Also, free fatty acid presented in the initial feedstock can react with the base catalyst to form soap which can soluble in the crude glycerol. In

addition, crude glycerol also contains salt of alkali catalyst and a variety of elements such as calcium, magnesium, phosphorous or sulfur (Thompson and He, 2006).

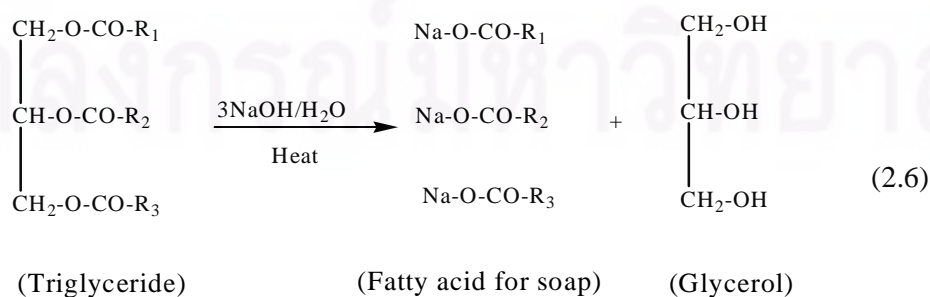
According to above transesterification reaction, 10 kilograms of glycerol is produced for every 100 kilograms of biodiesel. If the production of biodiesel increases as predicted, the surplus of glycerol will create a glut on the market and environment.

2.3 Glycerol

2.3.1 Glycerol and source of formation

Glycerol (HOCH₂CH(OH)CH₂OH), is also well known as glycerine and less commonly as propane-1,2,3-triol, 1,2,3-propanetriol, 1,2,3-trihydroxypropane, glyceritol or glycerol alcohol, is completely soluble in water and alcohols, slightly soluble in many common solvents like ether and dioxane but insoluble in hydrocarbons. Liquid glycerol boils at 290°C under normal atmospheric pressure. The specific gravity and molecular weight are 1.26 and 92.09, respectively. At low temperatures, it is usually in the forms of crystals which tends to melt at 17.9°C (Naresh and Brian, 2006).

Today, the name of glycerol refers to pure chemical and is commercially known as glycerin. The glycerol can be produced by fermentation or hydrogenolysis of carbohydrate or sugar and be recovered from waste oils by the addition of H₂SO₄ or HCl. The glycerol is a by-product of the industrial soap manufacturing process (saponification). This process uses animal or vegetable oil and alkali solution (NaOH or KOH) to produce fatty acids for soap (sweet water), water and glycerol by hydrolysis process (fat splitting process). The glycerol is removed from water and sweet water and is often processed into purified glycerol. The simplified saponification reaction is shown below.



Besides, glycerol is also the by-product of biodiesel production by transesterification reaction as described in 2.2.2. The production of soap and biodiesel is nearly similar (Figure 2.2) in that both processes produce glycerol as a by-product.

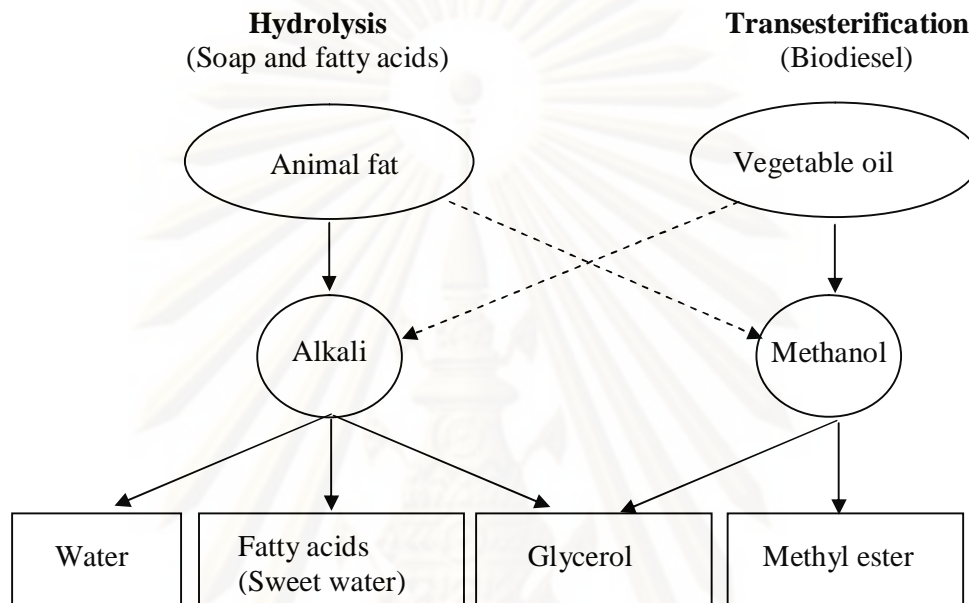


Figure 2.2. Comparison of saponification and transesterification ([Glycerine market analysis, 2009](#)).

Currently, large quantity of glycerol is generated from the transesterification of vegetables oils or animal fats but it has low value due to the presence of various contaminants. Usually, glycerol can be purified by treated and refined through filtration, chemical additions, and fractional vacuum distillation. The refining of the crude glycerol may be a costly affair depending on the economy of production scale and/or the availability of a glycerol purification facility. Many previous works have been conducted and innovated to utilize crude glycerol. It will be beneficial to the research community as well as biodiesel industry in understanding the progress of glycerol for value-added applications and for reference in manipulating their own integrated plans for sustainable and profitable biodiesel production.

2.3.2 Application of glycerol

A high purity glycerol is an important feedstock for industrial application including food products, personal care products such as skin creams, lotions shaving creams, makeup and deodorant, oral care product such as toothpastes, mouthwashes and sugar-free gum, pharmaceutical industries and others application. The applications of glycerol in food, personal and oral care products are 64% of refined glycerol consumption. Figure 2.3 shows the complete breakdown of glycerol consumption by end use.

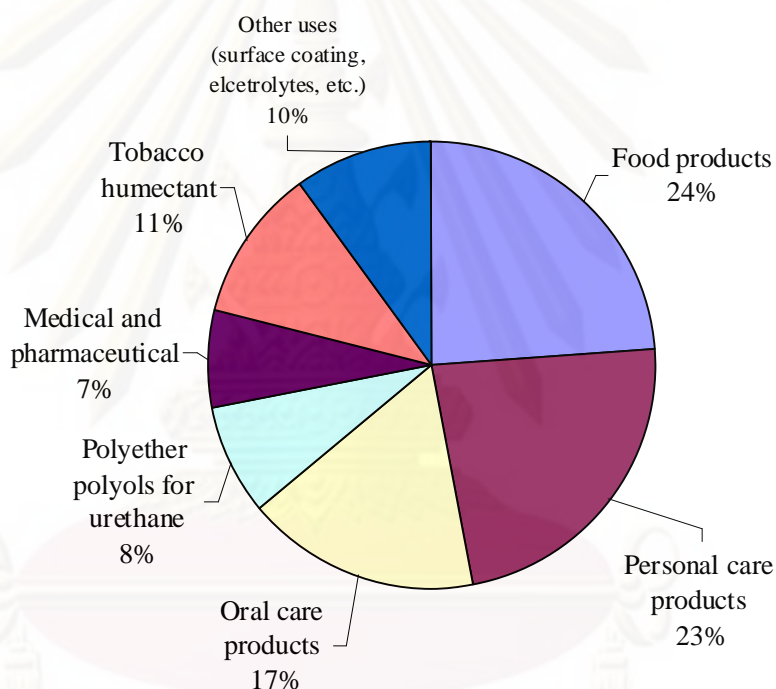


Figure 2.3. Application of refined glycerol ([Glycerin market analysis, 2009](#)).

For example, in food and beverages industries, glycerol is a humectant, solvent and sweetener and preservative. It acts as a solvent for flavors and food colors in drinks and softening agent in candy, cakes and cheese. It is also used as filler in commercially prepared low-fat foods (e.g., cookies). Glycerol is added to ice-cream to improve the texture, and its sweet taste decreases the amount of sugar needed. The monoglycerides, the glycerol esters of fatty acids are emulsifiers and stabilizers for many products. It is used in salad dressings, frozen desserts, candy, and food coatings

Monoglycerides also help to maintain moisture balance in a product and permit richer formulations with longer shelf life when added to margarine to increase plasticity and to dough mixes to promote dispersion of fat.

In cosmetics and other toiletry applications, glycerol is virtually nontoxic, non-irritating and odorless. It functions as a humectants, vehicle and emollient. Glycerol is a major toothpaste ingredient, preventing drying out and hardening in the tube and maintaining smoothness and shine. It is added during the manufacture of soaps in order to prepare shiny transparent bars. Glycerol is also added in hair shampoo to make them flow easily when pours from the bottle. Other uses include skin creams and lotions, shaving preparation, deodorant and make up. Glycerol esters of fatty acids are utilized as emulsifiers in cream, lotion, replaced waxes in lipstick.

In drug and pharmaceutical industries, glycerol is a solvent, moistener, humectants, and bodying agent in tinctures, elixirs, and ointments. Other well known uses include suppositories, ear infection remedies, anesthetics, cough remedies, lozenges, gargles and vehicles for antibiotics and antiseptics. Medically, glycerol serves as an emollient and demulcent preparation used on the skin and as an osmotic diuretic to manage cerebral edema, to reduce cerebrospinal pressure and to lower intraocular pressure. Nitroglycerin is the trinitrate derivative of glycerol, which is considered as a drug to relieve chest pains and to treat various heart ailments. One application of this chemical is as the key element in the manufactures of dynamite explosives and gun cotton.

In addition, glycerol is a standard component in the manufacture of these resins used in surface coatings of metals because of its chemical flexibility and process advantages. Glycerol is used as a humectants and sweetener in the industrial tobacco manufacturing. About 3%wt of glycerol is sprayed on leaves before processing to prevent crumbing, breaking, dehydration and freshness in packaged cigarettes. Glycerol is an important role in the lubricants used in many applications because of its stability over a broad range of temperatures and pressures and due to its viscosity and hygroscopicity in a textile conditioning agent. Glycerol provides one of the fundamental chemical building blocks for the construction of rigid polyurethane foams. The flexible foams have superior properties with respect to humid aging and resilience by using glycerol in the processes. It is employed for the manufacture of

electrolytes for electrolytic condensers used in radios and neon lights. A small in volume of glycerol is applied in photography, laboratory, cell preservation, and gas drying.

The low-grade glycerol obtained from biodiesel production cannot directly be used in food, drug, pharmaceutical and cosmetic industries. Some simple methods for low-grade glycerol direct utilization have been proposed such as the combustion, compost and animal-feed (Cerrate et al., 2006). Also, many researchers attempted to value-added low-grade glycerol by the other methods such as thermo-chemical conversions (Sabourin-Provost and Hallenbeck, 2009) and biological conversion (Tang et al., 2009).

2.3.4 Value-added products of glycerol

As the biodiesel production is increasing exponentially, the crude glycerol generated from the transesterification of vegetables oils has been increased in a large quantity. Many processes have been developed to make value-added crude glycerol, which will be beneficial to the research society and biodiesel industry. Reforming glycerol into value-added products can be carried out by both fermentation and catalytic process. For example, Lee et al., (2000) have been used glycerol in the fermentation of *A. Succiniciproducens* to produce the succinic acid. Also, glycerol has been used as a carbon source in the fermentation of *E. coli*. This leads to a mixture of products such as ethanol, succinate, acetate, lactate and H₂. Moreover, Cortright et al., (2002) have described an aqueous phase reforming process that will reform glycerol to H₂. It can be used as a fuel. Virent Energy Systems, Inc. is currently trying to commercialize this technology and claim that sodium hydroxide, methanol and high pH levels content crude glycerol lead to low-grade and value of crude glycerol actually help the process (A glycerin factor, 2005). In general, there has been much research using thermochemical processes or various microorganisms (Table 2.2) to produce the value-added industrial products using glycerol as a feed stock.

Table 2.2. Product derived from glycerol with some previous researches (Naresh and Brian, 2006).

Product name	Process method	Researchers/Scientists
1,3-propanediol	Continuous and batch microbial fermentations mainly by <i>C. Butyricum</i> and <i>K. Pneumoniae</i> .	Himmi et al. (1999) Papanikolaou and Aggelis (2003) Xiu et al. (2004)
	Selective hydroxylation technique	Wang et al. (2003)
	Continuous microbial fermentation by <i>E. Aerogenes</i> HU-101.	Ito et al. (2005)
Hydrogen	Catalytic reforming	Wood (2002)
	Steam reforming	Hirai et al. (2005)
	Pyrolysis and steam gasification	Huber et al. (2003)
	Aqueous-phase reforming by Sn/Ni catalyst.	Valliyappan (2001)
	Microbial fermentation by <i>A. succiniciproducens</i>	Lee et al. (2001)
1,2-propanediol	Low-pressure hydrogenolysis	Dasari et al. (2005)
	Selective hydrogenolysis with Ni catalyst	Perosa and Tundo (2005)
	Chemoselective catalytic oxidation with Pt catalyst.	Garcia et al. (1994)
Dihydroxyacetone	Selective oxidation with Pt-Bi catalyst.	Kimura (2001)
	Microbial fermentations by <i>gluconobacter oxydans</i>	Bauer et al. (2005)
Polyesters	Adipic acid in the presence of Sn catalysts.	Stumbe and Bruchmann (2004)
Polyglycerols	Selective etherification	Clacens et al. (2002)

For example, glycerol was hydrogenolyzed in the presence of supported metallic (Cu, Ni, Pt, Ru, Rh and Pd) and bimetallic (Pt/WO₃/ZrO₂) catalysts to produce propylene glycol or 1,3-propanediol (Wang et al., 2003, Miyazawa et al., 2006, Alhanash et al., 2008 and Kurosaka et al., 2008) and ethylene glycol (Lahr and Shanks, 2005), gaseous hydrogen (Marshall et al., 2008 and Valliyappan et al., 2008). Cameron et al. (1998) proposed a biocatalytic fermentation process for production of propanediol from glycerol. The dehydration of glycerol to acetol and 3-hydroxypropionaldehyde was catalyzed by the solid acid catalyst such as zeolites, sulfated zirconia, tungstic acid and ion exchange resins which exhibited the highest activity (Miyazawa et al., 2006). The cracking, dehydration and hydrogenation transfer of glycerol with acid sites of the zeolite can be converted into acrolein, short olefins, aromatics, acetaldehyde, hydroxylacetone and acetone. Acrolein can also be produced from the liquid and gaseous phase of glycerol by dehydration with phosphoric acid catalyst (Huber et al., 2008). In addition, glycerol can be reformed to fuel additives such as di-tert-butylglycerols and tri-tert-butylglycerol by sulfonic-acid-functionalized mesostructured silicas (Melero et al., 2008) and to value-added products of glycerol such as dihydroxyacetone, glyceraldehyde, glyceric acid, glycolic acid, hydroxypyruvic acid, mesoxalic, oxalic acid and tartronic acid as Au, Pd and Pt supported on carbon catalyzed oxidation of glycerol in liquid phase depicted in Figure 2.4.

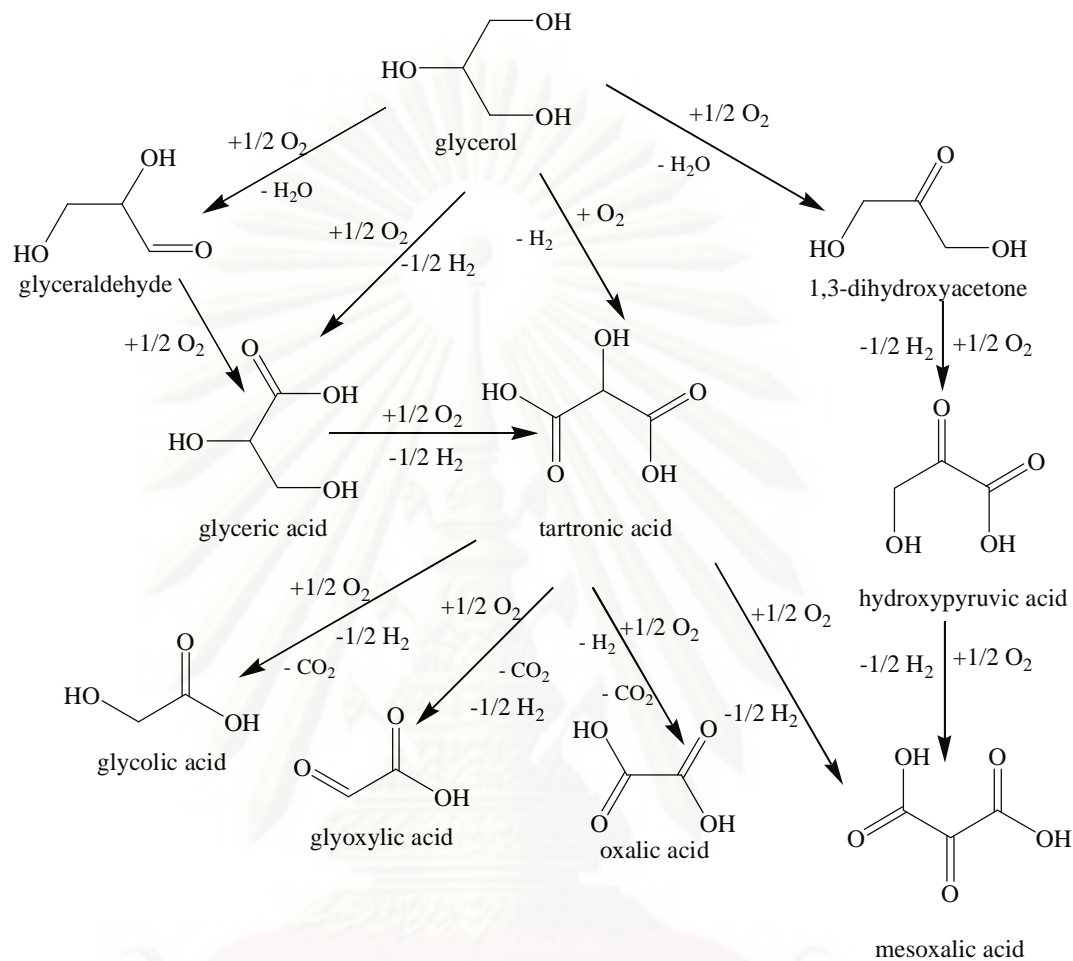


Figure 2.4. Chemical substances produced from glycerol (Demirel-Gülen et al., 2005).

2.4 1,3-propanediol

1,3-Propanediol (HOCH₂CH₂CH₂OH) or trimethylene glycol is a clear, colorless, odorless and innocuous liquid that is miscible with water, alcohol ethers and formamide. It is a valuable chemical intermediate that is potentially used as a monomer to produce polyesters, polyethers and polyurethanes. Currently, it has two routes to produce 1,3-propanediol as shown in Figure 2.5. Shell Chemical's Corterra™ has developed a process based on ethylene oxide, while Degussa-Uhde technology developed a process based on acrolein. Dupont's Sorona® acquired with

the Degussa-Uhde technology developed a process for 1,3-propanediol production by using renewable material such as glucose and sucrose as feedstock (Hass et al., 2005).

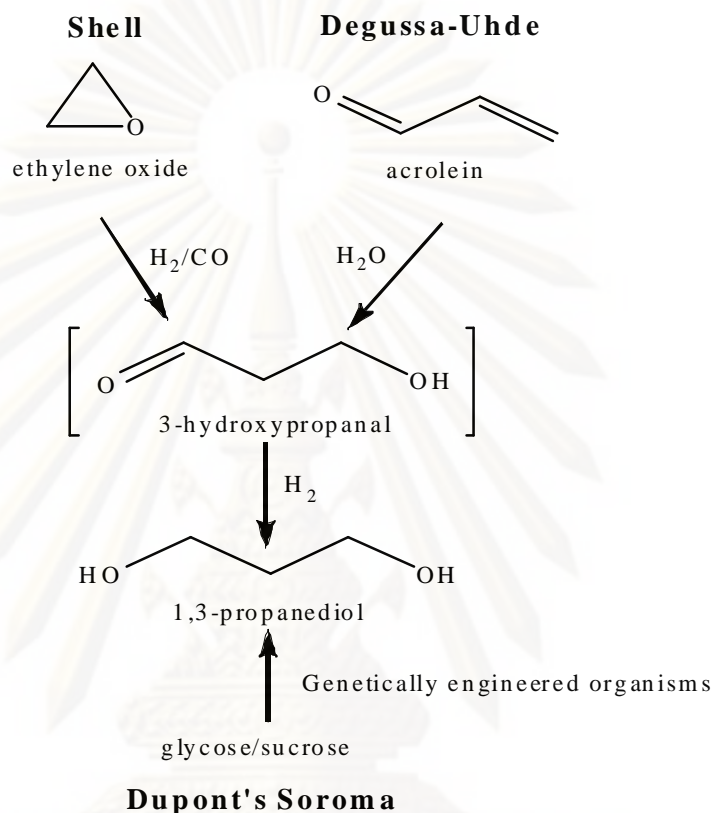


Figure 2.5. Industrial 1,3-propanediol processes (Hass et al., 2005).

2.4.1 1,3-propanediol based on acrolein

The 1,3-propanediol can be produced from acrolein with two reaction steps. The first step is acrolein hydration in an aqueous solution to form 3-hydroxypropanal at the temperature below 100°C. 3-hydroxypropanal is consecutively hydrogenated to 1,3-propanediol with catalyst. Both reaction steps run in adiabatic fixed bed reactors and continuous mode. The conversion of this process was about 85 - 90% in the pH ranging from 2 - 5 with buffer solution. Although the conversion and selectivity are about 100% in industrial scale at the optimum condition, it still contains the residual carbonyls in an extend of up to a few thousand ppm. These carbonyls are consisted of saturated aliphatic carbonyls and acetalization product as 2-(2'-hydroxyethyl)-1,3-dioxane (HED) (Haas et al., 2005).

2.4.2 1,3-propanediol process based on ethylene oxide

The hydroformylation of epoxides provides 3-hydroxyaldehydes and then hydrogenates to produce 1,3-propanediol. However, the hydroformylation reaction of epoxides can produce acrolein which can be hydrogenated to propanol and propanal. The condensation reactions of 3-hydroxypropionaldehyde from hydroformylation of epoxides can react with other aldehydes to produce C₅- or C₆-aldehyde compounds. In addition, the isomerization of ethylene oxide can be produced acetaldehyde and then hydrogenated to ethanol leading to yield and selectivity of 1,3-propanediol were decreased (Haas et al., 2005).

2.4.3 1,3-propanediol process based on fermentation of glycerol

Recently, Dupont's Sorona[®] developed process to produce 1,3-propanediol in a single step fermentation by genetically engineered strains as *E. coli* and changing a feetsocks from glucose and sucrose to glycerol. From the previous reviews, the fermentation by natural microorganisms, such as *K. pneumoniae*, *E. agglomerans*, *C. freundii*, *C. butyicum*, *C. pasteurianum*, *L. brevis* and *L. buchneri*, can produce 1,3-propanediol in two-step reaction. The *K. Pneumoniae*, *C. Freundii* and *C. Butyricum* provided a high yield and productivity because of their appreciable substrate tolerance (Himmi et al., 1999). Many researchers studied the fermentation method by using bacterial strain to produce 1,3-propanediol from glycerol as a carbon source (Shown in Table 2.3). The fermentation method using *K. Pneumoiae* was carried out both in batch and fed-batch cultures in which glycerol was reformed to 1,3-propanediol in good yields (61%), but the reaction proceeded very slow in water solution.

Table 2.3. Synthesis of 1,3-propanediol by *K. Pneumoiae* and *C. Butyicum*

Authors	Process	Initial concentration of glycerol (g/l)	Yield of 1,3- propanediol (%)
Menzel et al., (1997) ¹	Continuous culture	870	4.81
Papanikolaou et al., (2000) ²	Two-stage continuous fermentation	80	50.38

Authors	Process	Initial concentration of glycerol (g/l)	Yield of 1,3- propanediol (%)
Xiu et al., (2003) ³	Batch co-fermentation (glucose: glycerol)	92.4 (57.6:92.4)	100
Zhang et al., (2007) ⁴	Batch and fed-batch culture	66.4	61

Reaction condition:

¹Temp. 37°C, pH=7 and purged with N₂ at flow rate at 0.4 vvm.

²Temp. 33°C, pH= 7 and purged with N₂ at flow rate at 0.5 vvm.

³Temp. 37°C, pH= 8, aerating air at 40 vvm and agitation speed at 300 rpm.

⁴Temp. 40°C, time 48 h, pH= 8 and media was 12g/l of (NH₄)₂SO₄, 3.0g/l of NaCl and 54 g/l of agar.

Figure 2.6 shows the reviewed pathways of glycerol conversion to 1,3-propanediol and other products with anaerobic metabolism pathways. It was found that glycerol was oxidized by glycerol dehydrogenase (GDH) catalyst to form dihydroxyacetone (DHA) which was coupled with reducing equivalent (NADH₂) generator. The phosphorylated glycerol produced two dihydroxyacetone kinases (DHAK I and DHAK II), that were reformed to ATP and PEP-dependent, respectively. In parallel pathway, glycerol was dehydrated to 3-hydroxypropionaldehyde by glycerol dehydratase (GDHt), then reformed to 1,3-propanediol under the reducing condition.

Table 2.4. Glycerol hydrogenolysis to 1,3-propanediol with various supported metal catalysts.

Authors	Catalysts	Initial concentration of glycerol (g/l)	Yield of 1,3-propanediol (%)
Chaminand et al.,(2004) ¹	Ru/C	15	26.67
Kusunoki et al., (2005) ²	Ru/C	20	12.8
Kurosaka et al., (2008) ³	Pt/WO ₃ /ZrO ₂	0.1386	24.2

Reaction condition:

¹Temp. 180 °C, time 168h., pressure 80 bar with H₂ and use sulfolane as solvent.

²Temp. 120 °C, time 10h., pressure 80 bar with H₂.

³Temp. 170 °C, time 18h., pressure 80 bar with H₂ and use 1,3-dimethyl-2-imidazolidinone as solvent.

As mentioned above, although various methods are effective to reform glycerol to 1,3-propanediol, the hydrogenolysis was still provided a low production yield and required specific conditions such as high temperature (120 - 180°C) and pressure (4 - 10 MPa) or the fermentation process required long production time due to its two-step reaction. Besides some previous methods, electrochemical technique is an alternative method to reform glycerol. With unique features such as simplicity and robustness in structure and operation, the electrochemical technique has the potential to develop a cost-effective technology for glycerol reforming to 1,3-propanediol.

2.5 Fundamental of electrochemical (Pleteher and Weinberg, 1990, Prentice, 1991, Bard and Faulkner, 2001, Bard and Stratmann, 2007 and Macdonald and Schmuki, 2007)

The application of electrochemistry which has become an established discipline and optimization of electrochemical processes based on the fundamental laws of chemistry and electrochemistry. Essentially, it is an interdisciplinary field providing the tools of unit operations for the systematic description and treatment of chemical processes in a way that linked the underlying physical and physicochemical principles to chemical technology.

Now, the environmental aspect has become a major issue and a crucial factor in the industrial process to meet the requirement of sustainable development. In this field, electrochemistry offers some promising approaches due to its environmental compatibility and use of the electron as a “clean reagent”. There is common agreement among scientists that electrochemically based processes will be increasing importance in the future to meet the economic and social challenges resulting from urgent demand of low-grade raw materials utilization, energy saving and friendly of the environment.

2.5.1 Nature of electrode reactions

Electrode reactions are heterogeneous and take place in the interfacial region between electrode and a species in solution. The electrode process is affected by the structure of this region. The electrode reaction usually referred as electrolysis, typically involving a series of elementary steps. The reactant (O) moves to the electrode interface and reacts with electron (e^-) donated from electrode to form product (R), which consequently moves away from the surface of electrode to bulk solution, allowing a fresh reaction site for the next step of electrochemical reaction as shown in Figure 2.7.

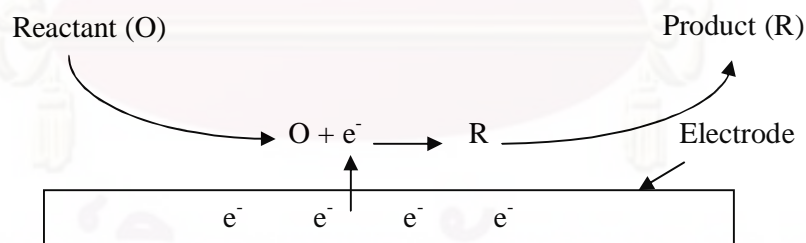


Figure 2.7. Schematic of a simple electrode reaction (Bard and Stratmann, 2007).

The electrochemical reaction on electrode surface depends upon the applied voltage on the electrode, the reactivity of the species, the nature of the electrode surface and the structure of the interfacial region where the electron transfer occurs.

2.5.2 Half-cell reaction

The electrochemical half-cell reaction is expressed by the conversion of the reversible processes, the simplified equation is Eq. (2.8)



The equation relating the equilibrium potential for the involved species is an electron transfer reaction derived by Nernst equation (Eq. 2.9)

$$E = E^0 + \frac{RT}{F} \ln \left(\frac{a_{O_x}}{a_{R_{ed}}} \right) \quad (2.9)$$

The activity of dissolved species in solution is commonly related to concentration by Eq. (2.10)

$$a_i = g_i C_i \quad (2.10)$$

When concentration are used instead of activity, the Nernst equation becomes

$$E = E^0 + \frac{RT}{F} \ln \left(\frac{g_{ox} [O_x]}{g_{re} [R_{ed}]} \right) \quad (2.11)$$

2.5.3 Standard electrode potential (E^0)

The quantity of E^0 in Eq. (2.11) is the standard electrode potential of the half-cell reaction. It is the actual cell potential when the concentration of species in solution is 1 M, the hydrogen pressure of 1 atm and pH = 0. E^0 can be related to the free energy change when all species are in standard states.

$$\Delta G^0 = -F\Delta E^0 = RT \ln K \quad (2.12)$$

The basic database for aqueous electrochemistry consists of the standard potential. This property is different for each combination on the half-cell that constitutes the overall cell.

2.5.4 Potential of an electrochemical cell

The cell potential of an electrochemical cell can be calculated from the electrode potential of the half-cell reaction. In general, the standard electrode potentials of the half-cell reactions allow directly the favored thermodynamics of the half-cell. Then, the standard potential of a cell can be calculated by the difference of the electrode potential between the cathode and anode.

$$E_{cell}^0 = \Delta E^0 = E_{cathode}^0 - E_{anode}^0 \quad (2.13)$$

From Eq. (2.13) and (2.14), the potential of an electrochemical cell is given by

$$\Delta E^0 = (RT / F) \ln K \quad (2.14)$$

2.5.5 Reference electrode

The reference cell is used for the hydrogen half-cell vs. $Pt / 1/2H_2(g) / H^+(aq) // M^{2+}(aq) / M$ in which hydrogen gas is allowed to bubble over a platinum electrode having a specially treated surface which catalyzes the reaction.



This electrode couple is arbitrarily defined as 0.00 volts. It is easy to use an electrode couple that has a clearly defined potential relative to the standard hydrogen electrode (SHE) (Figure 2.8 (a)). A commonly employed system is Ag/AgCl. The potential of this system is determined by the concentration of Cl^- ions in the solution from the Nernst equation (Figure 2.8 (b)).

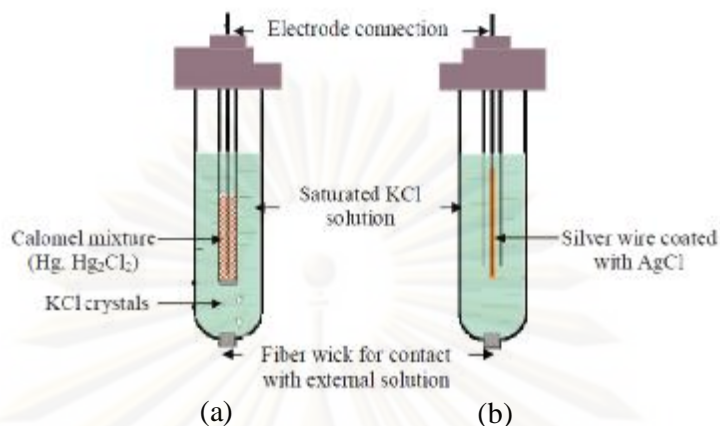


Figure 2.8. Reference electrodes SCE (a) and Ag/AgCl (b).

2.5.6 Nernst equation

The equilibrium reduction potential of a half-cell in an electrochemical cell can be calculated by the Nernst equation.

The expression for the Gibbs depends on activity and turns this around for expression in terms of the cell potential.

$$\Delta G = \Delta G^0 + RT \ln K \quad (2.16)$$

The relation between cell potential (E^0) and free energy gives

$$-nFE = -nFE^0 + RT \ln K \quad (2.17)$$

This can be rearranged to the Nernst equation as

$$E = E^0 - \left[\frac{RT}{nF} \right] \ln K \quad (2.18)$$

At 25°C, Eq. (2.18) becomes

$$E = E^0 - \frac{0.0257}{n} \ln K \quad (2.19)$$

or

$$E = E^0 - \frac{0.0592}{n} \log K \quad (2.20)$$

2.5.7 Thermodynamics of electrochemical reactions

From the first law of thermodynamic and some standard thermodynamic reactions, we find

$$dU = TdS - PdV + dw_{\text{electrical}} \quad (2.21)$$

And therefore, the Gibbs function is at the heart of electrochemical

$$dG = TdS - PdV + dw_{\text{electrical}} + PdV - TdS \quad (2.22)$$

All constants P and T , $dP = 0$ and $dT = 0$ and the maximum amount of work is produced by a reversible process ($dq = TdS$), which upon implies

$$dG_{T,P} = dw_{\text{electrical}} \quad (2.23)$$

The free energy function is the key to assess the way in which a chemical system will spontaneously evolve.

$$\Delta G_{T,P} = -w_{\text{electrical}} = -nFE \quad (2.24)$$

Integration of the expressions for the dependence of amount of material on the Gibbs function leads to the following relationship:

$$m = m_0 + RT \ln a \quad (2.25)$$

Same dependence as with the chemical potential,



In order to analyze a chemical process mathematically, we formulate this reaction quotient.

$$K = \frac{a_C^c a_D^d}{a_A^a a_B^b} \quad (2.27)$$

Same dependence as with the chemical potential, we have

$$G = G^0 + RT \ln a \quad (2.28)$$

When we apply this to a reaction, the reaction quotient comes into play, giving us

$$\Delta G = \Delta G^0 + RT \ln K \quad (2.29)$$

When all participants have unit activity ($a=1$), then $K=1$ and $\ln K = 0$.

And
$$\Delta G = \Delta G^0 \quad (2.30)$$

When the reaction is reach to equilibrium state, ΔG is finally zero. Thus, Equation (2.29) can be written as

$$\Delta G^0 = -RT \ln K^* \quad (2.31)$$

This special K^* is renamed K_{eq} , the equilibrium constant.

2.5.8 Faraday's law

The relation of reactant molecules involved in an electrode reaction is related stoichiometrically to number of charges flowing in the process. This is the basic

argument of this laws formulated by Michael Faraday. The most common ideas of the laws are resembled to two statements as the following:

1. The quantities of substance involved in the chemical changes are relative to the quantity of electricity which passes through the electrolyte.
2. The same quantities of electrical charge set free the same number of equivalent of different substance at the electrode.

Faraday's laws can be summarized by

$$m = \left(\frac{Q}{F}\right)\left(\frac{M_w}{n}\right) \quad (2.32)$$

A charge transfer reaction provides an additional channel for current to flow through the interface. The amount of electricity flowing through this channel depends on the amount of species being oxidized or reduced according to the Faraday law. In the simple case of constant-current electrolysis leads to

$$m = \left(\frac{it}{F}\right)\left(\frac{M_w}{n}\right) \quad (2.33)$$

And then to

$$n' = \left(\frac{it}{F}\right)\left(\frac{1}{n}\right) \quad (2.34)$$

2.5.9 Tafel Plots

The overpotential (h') is the difference potential between the working electrode potential and the reversible reaction potential and was related to the current density by Tafel equation (2.35)

$$h' = a + b \log(j) \quad (2.35)$$

From the Nernst equilibrium potential, the term of exchange current density (j_0) has the value of the forward and backward current density at the reversible Nernst potential. Then, the Tafel equation can be written in form of Eq. (2.36)

$$h' = b \log(j - \log j_0) \quad (2.36)$$

The equation (2.36) can be modified by changing the Tafel's constant and b with the expression of $RT/\alpha F$ and rearranged to Eq. (2.37)

$$j = -nFk'C' \exp(-a'h'F/RT) \quad (2.37)$$

From a general point of new electrochemical reaction, the potential-dependent rate equation takes the form of Eq. (2.36) when the potential is disturbed from the equilibrium value.

$$j = nFk'C_{red} \exp(bh'F/RT) - nFk'C_{ox} \exp(-a'h'F/RT) \quad (2.38)$$

A schematic Tafel plot is shown in Figure 2.9. At larger values of the overpotential, one reaction dominates and the polarization curve shows a linear behavior. At low values of the overpotential, both the forward and backward reactions are important to determining the overall current density, and the polarization curve is no longer linear.

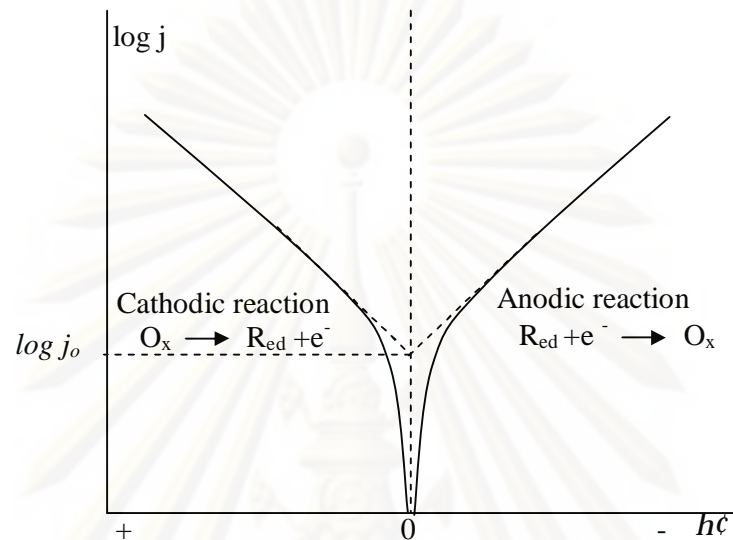


Figure 2.9. Tafel-plot diagrams for the cathodic and anodic process (Bard and Faulkner, 2001).

2.5.10 Electrode kinetics and mass transport phenomena

A charge transfer reaction provides the current to flow through the interface of electrode. The amount of electricity depends on the amount of species being oxidized or reduced according to the Faraday's law.

From Eq. (2.33), it can be rearranged to give the current term.

$$i = nF\left(\frac{N}{t}\right) \quad (2.39)$$

This equation describes average current flowing through the electrode during time and the expression for the instantaneous current is

$$i = nF\left(\frac{dN}{dt}\right) \quad (2.40)$$

Hence faradaic current is a measure of a chemical reaction rate

$$i = nF\left(\frac{dN}{dt}\right) = nFr \quad (2.41)$$

A general scheme of a faradaic process can be summarized in five steps as shown in Figure 2.10. First, the mass transfer of species is diffused from the bulk solution to the surface of electrode. Then, they are adsorbed and generated the chemical reaction (oxidation and reduction) at the surface of electrode. Finally, the mass transfer of species is desorbed and diffuse from the surface of electrode to the bulk solution. The current flowing through the cell is limited by the current corresponding to the slowest reaction step.

The types of faradaic currents consist of charge transfer currents, adsorption currents, kinetic currents and mass transfer currents.

The electron transfer reaction is influenced by the nature and the structure of the reacting species, solvent, potential, adsorbed layers on the surface of electrode and material of electrode.

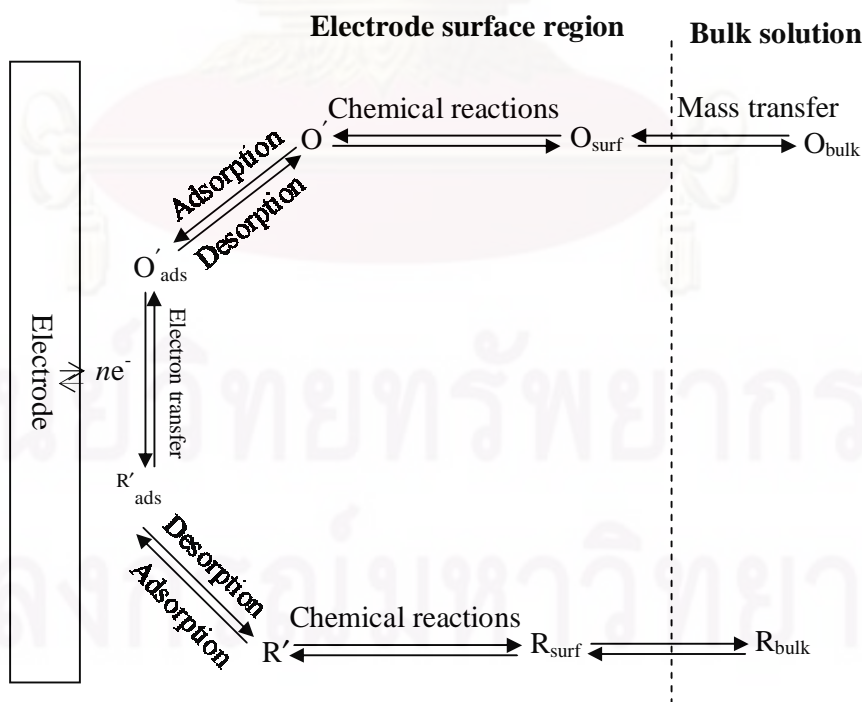


Figure 2.10. General scheme of a faradaic process (Bard and Faulkner, 2001).

Mass transfer to an electrode is governed by the Nernst-Planck equation which is written for one-dimensional mass transfer along the y-axis as

$$J_i = -D_i \frac{\partial C_i(y)}{\partial y} - m_i C_i \frac{\partial f(y)}{\partial y} + C_i n_i \quad (2.42)$$

A schematic representation of a concentration profile of a species reacting on the electrode surface is given in Figure 2.11. The species moving to the electrode surface is determined the thickness of the Nernst diffusion layer (δ_N) and the concentrations of species outside this layer can be assumed to be constant.

The current transport rate is determined by diffusion and Fick's first law according to following equation;

$$i = nFD \left(\frac{C_b - C_s}{d} \right) = nFDk_m (C_b - C_s) \quad (2.43)$$

When $C_s = 0$, the limiting diffusion current density is

$$i_l = nFD(C_b / d_N) = nFDk_m C_b \quad (2.44)$$

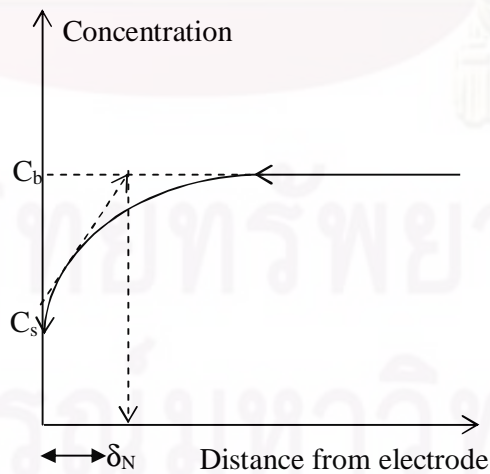


Figure 2.11. Schematic representation of a concentration profile of a species reacting on the electrode surface (Bard and Faulkner, 2001).

2.5.11 Cyclic voltammetry

Cyclic voltammetry (CV) is one of the most accepted techniques to characterize the oxidation and reduction reaction of some compounds and to explain the kinetics of electrode reactions. Generally, an electrochemical cell for cyclic voltammetry measurement contains with three different electrodes including working, reference and counter electrodes. The current flows between the working and counter electrodes. The potential is relatively controlled to the reference electrode. In cyclic voltammetry, the applied current in the cell is measured as a function of potential. During the measurement, the potential of working electrode is linearly cycled from a starting to a final potential and then back to the initial potential. Figure 2.12 shows plot of potential versus current.

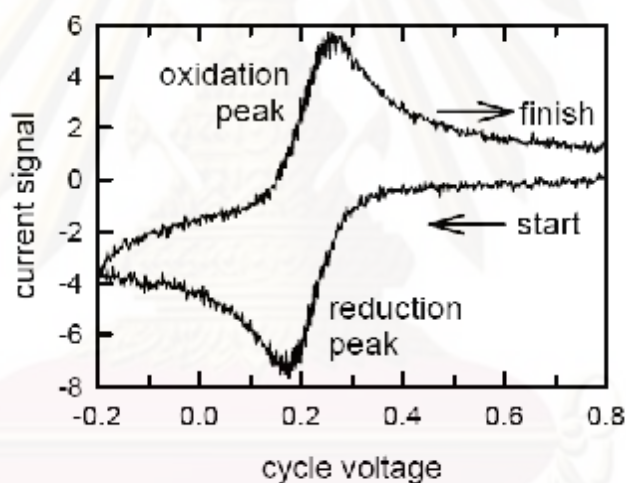


Figure 2.12. The oxidation -reduction peaks from cyclic voltammogram (Cyclic voltammetry, 2004).

Cyclic voltammetry can be used to investigate the chemical reactivity of species. To demonstrate this, let us consider a few possible reactions.

First, we consider the electrochemical reaction



The mass transport equation for this reaction when diffusion transport is dominant is

$$\frac{\partial[O]}{\partial t} = D_0 \left(\frac{\partial^2[O]}{\partial x^2} \right) \quad (2.46)$$

$$\frac{\partial[R]}{\partial t} = D_0 \left(\frac{\partial^2[R]}{\partial x^2} \right) - k_{EC}[R] \quad (2.47)$$

The mass transport equation for (*O*) is identical to the case when no chemical reaction occurs and the species (*R*) has an additional term to account for the fact that it is destroyed chemically by a first order reaction.

It is possible to gain information about the chemical rate constant k_{EC} by studying the reaction via cyclic voltammetry (Figure 2.13).

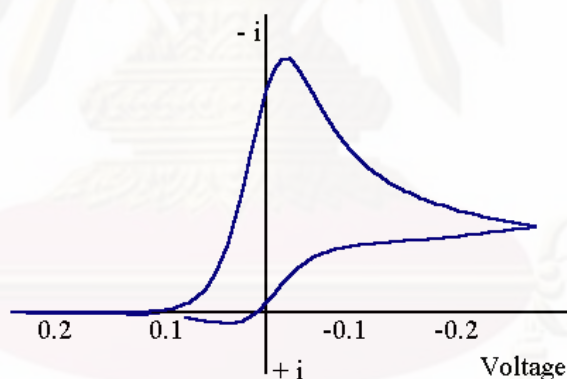


Figure 2.13. Cyclic voltammogram showing reduction and oxidation peaks of one reaction (Cyclic voltammetry, 2004).

Many oxidation and reduction reactions can be occurred as demonstrated in Figure 2.14.



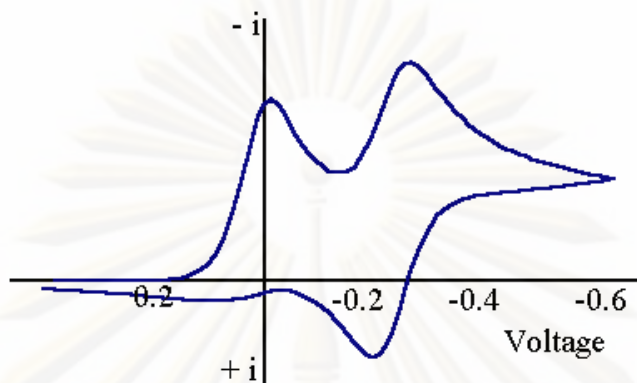
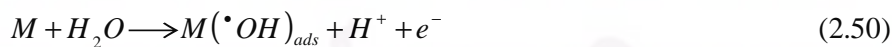


Figure 2.14. Cyclic voltammogram showing reduction and oxidation peaks of many reactions (Cyclic voltammetry, 2004).

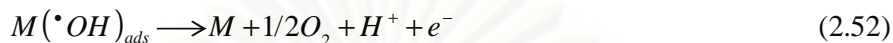
2.6 Application of electrochemical technology for organic reforming

The principle concept of organic reforming by electrochemistry is the generation of strong oxidizing agent in-situ by electricity at ambient temperature and atmospheric pressure conditions (Ciriminna et al, 2006, Piya-areetham et al., 2006 and Macrdonald and Schmuki, 2007). A generalized scheme of the electrochemical oxidation/combustion of organic compounds or organic pollutants on nature of electrode material anode (M_x) is given below.

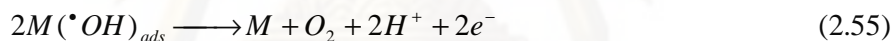
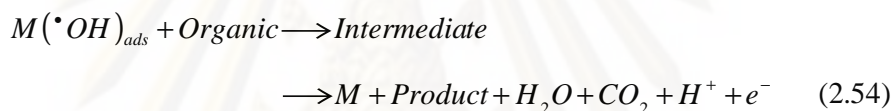
Firstly, H_2O is discharged at the anode to produce adsorbed hydroxyl radical (OH^\bullet) according to the reaction (2.50). Then, the adsorbed OH^\bullet reacts with the anode with possible transition of the oxygen from the adsorbed OH^\bullet to the anode surface, forming the higher oxide MO (reaction (2.51)) (Simod et al., 1997 and Mohan et al., 2007).



In the absence of any oxidizable organics, the active oxygen can dissociate to gas oxygen according to the following reactions;



However, in the presence of oxidizable organics, OH^\bullet will attack the organic substrate and form the stable and/or value end products (reaction 2.54) and the parallel reaction (reaction (2.55)).



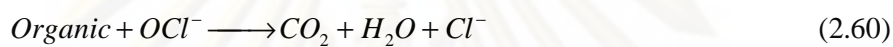
If chloride is presented in the electrolysis, an indirect oxidation via active chlorine can be operative (Rajkumar et al., 2005). In direct electrooxidation, chloride salts of sodium or potassium are added to the electrolyte for better conductivity and generation of hypochlorite. The reaction of anodic oxidation of chloride ions to chlorine is given as



The liberated chlorine form hypochlorous acid (reaction (2.57)) and further dissociated to give hypochlorite ion (reaction (2.58))



The hypochlorite (OCl^-) is collectively often referred to “active chlorine” which can react with the various organic substrates leading to the formation of selective oxidation products or some intermediate species according to reaction (2.59). If the complete oxidation occurs, the final product is CO_2 and H_2O according to reaction (2.60).

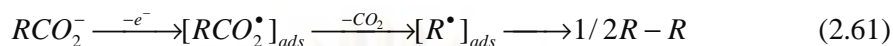


2.7 Electrochemical synthesis (Bard and Stratmann, 2007)

The organic, organometallic and inorganic can be synthesized by electrochemical method. The fundamental of electrochemical rests on the capability of molecules, ions and radicals of chemical substances to react at the surface electrode that facilitates electron transfer. In this regard, electrochemical synthesis is obviously based on the electron from the electricity supplier because it can be added to electron-poor functional groups of organic compounds in order to convert them from electrophiles (E^+) into nucleophiles (Nu^-) or remove from electron-rich functional groups in order to convert them from nucleophiles into electrophiles and is nonpolluting at the level of its use in electrochemical synthesis.

The performance of electrochemical synthesis depends on the parameters such as material of working electrode, type of solvent, applied potential in system, pH of solution and other parameter that need to be examined including cell geometry, reactant concentration and temperature.

The electroorganic synthesis is performed by pioneering works of Michael Faraday, Kolbe, Haber, Fitcher, Tafel and other notable contemporaries who expanded the foundation of organic electrochemical technology. It is the anodic decarboxylation of acetic acid in high concentration, high current density and mild experimental conditions with Pt material of electrode leads to the formation of adsorbed radicals, which dimerize to a corresponding hydrocarbon (Eq. (2.61))



The electroorganic synthesis can provide value-added products of organic compound and environmentally friendly contributions to industrial process development and waste of organic compound.

2.7.1 Main reactions of organic electrochemistry

Figure 2.15 summarizes the principal reactions achievable of organic electrochemistry. In particular, the electrolysis of organic substrates (molecules or ions) in aprotic polar solvents provides new form of organic compounds with electron transfer activation. It consists of nucleophiles such as radical anions and cations, electrophiles such as radical anions and anions, and free radicals by means of oxidation of anions or scission of radical.

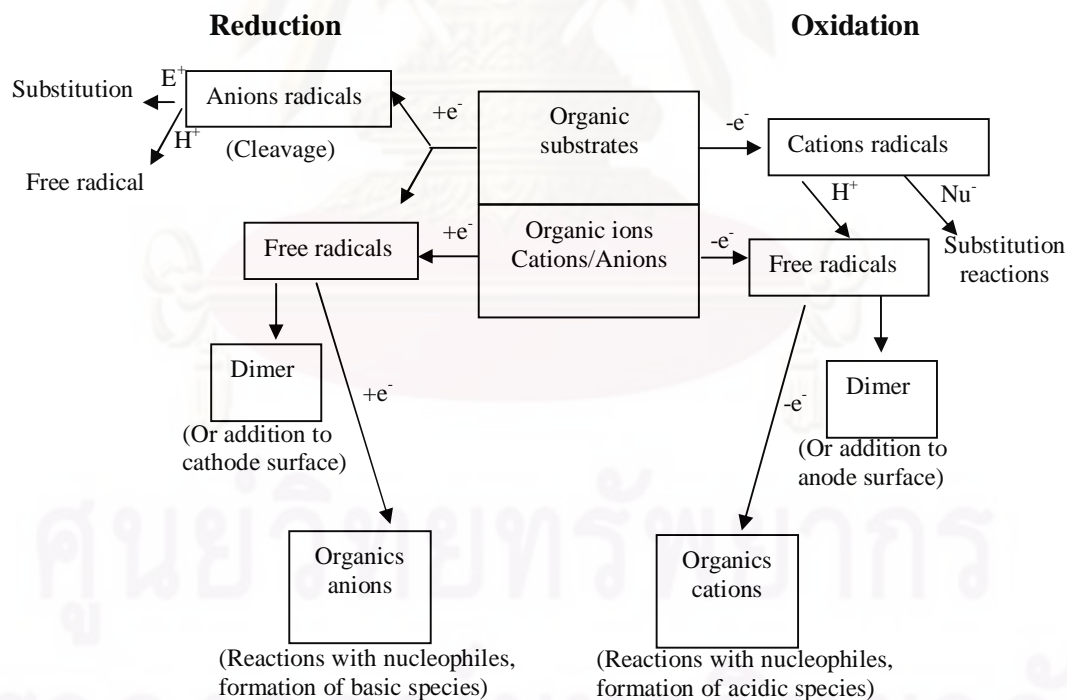


Figure 2.15. Principal reactions of organic electrochemistry (Bard and Stratmann, 2007).

2.7.2 Reaction mechanisms, kinetics and thermodynamics

In electrochemical studies of organic compounds, one-electron bond cleavages can be seen as a potential source of free radicals such as alkyl and aryl radicals. Therefore this might be utilized in radical chemistry. The electron transfer follows a stepwise mechanism and can be described by the Savéant's theory when the initial electron transfer step is the rate-determining step which demonstrates in Figure 2.16.

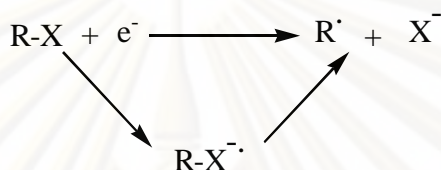


Figure 2.16. The dissociative electron transfer or Savéant's Theory (Bard and Stratmann, 2007).

2.7.3 Electron transfer mechanism

Both thermodynamic and kinetic factors are involved in the competition between concerted and stepwise mechanisms as shown in Figure 2.17. When the splitting of ion-radical becomes faster, the passage from the stepwise to the concerted mechanism is expected to arise. Under these conditions, the rate-determining step of the stepwise process becomes the initial electron transfer. Then thermodynamics will favor the mechanism according to Eq. (2.62)

$$\Delta G_{RX+e \rightarrow R+X^\cdot}^0 = D_{R-X} - E_{RX/R^\cdot+X^-}^0 + E_{RX/RX^{\cdot-}}^0 - T\Delta S_{RX+e \rightarrow R^\cdot+X^-} \quad (2.62)$$

Thus, as the driving force for cleaving the ion-radical, the passage from the stepwise to the concerted mechanism becomes larger and larger.

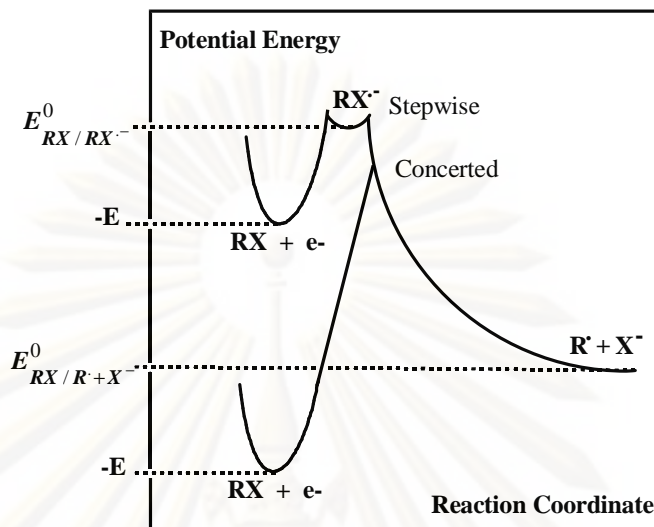


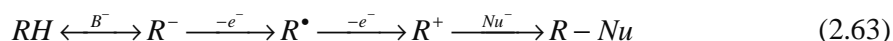
Figure 2.17. Passage from the stepwise to the concerted mechanism upon decreasing the driving force (Grimshaw, 2000).

A weak RX bond, a negative value of $E^0_{RX/RX^{\cdot-}}$ and a positive value of $E^0_{RX/R'+X^-}$ will favor the concerted mechanism and vice versa. All three factors may vary from one molecule (RX) to another. However, there are families of compounds where the passage from one mechanism to the other is mainly driven by one of them. (Grimshaw, 2000).

2.7.4 Electrochemical reforming of alkane compounds

Alkanes are easily oxidized with carbanions in acidic solvents such as trifluoroacetic acid and fluorosulphuric acid. The anode material may be platinum, vitreous carbon, graphite, and titanium oxide.

The first stage of these reactions involves the removal of an electron from either a carbon-hydrogen or a carbon-carbon π -bond, with simultaneous bond cleavage to yield the most stable carbon radical and carbonium anion (Reaction 2.63). These are dissociative processes where the radical cation cannot be detected as an intermediate.



For the electrochemical reforming of alkane to acetonitrile, carbon ions will combine with the solvent to form a nitrilium ion and reacts with water to form the N-substituted acetamide as shown in Figure 2.18.

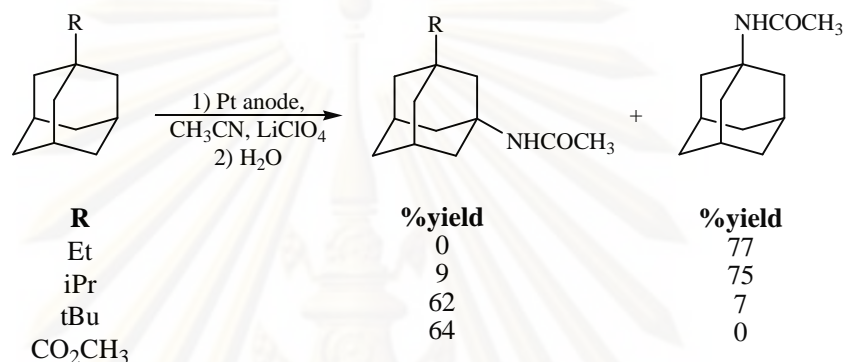


Figure 2.18. Electrochemical reforming of alkane compounds (Bard and Stratmann, 2007).

2.7.5 Electrochemical reforming of alkene compounds

Alkenes are electrochemically reformed in nucleophilic solvents such as alcohols, acetic acid or acetonitrile using an undivided cell. Figure 2.19 shows the electrochemical reforming of alkene compounds. The alkene molecule reacts with the nucleophile to form a radical intermediate, which is then oxidized to the carbonium ion at less positive potential.

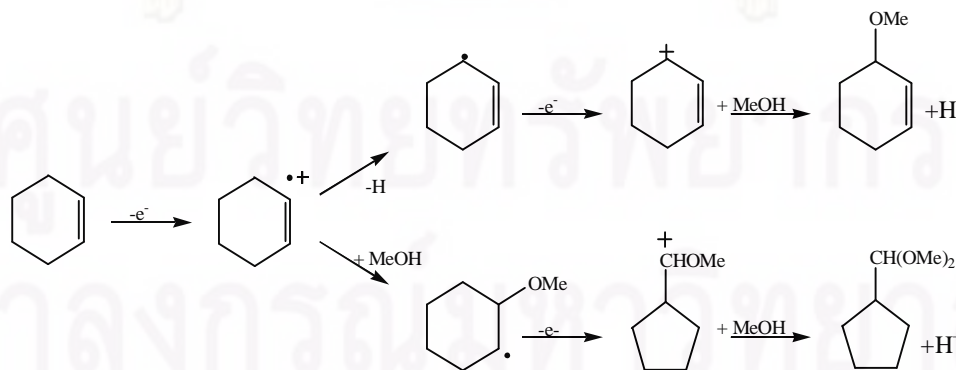


Figure 2.19. Electrochemical reforming of alkene compounds (Bard and Stratmann, 2007).

2.7.6 Electrochemical reforming of alcohol and ester compounds

The direct reform of alcohols is carried out in absence of solvents or in acetonitrile and in the presence of perchlorates or tetrafluoroborates as supporting electrolytes. Depending on the structures of the alcohols and the electrolytic systems, the electrochemical reforming of alcohols may lead to the formation of aldehydes, acetals acids and esters as shown in Figures 2.20 and 2.21.

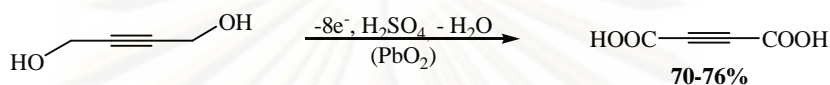


Figure 2.20. Electrochemical reforming of alcohol compounds (Bard and Stratmann, 2007).

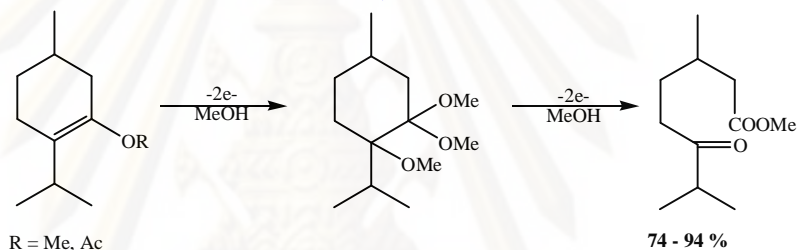


Figure 2.21. Electrochemical reforming of ester compounds (Bard and Stratmann, 2007).

2.7.7 Electrochemical reforming of amine compounds

The aliphatic amines have relatively low oxidation potentials. The course of oxidation depends on the structure of amine on the anode material and the composition of electrolyte. For example, the amidoalkylation of α -methoxyamides and α -carbamates generated the iminium ions as intermediates in acid condition. Then, they can be sufficiently reacted with nucleophilic substrates such as aromates, alkenes and other to produce the electrophilic substitution as shown in Figure 2.21.

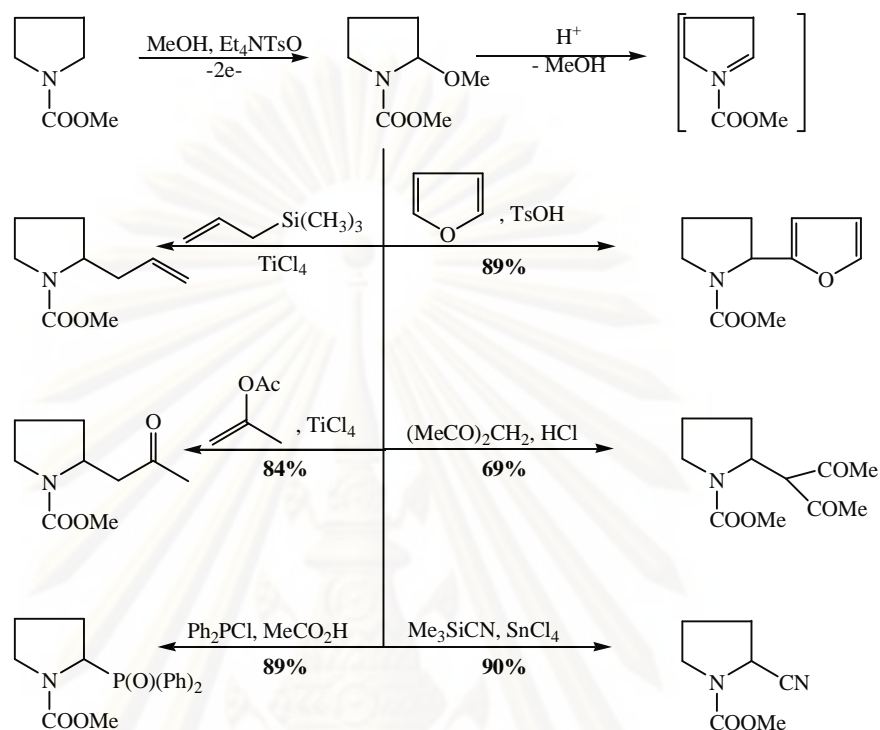


Figure 2.22. Electrochemical reforming of amine compounds (Grimshaw, 2000).

2.7.8 Electrochemical reforming of aromatic compounds

Simple aromatic compounds such as benzene, naphthalene, toluene, xylene have relatively very positive oxidation potentials. A radical cation is usually formed which, in general, dimerizes (Figure 2.23) or reacts with a nucleophile to yield a substitution product (Figure 2.24).

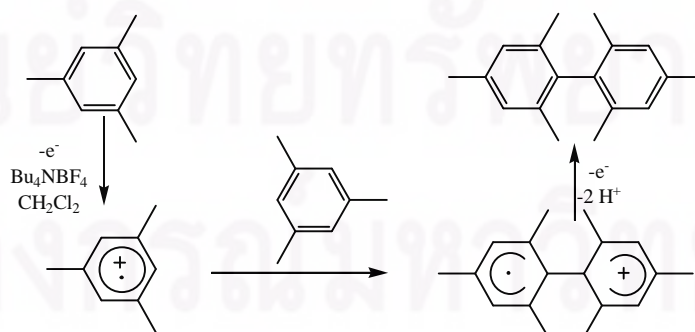


Figure 2.23. Electrochemical reforming of aromatic compounds with nucleophilic (Grimshaw, 2000).

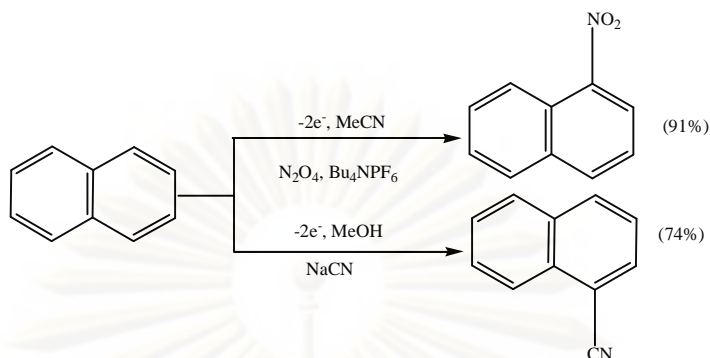


Figure 2.24. Electrochemical reforming of aromatic compounds (Grimshaw, 2000).

2.7.9 Electrochemical reforming of sulfur and selenium compounds

Figure 2.25 shows the anodic reforming of thiols and dialkyl or diaryl sulfides to prepare sulfur compounds at different degrees of oxidation. It is influenced by potential, electrode material such as carbon, platinum, stainless steel and composition of electrolyte.

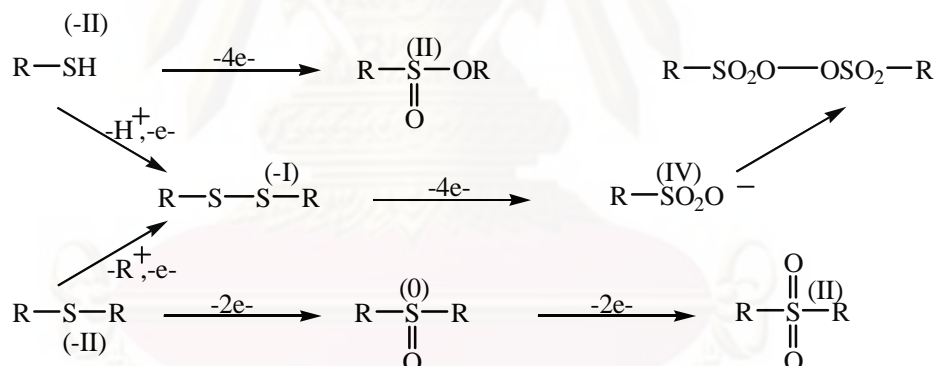


Figure 2.25. Electrochemical reforming of sulfur and selenium compounds (Grimshaw, 2000).

2.7.10 Electrochemical reforming of functional group at cathode electrode

Hydrogenation double bonds of C-C can proceed by a direct electron transfer to the single bond. This reaction can proceed with good selectivity as shown in Figure 2.26.

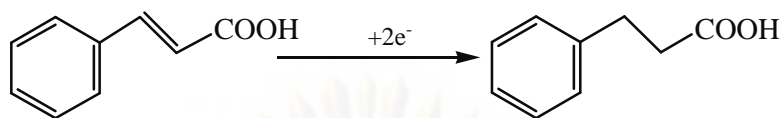


Figure 2.27. Electrochemical reduction of alkene compounds (Grimshaw, 2000).

Electrochemical reforming of nitroaromatic to amines can be obtained with the reduction of nitroaromatics. It carries a group in the para-position which prevents a rearrangement (Figure 2.27).

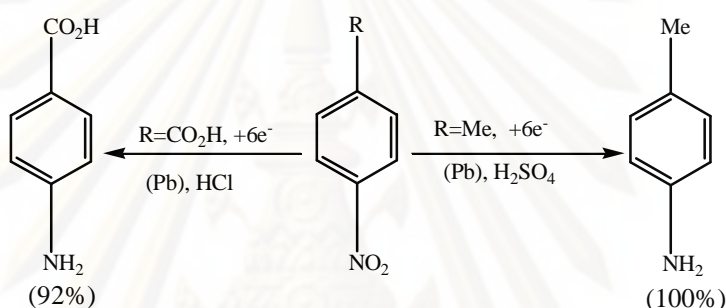


Figure 2.28. Electrochemical reduction of nitroaromatic compounds (Grimshaw, 2000).

2.8 Literature reviews

In the past, some microorganisms such as *K. pneumoniae*, *E. agglomerans*, *C. freundii*, *C. butylicum*, *C. pasteurianum*, *L. brevis* and *L. buchneri* were used to produce 1,3-propanediol (Zeng et al., 1993).

Menzel et al., (1997) attempted to synthesize 1,3-propanediol in continuous culture of *K. pneumoniae*. The reactor was agitated at 300 rpm and purged with N_2 at a flow rate of 0.4 volume of air per volume of liquid per minute (vvm). The pH was controlled at 7.0 by the addition of 30% KOH and the culture temperature was around 37°C . A glycerol solution of 870 g/l was separately fed to the medium reservoir instead of to the bioreactor according to the normalized concentration required in the feeding medium. The continuous culture provided the relatively high productivities (4.9 - 8.8 g/l-h with 1,3-propanediol concentrations of 35.2 - 48.5 g/l) at low dilution rates.

Himmi et al., (1999) produced 1,3-propanediol from glycerol and industrial glycerin in batch fermentation with a low-nutrient medium (LNM) based on biotin by *C. Butyricum*. The culture inoculum was consisted of 11 (6%vol) of pH-controlled inoculum culture using industrial glycerin equivalent to 50 g/l of pure glycerol. It was shown that the optimized biotin and glycerol as carbon sources were 4 $\mu\text{g/l}$ and 129 g/l of glycerol or 121 g/l of industrial glycerol, respectively can be produced 1,3-propanediol at about 67 and 65 g/l, respectively

Papanikolaou et al., (2000) attempted to produce 1,3-propanediol by *C. butyricum* strain by using industrial glycerol as a carbon source and compared the obtained yield between batch and continuous systems. Batch and single-stage continuous cultures were conducted in a 2 l reactor filled with 0.9 l of medium and inoculated with 0.1l of preculture. The agitation speed was 200 rpm and the pH was adjusted to 7 ± 0.05 by automatic addition of 2 M KOH and N_2 at a rate of 0.5 vvm into the culture. The incubation temperature was 33°C . For both types of cultures, the obtained conversion yield was around 0.55 g of 1,3-propanediol per 1 g of glycerol consumed whereas the highest 1,3-propanediol concentration, achieved during the single-stage continuous cultures, was 35 - 48 g/l. A two-stage continuous fermentation was also carried out. The first stage presented high 1,3-propanediol volumetric productivity, whereas the second stage (with a lower dilution rate) served to further increase the final product concentration. High 1,3-propanediol concentration was achieved (41 - 46 g/l) with a maximum volumetric productivity of 3.4 g/l.h.

Wang et al., (2001) studied the conversion of glycerol solution to 1,3-propanediol by fermentation process under anaerobic and microaerobic conditions in batch and continuous systems. The 1,3-propanediol conversion rates of both processes were similar, but the productivity of 1,3-propanediol under microaerobic condition was higher than that under anaerobic condition. In the continuous culture at a dilution rate of 0.1 h^{-1} and glycerin limitation, both yield and productivity of 1,3-propanediol under 5 microaerobic condition were higher than that under anaerobic condition.

Chen et al., (2003) studied the glycerol conversion to 1,3-propanediol in batch cultures by *K. pneumoniae*. They showed that a microaerobic condition was better for production of 1,3-propanediol from glycerol than anaerobic and aerobic conditions.

The maximum theoretical yield of 1,3-propanediol to glycerol could reach to 0.85 M if all acetyl-CoA entered into molecular oxygen in tricarboxylic acid cycle (δ) instead of acetic acid pathway under anaerobic conditions. The yield of 1,3-propanediol was still high in a range of δ between 0.11 and 0.48. In addition, aeration could not improve the yield of 1,3-propanediol by an anaerobic or aerobic culture.

Xiu et al., (2003) synthesized 1,3-propanediol in batch culture of *K. pneumoniae* by using biomass and glucose as a co-substrate of a carbon source to compare the results with glycerol fermentation without co-substrate. The experimental results of batch cultures demonstrated that the biomass concentration and yield of 1,3-propanediol could be enhanced by using glucose as a co-substrate. The maximum ratio of 0.32 mol glucose per mol glycerol was needed to convert glycerol completely to 1,3-propanediol under anaerobic conditions. The minimum ratio of glucose to glycerol could reach to 0.11 mol glucose per mol glycerol. The batch co-fermentation of glucose and glycerol showed that the yield of 1,3-propanediol on glycerol and biomass concentration increased as compared with glycerol fermentation.

Xiu et al., (2004) reported the best condition of glycerol conversion to 1,3-propanediol in batch and continuous fermentations by *K. pneumoniae* was based on the growth kinetics of multiple inhibitions, the metabolic overflow of substrate consumption and product formation. In the batch culture with 0.1g of biomass/l, the optimal initial glycerol concentration was found to be 0.96 M, which led to the highest of 1,3-propanediol about 0.0526 M/h. For continuous fermentations, the optimal dilution rate and initial glycerol concentration in feed were 0.29 h⁻¹ and 0.731 M, respectively. The productivity was 0.114 M/h, twice times higher than the productivity of an optimal batch culture. They proposed two-stage continuous process in which the first stage was operated at the optimal conditions and the second one was used to consume the residual glycerol in the first one. The dilution rate was higher in the second stage than in the first one. A two-step bioprocess of two bioreactors in series appeared to be more favorable than a single bioreactor system with the same volume in terms of the concentration, yield and productivity of 1,3-propanediol.

Chen et al., (2004) examined different carbon sources, organic nutrients, nitrogen sources and salts on key enzymes formation for fermentation process. They reported that at optimum conditions (37°C, pH of 7, shaker speed of 200 rpm, 30 g/l

glycerol, 1.6 g/l KCl, 6.7 g/l NH₄Cl, 0.28 g/l CaCl₂, and yeast extract 2.8 g/l), the appearance of maximum activities of key enzymes was earlier than that of maximum concentration of 1,3-propanediol.

González-Pajuelo et al., (2005) produced 1,3-propanediol in fed-batch cultured by *C. acetobutylicum* and *C. butyricum*. The fed-batch cultures were performed in a 2 l bioreactor Biostat MD with a working volume of 1.250 l. Cultures were stirred at 200 rpm and the temperature of 35 °C. The pH of system was maintained constant by automatic addition of NH₄OH 6 M. To create anaerobic conditions, the sterilized medium in the vessels was flushed with sterile O₂-free nitrogen until room temperature was attained. It was found that 1,3-propanediol concentration could be increased up to 1.104 M when *C. acetobutylicum* DG1 (pSPD5) was grown in fed-batch cultures. The maximum 1,3-propanediol concentration achieved in fed-batch cultures of *C. butyricum* VPI 3266 was 0.854 M.

Hongwen et al., (2005) studied the effect of key enzymes, such as glycerol dehydrogenase (GDH), 1,3-propanediol oxidoreductase (PDOR) and glycerol dehydratase (GDHt), to produce 1,3-propanediol by using *K. pneumoniae* in batch fermentation process. The results were found that the carbon sources, organic nutrients, nitrogen and salts were examined for their effects on key enzymes formation. The maximum activities of GDH, PDOR and GDHt were 3700, 3840 and 8.70 μmol/min per liter of fermentation broth (U/l) after 20 h cultivation, which provided the maximum concentration of 1,3-PD of about 10.5 g/l.

Lin et al., (2005) enhanced the rate of glycerol consumption and the production of 1,3-propanediol by *K. pneumoniae* by the addition of fumarate. The initial glycerol concentration of 20 g/l and fumarate was added in the range of 0- 25 mM. The fermentation was carried out for 4 h. It was found that the cell grew faster with the addition of adding fumarate. They proposed two reasons for this increase. First, fumarate addition may speed up the metabolic activities of the key enzymes in the metabolic pathways of 1,3-propanediol production. Second, the NAD⁺/NADH ratio was decreased by fumarate addition, which reduced a power for converting 3-hydroxypropionaldehyde into 1,3-propanediol.

Zhang et al., (2007) synthesized 1,3-propanediol in fed-batch cultured by *K. pneumoniae* XJ-Li using glycerol. The optimal cultivation parameters for pH and

temperature were determined as 8.0 and 40°C, respectively. A higher molar yield of 0.70 was also achieved in fed-batch fermentation, and 38.1 g/l of 1,3-propanediol was produced by consuming glycerol with a concentration of 66.4 g/l during 48 h of fermentation.

Zheng et al., (2008) attempted to synthesize 1,3-propanediol in batch culture of *K. pneumoniae* AC 15. The optimum cultivation parameters for rate of stirring, air aeration, and pH were determined as 318 rpm, 0.6 vvm and 6.48, respectively. The optimized nitrogen and carbon sources were 6.0 g/l of $(\text{NH}_4)_2\text{SO}_4$ and 50 g/l of glycerol, respectively. The subsequent fed batch experiments produced 1,3-propanediol of 70 g/l at a fermentation of 30 h. In 2009, Zheng et al studied scaled up from 5 to 50,000 l in batch culture for synthesize 1,3-propanediol from glycerol by *K. pneumoniae* CGMCC 1.6366 under aerobic condition. It was found that the fermentation in 500 l bioreactor produced 1,3-propanediol about 66.8 g (0.5 mol/mol) at agitation rate of 130 rpm and air flow of 0.14 vvm. The final concentrations of 1,3-propanediol in 5000 and 50,000 l bioreactor amounted to 66.1 and 63.3 g/l with the yield of 0.52 and 0.5 mol/mol, respectively.

The direct hydrogenolysis of glycerol to 1,3-propanediol was particularly interesting because it may be produced in organic solvents and in one step reaction. Besson et al., (2003) studied the catalytic hydrogenation of aqueous 3-hydroxypropanal solution to 1,3-propanediol at 40 - 60°C and 40 bar H_2 pressure with heterogeneous Ru catalysts in a trickle-bed reactor. Catalysts were optimized to obtain stable activity and selectivity as a function of time on stream. The reported that catalyst deactivation was attributed to the deposit of heavy organic impurities on the surface of catalyst

Kurosaka et al., (2008) attempted to examine the hydrogenolysis of glycerol in the presence of solid acids (tungsten oxide and noble metals) by using 1,3-dimethyl - 2-imidazolidinone (DMI) as a solvent. Yield of 1,3-propanediol obtained from glycerol hydrogenolysis in the presence of $\text{Pt}/\text{WO}_3/\text{ZrO}_2$ was up to 24%. The catalytic activities and the selectivity toward 1,3-propanediol were remarkably affected by the type of support, loaded noble metal and the preparation/impregnation procedure.

Leifeng et al., (2009) studied the effect of different protic solvents such as ethanol and water for dehydroxylation of glycerol reforming to 1,3-propanediol over a Pt/WO₃/ZrO₂ catalyst. The binary solvents, such as 1,3-dimethyl -2-imidazolidinone (DMI)-water, ethanol-water, and DMI-ethanol mixtures which was showed a synergetic solvent effect on the selectivity and the percent yield of 1,3-propanediol. It was found that ethanol and the binary solvents containing ethanol gave a higher glycerol conversion than those without ethanol. The water content in the DMI-water binary solvent influenced the performance of the Pt/WO₃/ZrO₂ catalyst for glycerol reforming to 1,3-propanediol.

The low-grade glycerol obtained from biodiesel production can be applied. For example, Cerrate et al., (2006) used low-grade glycerol obtained from biodiesel production as a pure energy source for feeding to broiler diets. It was found that low-grade glycerol obtained from biodiesel production can be effectively used in broiler diets as level of 2.5 or 5% low-grade glycerol. However, low-grade glycerol content about 10% was reduced performance with feeds flow and had highly related to problems with feed flow.

Lammers et al., (2008) studied supplementing the diet of growing pigs with crude glycerol. It was found that the metabolizable to digestible energy ratio of glycerol was similar to corn or soybean oil when fed to pigs. They concluded that crude glycerol can be used as an excellent source of energy for growing pigs, but also cautions that little was known about what the impacts of impurities in the glycerol may be.

Sbourin-Provost and Hallenbeck (2009) attempted to synthesize H₂ from crude glycerol from biodiesel production in batch culture of the photosynthetic bacterium *R. palustris*. The results found that yields of H₂ obtained with the crude glycerol were up to 6 molH₂/glycerol, which is 75% of theoretical. The yield of H₂ was nearly or only slightly lower than the pure compound. Addition of nitrogen appears to be useful in improving yields and can also control rates.

CHAPTER III

METHODOLOGY

This chapter shows the details about the experimental set up for studying the polarization curve of synthetic glycerol, crude glycerol and the purified crude glycerol from biodiesel plant. Descriptions of electrochemical reactor and experimental set up, utilized chemical substances and experimental procedure were described here.

3.1 Experimental set up of polarization curve

The possibility of reduction - oxidation reaction of glycerol solution was investigated with the Potentiostat/Galvanostat apparatus (Auto Lab, model PG stato). Measurement was carried out in the electrolytic cell containing a Ag/AgCl reference. The platinum sheet and platinum rod were used as counter and working electrodes, respectively. Prior to perform each experiment, nitrogen gas was purged through the electrolyte for 20 min to decrease the oxygen content in the electrolyte. The measurement was performed at room temperature at constant stirring rate of 400 rpm. The scan potential was varied from +2.50 to -2.50 V/Ag/AgCl with a scan rate of 5 mV/s. The final pH of all investigated solutions was adjusted to a final value of around pH 1 - 12 with conc. of H_2SO_4 or 1.0 M NaOH.

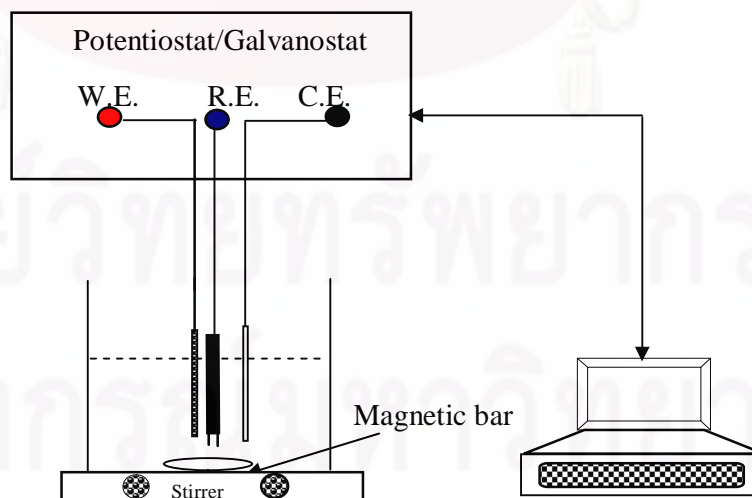


Figure 3.1. Schematic diagram of apparatus for current density-potential studies.

3.2 Electrochemical reactor

Figure 3.2 shows the experimental set up of electrochemical reactor. The system was composed of the following equipments

- Electrochemical reactor made from Pyrex glass having a total capacity of 0.5 l
- Regulated DC power supply: type ZS 3205-2X (0 – 32 VDC; 0 – 10 A)
- Magnetic bar
- Cooling system
- Cathode: Pt grid in cylindrical shape having a total surface area of 124.34 cm²
- Anode: Pt grid, Ti/RuO₂ grid and graphite sheet having a total surface area of 66.49 cm²

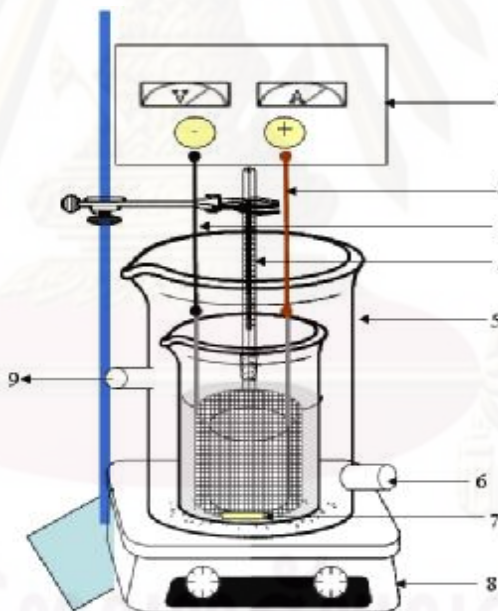


Figure 3.2. Schematic diagram of experiment set up: (1) DC power supply, (2) anode, (3) cathode, (4) thermometer, (5) electrochemical reactor, (6) cooling water inlet, (7) magnetic bar, (8) magnetic stirrer and (9) cooling water outlet.

3.3 Chemical substances

The synthetic glycerol solution and other chemical substances were prepared from the following reagents:

- Ammonia solution (NH_4OH) (99.9 % purity, Merck)
- Ammonium peroxydisulfate ($(\text{NH}_4)_2\text{S}_2\text{O}_8$) (99.5% purity, Ajex Finechem)
- Ethanol ($\text{C}_2\text{H}_5\text{OH}$) (99.9 % purity, Merck)
- Glycerol ($\text{C}_3\text{H}_8\text{O}_3$) (99.5% purity, Fisher)
- Hydrogen peroxide (H_2O_2) (30% purity, Merck)
- Methanol (CH_3OH) (99.9 % purity, Fisher)
- n-Hexane ($\text{n-C}_6\text{H}_{14}$) (99% purity, Fisher)
- Phosphoric acid (H_3PO_4) (98% purity, Mallinckrodt)
- Potassium hydroxide (KOH) (97% purity, Ajex Finechem)
- Potassium permanganate (KMnO_4) (98% purity, Carlo Erba)
- Silver sulfate (Ag_2SO_4) (99% purity, Fisher)
- Sodium chloride (NaCl) (99% purity, Lab scan)
- Sodium hydroxide (NaOH) (97% purity, Carlo Erba)
- Sodium sulfate (Na_2SO_4) (99.5% purity, Rankem)
- Sulphuric acid (H_2SO_4) (98% purity, Mallinckrodt)
- 1,2-propanediol ($\text{C}_3\text{H}_8\text{O}_2$) (99.8% purity, Fluka)
- 1,3-propanediol ($\text{C}_3\text{H}_8\text{O}_2$) (99.8% purity, Fluka)
- 2,4-dinitrophenylhydrazine ($\text{C}_6\text{H}_3(\text{NO}_2)_2\text{NHNH}_2$) (99% purity, Mallinckrodt)

3.4 Experimental set up for glycerol reforming

The experimental of glycerol reforming was separated into three parts. The first part was electrochemical reforming of synthetic glycerol. The second part was the purification of crude glycerol from biodiesel plant and the last part was the electrochemical reforming of the purified crude glycerol.

3.4.1 Electrochemical reforming of synthetic glycerol

The reforming of synthetic glycerol to 1,3-propanediol by electrochemical technique was carried out in electrochemical reactor (Figure 3.2) at ambient temperature (around 30°C). The investigated parameters were

- Type of anode: Pt, Ti/ RuO_2 and graphite material
- Type of acid: conc. H_2SO_4 and H_3PO_4
- Current intensity: 3 - 5 A
- Initial pH of glycerol solution: 0.5 - 4

- Type of additives: NaCl, Na₂SO₄ and (NH₄)₂S₂O₈

- Concentration of NaCl: 0 - 8.78 g/l

3.4.2 Purification of crude glycerol from biodiesel plant

Crude glycerol, the by product from biodiesel plant via the alkali mediated transesterification process, was used in this work. The purification of crude glycerol was carried out by chemical treatment shown in Figure 3.3.

There were two routes for glycerol-rich layer purifying. For the first route, the pH of crude glycerol was adjusted to 1, 2.2, 3.5 and 6 by the addition of 1.19 M H₂SO₄ or H₃PO₄, and then left for 3 h. The original crude glycerol automatically phase separated into four distinct layers during the purification stage. The upper layer was free fatty acid, the second layer was char and soap layer, the third layer was glycerol-rich layer and the bottom layer was alkaline-catalyst. The alkaline-catalyst, the free fatty acid and char were removed from glycerol-rich layer by gravitational decantation. The glycerol-rich layer was neutralized with 12.50 M NaOH or KOH followed by filtration to eliminate the precipitated salt and evaporated at 105°C to eliminate the residual water. The enriched glycerol solution was then extracted with excess C₂H₅OH to encourage the precipitation of the salts, harvesting the glycerol-ethanol solution and filtered again to eliminate the crystallized salt. The purified crude glycerol was then obtained after evaporation of the C₂H₅OH at 80°C. After that, it was extracted by n-C₆H₁₄, and then left until it was separated into two phases. The contaminants in glycerol were dissolved to n-C₆H₁₄ as upper phase. So, the glycerol phase was separated by gravitational decantation. Finally, the purified crude glycerol was then obtained after evaporation of the remained n-C₆H₁₄ at 60°C.

For the second route, the pH of crude glycerol was adjusted to 2.2 by the addition of 1.19 M H₃PO₄, and then left for 3 h for phase-separation. The glycerol-rich layer was extracted by n-C₆H₁₄, and then left until it was separated into two phases. After that, the glycerol-rich layer was neutralized with 12.50 M KOH followed by filtration to eliminate the precipitated salt and evaporated at 105 °C to eliminate the residual water. The enriched glycerol was then extracted with excess C₂H₅OH. At last, the purified crude glycerol was then obtained after evaporation of the remained C₂H₅OH at 80°C.

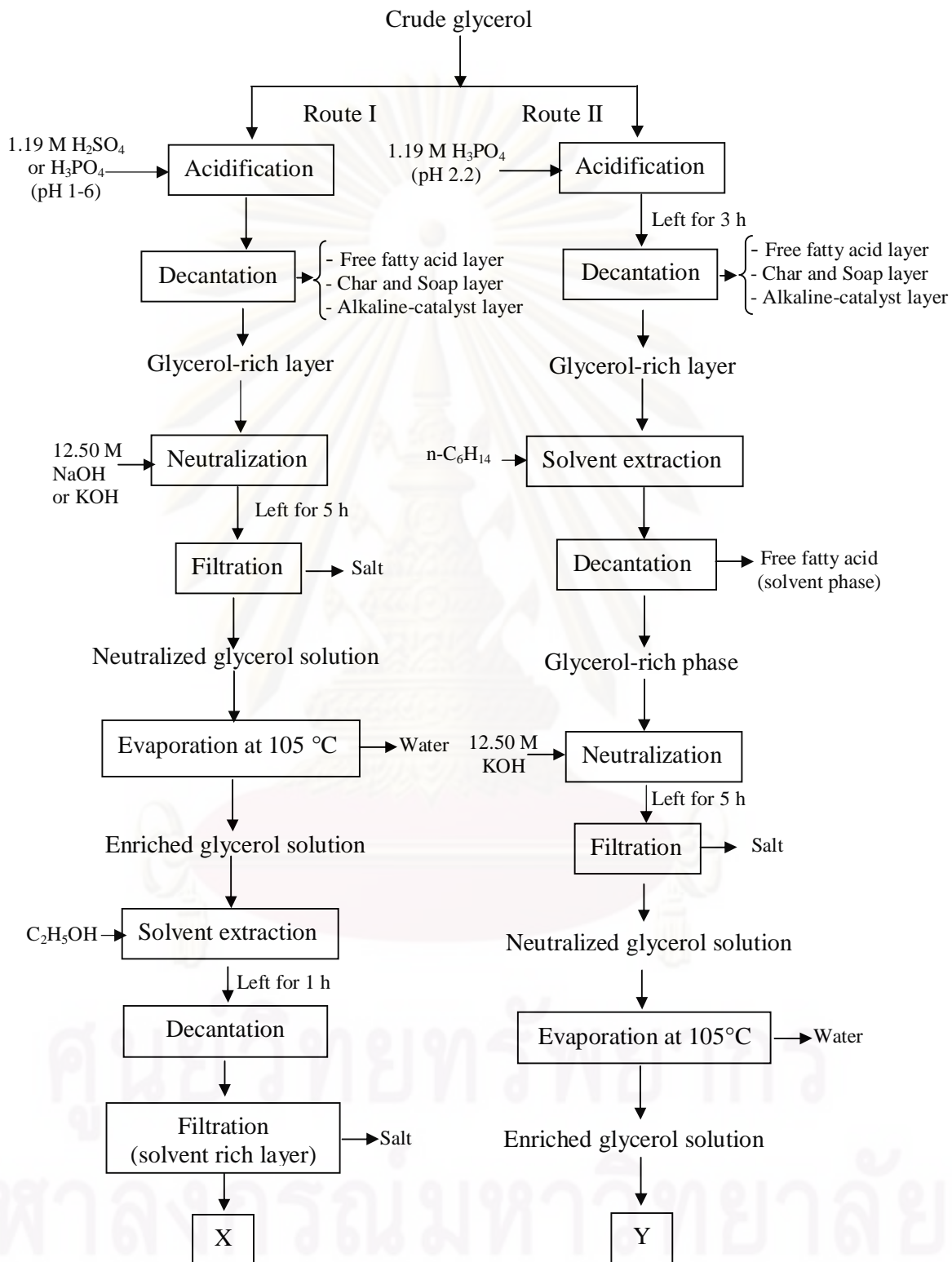


Figure 3.3. Schematic diagram of the chemical treatment of crude glycerol obtained from biodiesel production.

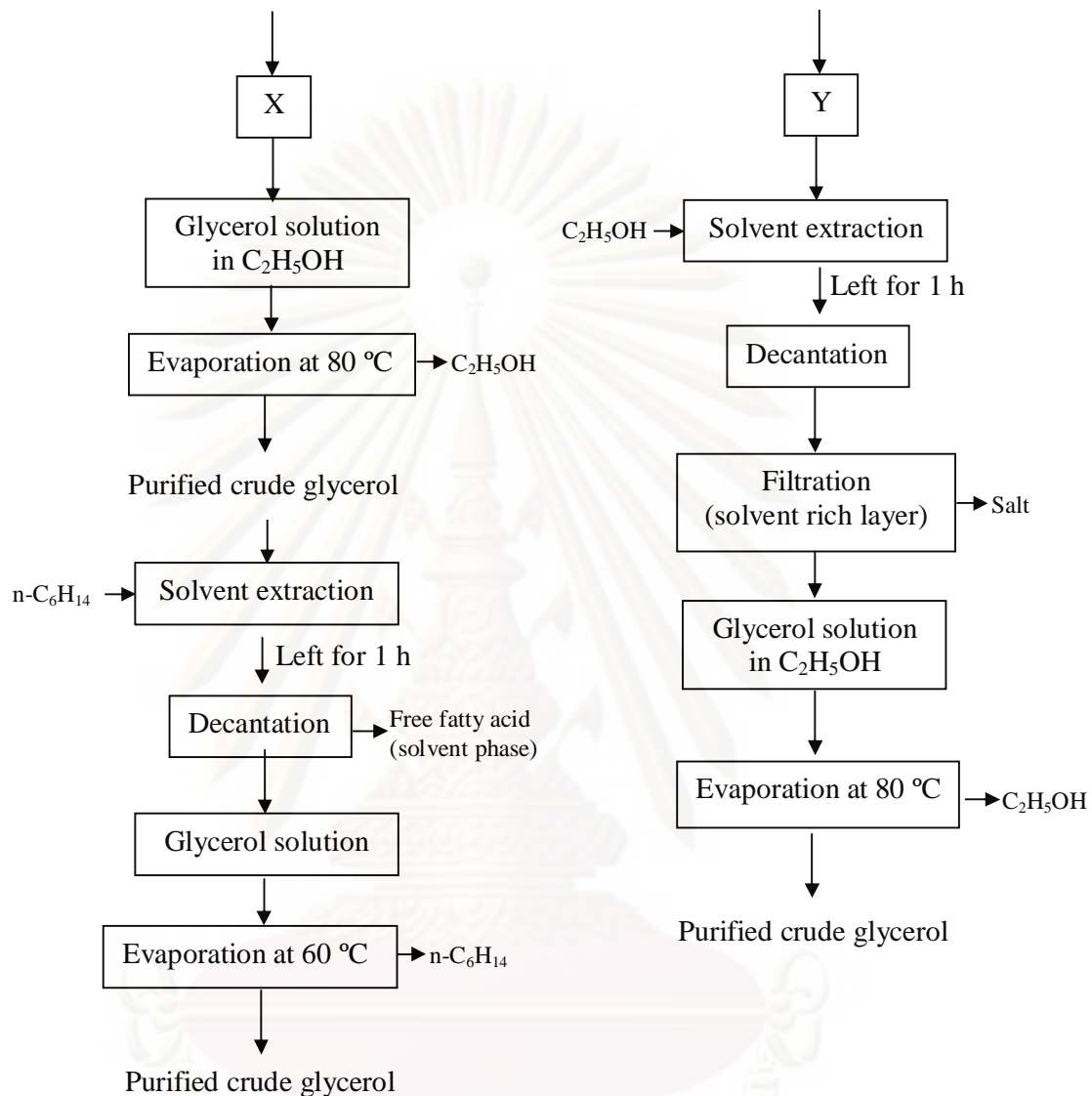


Figure 3.3. Schematic diagram of the chemical treatment crude glycerol obtained from biodiesel production (*cont.*).

The properties of purified crude glycerol were analyzed in terms of glycerol, ash, water and matter organic non glycerol (MOMG) contents according to the ISO standards (Appendix B). The structure, composition and functional groups of purified crude glycerol were analyzed by FTIR, GC/MS and ^{13}C -NMR.

3.4.3 Electrochemical reforming of purified crude glycerol

The reforming of purified crude glycerol to 1,3-propanediol by electrochemical technique was carried out in electrochemical reactor (Figure 3.2) at ambient temperature (around 30°C). Two Pt grids in cylindrical shape having a total surface area of 66.49 and 124.34 cm² were used as the anode and cathode, respectively. The concentration of glycerol prepared from purified crude glycerol was of 46.2 g/l at the initial pH of 1 with conc. H₂SO₄. The investigated parameters were

- Current intensity: 3.75 - 6.5 A
- Concentration of NaCl: 0 - 8.78 g/l

3.5 Characterization

3.5.1 High performance liquid chromatography

The concentration of glycerol and 1,3-propanediol was analyzed at particular time by high performance liquid chromatography (Shimadzu LC-10ADvp) equipped with a RID-10A refractive index detector (Figure 3.4). The stationary phase was a Pinnacle II C18 column (240 x 4.6 mm) and the mobile phase was a 96.7: 3.3 (v/v) ratio of 5 mM H₂SO₄ with pure methanol at flow rate of 0.7 ml/min. The column temperature was controlled at 40 °C.



Figure 3.4. High performance liquid chromatography (HPLC).

3.5.2 Fourier transform infrared spectroscopy

For the FTIR analysis (Figure 3.5), the functional groups of glycerol, crude glycerol and purified crude glycerol and its derivatives were monitored between 400 - 4000 cm^{-1} with the resolution of 4 cm^{-1} at room temperature by a Nicolet, model NEXUS 470, FTIR spectrometer equipped with a Smart Multi-Bounce HATRTM detector. All the recorded spectra were corrected for IR penetration depth using the ATR correction procedure implemented in the OMNIC[®] (Thermo Nicolet Corp.) software. Consequently, the ATR-corrected spectrum was evaluated using OMNIC[®] and MicroCal[®] Origin software.



Figure 3.5. Fourier Transform Infrared spectroscopy (FTIR).

3.5.3 Gas chromatograph and mass spectrometry

The generated compounds from the electrochemical reforming of glycerol, crude glycerol and purified crude glycerol were characterized by gas chromatograph and mass spectrometry (Agilent, G3174A) equipped with a flame ionization detector as shown in Figure 3.6. Hewlett-Packard Chemstation software was used to collect and analyze the data. A Restek Crop (Bellefonte, PA) DB-WAX GC-column (30m x 250mm x 0.25 μm) was used to analyze some products from the reaction of synthetic glycerol reforming and the DB- 5MS GC-column (30m x 250mm x 0.25 μm) was used to analyze the parts from crude glycerol and purified crude glycerol. The utilized solvent was 2-propanol.



Figure 3.6. Gas chromatograph and mass spectrometry (GC/MS).

ศูนย์วิทยทรัพยากร
จุฬาลงกรณ์มหาวิทยาลัย

CHAPTER IV

RESULTS AND DISCUSSION

This chapter presents the results and discussion of the glycerol reforming from synthetic and purified crude glycerol to 1,3-propanediol by an electrochemical technique and also presents the results and discussion of the purification of crude glycerol by chemical and physical treatments.

4.1 Electrochemical reforming of synthetic glycerol

4.1.1 Current density–potential curve

The possibility of the electrochemical reforming of glycerol was first explored with a cyclic voltammetry method using Pt sheet, Pt rod with a total surface area of 0.79 cm^2 , and Ag/AgCl electrode as the counter-, working- and reference electrodes, respectively. The scan potential was varied in the range of +2.50 to -2.50 V/Ag/AgCl with a scan rate of 5 mV/s. Prior to the start up of the experiment, gaseous N_2 was passed through the electrolyte for 20 min to decrease the oxygen concentration in the electrolyte solution. For each experiment, the system was agitated by using a magnetic stirrer at constant stirring rate of 400 rpm. Figure 4.1 shows the polarization curves of solvent solution (water) adjusted to final pH of 2, 4, 6, 8, 10 and 12 by the addition of the appropriate amount of conc. H_2SO_4 or NaOH (1.0 M). For the solution with pH of 2, the reduction of proton at strong acidic condition or H_2O was initially observed at the potential of -0.25 V/Ag/AgCl leading to the formation of hydrogen gas (reaction 4.1) and the oxygen gas evolution (reaction 4.2) corresponding to the oxidation reaction of water was initially observed at potential greater than +1.20 V/Ag/AgCl. For the solution with pH of 4, the reduction of water was found for potential -0.87 V/Ag/AgCl resulting to the formation of hydrogen gas and the oxidation reaction of water was significantly observed at potential more than +1.52 V/Ag/AgCl. For the solution pH as 6, 8, 10 and 12, the reduction and oxidation peaks of water were not observed in the studied potential range because the reduction and oxidation peaks of water will be observed at too lower negative potential and too high positive potential, respectively (Gerger and Haubner, 2005).

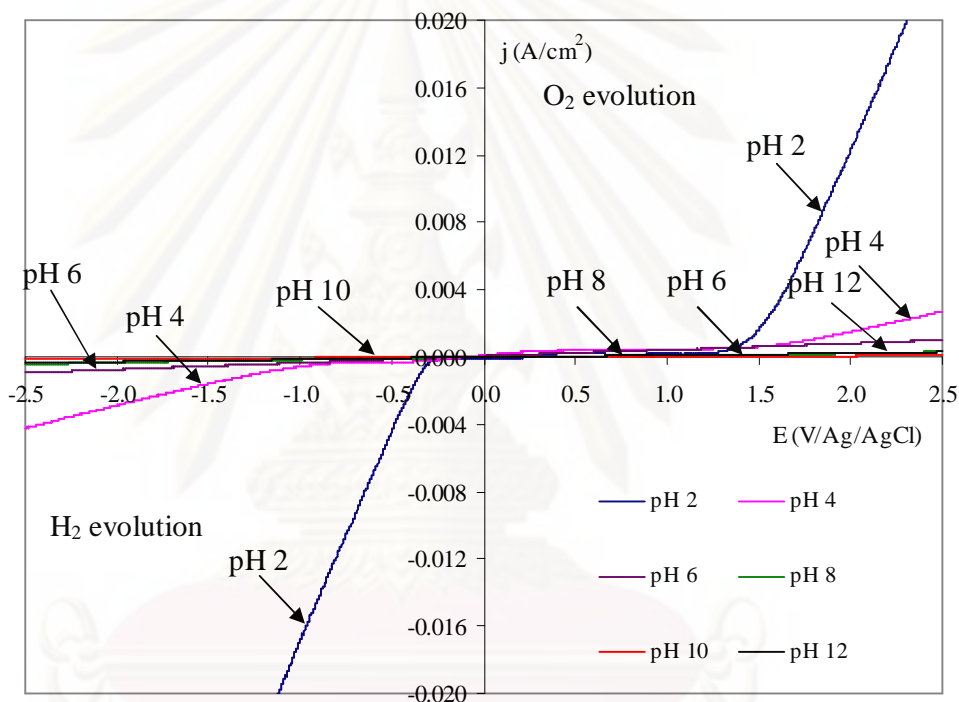
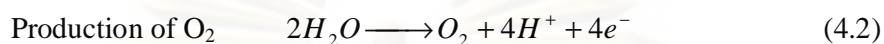
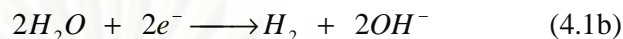
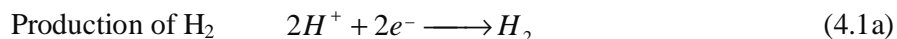


Figure 4.1 Current density-potential curves of solvent solution (water) at different pH with Pt electrode at constant stirring rate of 400 rpm and scan rate of 5 mV/s with Ag/AgCl reference electrode.

The current density-potential curves of synthetic glycerol solution with a final pH of 2, 4, 6, 8, 10 and 12 by the addition of the appropriate amount of conc. H_2SO_4 or NaOH (1.0 M) were preliminarily tested. The results revealed that the oxidation-reduction peaks of glycerol were not observed both in weak acidic (pH 6) and basic (pH 8 and 10) solutions while they were clearly observed in strong acidic solutions (pH 2 and 4) (Figure 4.2 (a)) and strong basic solution (pH 12) (Figure 4.2 (b)). For

both acid conditions, the peak shapes were practically the same in each of two media; two oxidation peaks (peaks A and B) during the forward sweep and one reduction peak (peak C) and one oxidation peak (peak D) during the backward sweep. The principle differences were the oxidation peak potential and current density. Namely, the oxidation peaks (A) were observed at a potential of -0.18 and -0.20 V/Ag/AgCl corresponding to the current density of 0.96 and 0.93 mA/cm² for solution pH 2 and pH 4, respectively whereas the oxidation peaks (B) of both solutions were observed at the same potential of 0.63 V/Ag/AgCl with a maximum current density of 1.6 and 0.83 mA/cm² for solution pH 2 and pH 4, respectively. During the backward sweep, the peak shapes were also practically the same for both pH 2 and pH 4, with a single reduction (peak C) and oxidation (peak D) peaks. The maximum reduction peaks of the synthetic glycerol solution at pH 2 and pH 4 were observed at 330 and 360 mV/Ag/AgCl, corresponding to a current density of 0.35 and 0.32 mA/cm², respectively. Also, for the oxidation peaks, they were observed at a potential of 0.29 and 0.28 V/Ag/AgCl, relating to the current density of 2.6 and 1.0 mA/cm² for glycerol solution with pH 2 and pH 4, respectively. With respect to the polarization curve of glycerol solution under strong basic condition (pH 12), a strong oxidation peak (peak B) was observed at the potential of 0.08 V/Ag/AgCl during the forward scan, corresponding to the current density of 7.07 mA/cm² while peak A was not strongly observed, it appeared as a broad shoulder. For the backward scan, only one peak (peak C) with low current density (0.76 mA/cm²) was observed at the potential of -0.38 V/Ag/AgCl.

The composition of residual solution obtained from the current density-potential curve study was then analyzed by HPLC. For all samples, the glycerol peaks in the HPLC chromatograms appeared at the retention time of 7.50 min (Figure 4.3). For solutions of pH 6, 8, 10 and 12, no other peaks were observed for all investigated retention times. This implied that the reforming product(s) alluded above were clearly not propanediol. However, peaks of 1,2-propanediol and 1,3-propanediol were observed in solutions with an initial pH 4 and, especially, pH 2 with retention times of 9.85 and 8.90 min, respectively.

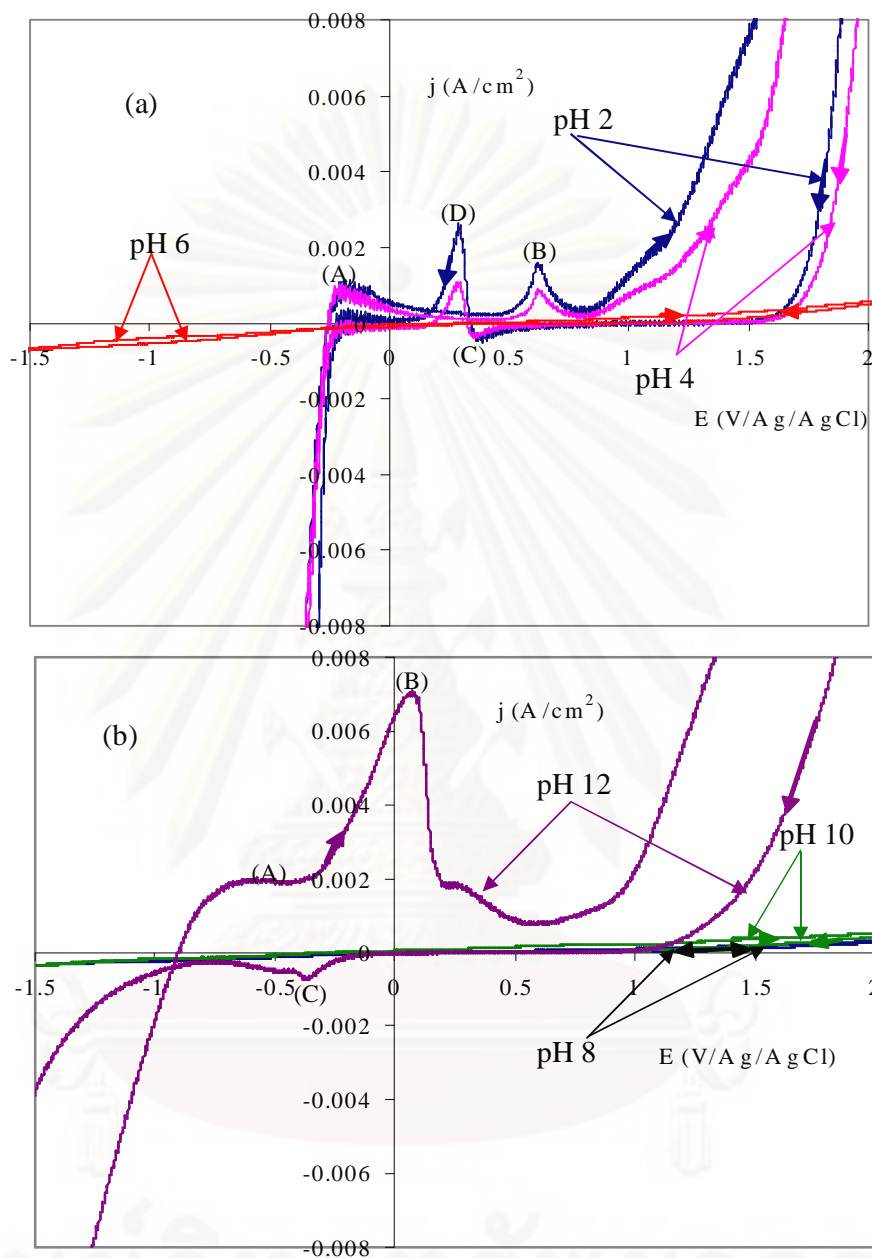


Figure 4.2 Current density-potential curves of synthetic glycerol solution pH 2, 4 and 6 (a), and synthetic glycerol solution 8, 10 and 12 (b) with Pt electrode at constant stirring rate of 400 rpm and scan rate of 5 mV/s with Ag/AgCl reference electrode.

The amount of 1,2-propanediol and 1,3-pepanediol generated in the system were presented in terms of yield percentages as demonstrated in Figure 4.4. The yield

of 1,3-propanediol obtained from glycerol reforming during the current density-potential curve study at pH 2 and pH 4 were higher than that of 1,2-propanediol at the same reforming conditions. According to the obtained results, it was clear that the oxidation-reduction of glycerol was principally observed in very strong acid condition. Therefore, for further study, the glycerol reforming to 1,3-propanediol by electrochemical was carried out under acidic conditions.

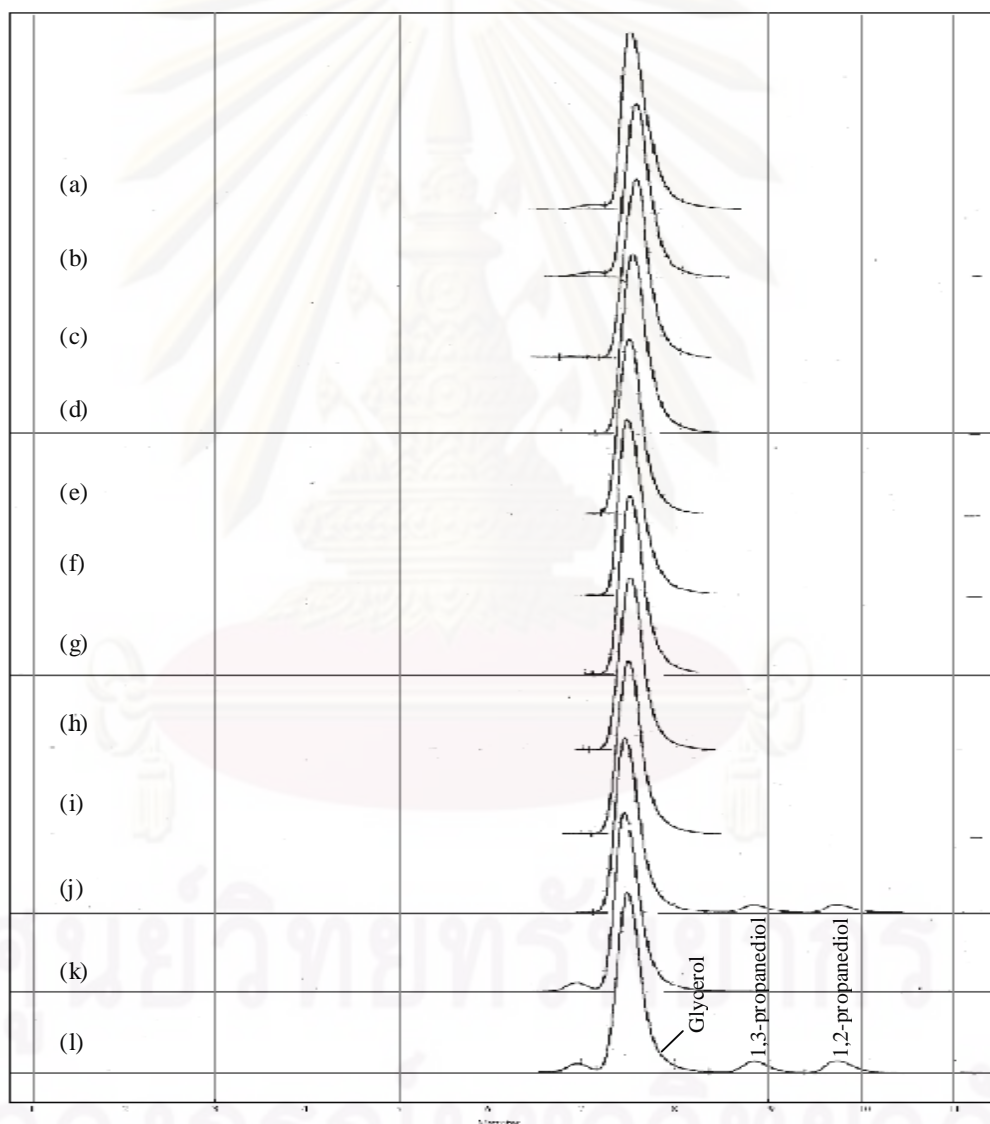


Figure 4.3. Representative HPLC chromatograms of solutions at pH 12 (a, b), pH 10 (c, d), pH 8 (e, f), pH 6 (g, h), pH 4 (i, j) and pH 2 (k, l), before (a, c, e, g, i, k), and after (b, d, f, h, j, l) running the polarization curve.

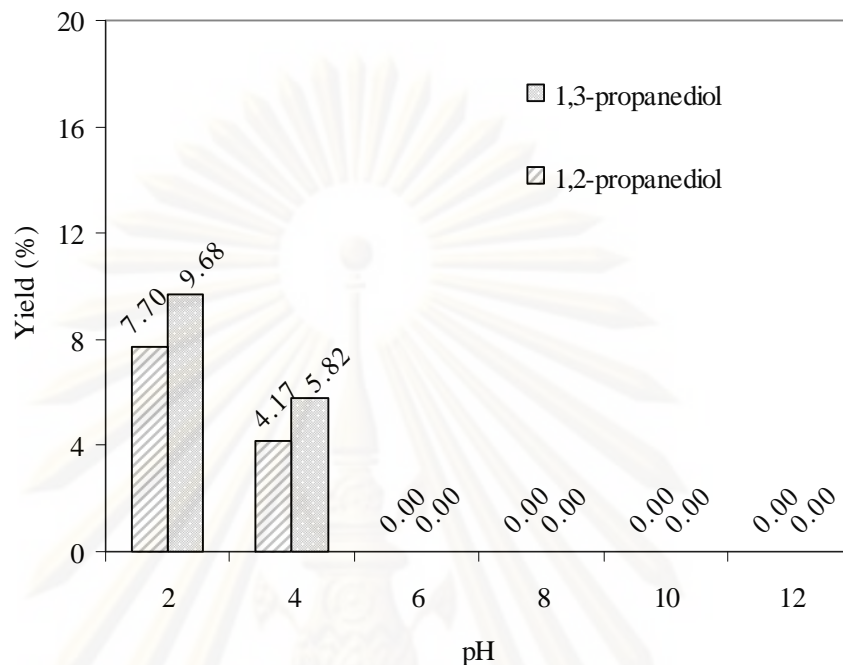


Figure 4.4. The yield of 1,2-propanediol and 1,3-propanediol obtained from synthetic glycerol solution at various pH by the cyclic voltametry.

4.1.2 Effect of parameters on synthetic glycerol reforming

Effects of various parameters including type of electrode, type of acid, current intensity, initial pH of glycerol solution, types of additive and concentrations were determined. At the end of this part, mechanism of synthetic glycerol reforming was explained.

- Effect of anode type

The effectiveness of organic substance reforming by electrochemical technique depends significantly on the nature of the electrode employed in the process (Rajeshwar et al., 1994, Tanaka et al., 2002 and Samet et al., 2006). Therefore, the efficiency of glycerol reforming to 1,3-propanediol was first explored by using three types of anode, that is Pt grids, Ti/RuO₂ grids and graphite sheet, with an initial pH of electrolyte of 2 and current intensity of 1 A. Under these conditions, the Pt grid promoted the highest normalized concentration and glycerol reforming (h_{gly} , Eq.(4.3)) compared with the other electrodes (Figure 4.5). Namely, approximately 0.029 mg glycerol/C of glycerol was reformed at an electrical charge of 10.3 Ah/l whereas they

were respectively around 0.022 and 0.019 mg glycerol/C for Ti/RuO₂ and graphite at the same operating conditions.

$$h_{gly} = \frac{([C_3H_5(OH)_3]_i - [C_3H_5(OH)_5]_i) V}{C'} \quad (4.3)$$

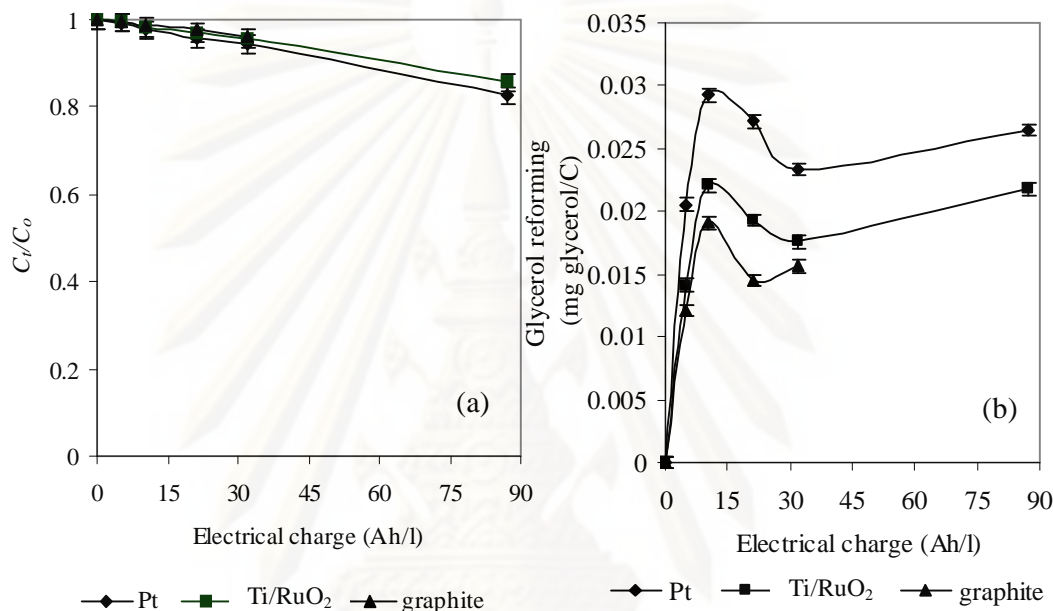
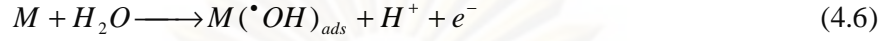


Figure 4.5. Evaluation of the normalized concentration (a) and glycerol reforming (b) as a function of electrical charges in the presence of different electrodes by using synthetic glycerol solution at the concentration of 46.2 g/l, pH of 2 and current intensity of 1 A.

The kinetic model supposed that the rate of the electrochemical reforming of glycerol can be explained with electrogenerated OH⁻ and/or direct electrochemical oxidation. In this region, we can control the amount of electrogenerated OH⁻ and nature of oxidation product by a proper choice the applied current intensity.

In fact, bulk electrolyte has known that, depending on the experimental condition, it was possible to obtain the partial reforming of glycerol to 1,3-propanediol or others products or complete reforming products as CO₂ and H₂O. Regarding the rate of glycerol reforming, it was found that the first step in the direct electrolysis of water molecule is the generation of the adsorbed hydroxyl radical

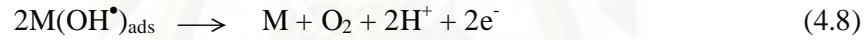
(OH[•]) as the oxidizing species by the adsorption of H₂O on the electrode surface (M), according to reaction (4.6) (Rajeshwar et al., 1994).



The generated OH[•] can attach the glycerol molecule leading to the formation of intermediate species X_i which is consequently reformed to stable and/or final products such as CO₂ and H₂O according to reaction (4.7).



In addition, the adsorption of the adsorbed OH[•] species from the electrode surface (reaction (4.6)) occurs parallel as reaction (4.8).



If reaction (4.7) is a first order rate reaction relating to the glycerol concentration, and if the concentration of OH[•] is constant during the electrolytic reforming of glycerol, then the reaction rate of glycerol reforming in reaction (4.7) can easily be deduced by the following expression (Samet et al., 2006).

$$\begin{aligned} -r_{C_3H_5(OH)_3} &= \frac{d[C_3H_5(OH)_3]}{dt} = k_{C_3H_5(OH)_3} [OH\cdot]_{ads}^a [C_3H_5(OH)_3] \\ &= k_{app, C_3H_5(OH)_3} [C_3H_5(OH)_3] \end{aligned} \quad (4.9)$$

Solving the above equation provides:

$$\ln \frac{[C_3H_5(OH)_3]_i}{[C_3H_5(OH)_3]_t} = k_{app, C_3H_5(OH)_3} t = k_m \frac{A_e}{V_R} t \quad (4.10)$$

The efficiency of different anode material for glycerol reforming can be also compared by fitting the rate of glycerol reforming with pseudo-first order kinetics model (Eq. (4.10)). The resulting pseudo-first order rate constants of material different electrode for the glycerol reforming at 1 A current intensity applied to an initial concentration 46.2 g/l of synthetic glycerol and pH of 2 was shown in Figure 4.6. The Pt electrode had the highest rate constant followed by the Ti/RuO₂ anode and then the graphite anode. Namely, the rate constants of glycerol reforming by using Pt, Ti/RuO₂ and graphite were 0.078, 0.0062 and 0.0042 h⁻¹, respectively. This emphasized that efficiency of electrochemical reforming of glycerol depended on the nature of the anodes used in the process.

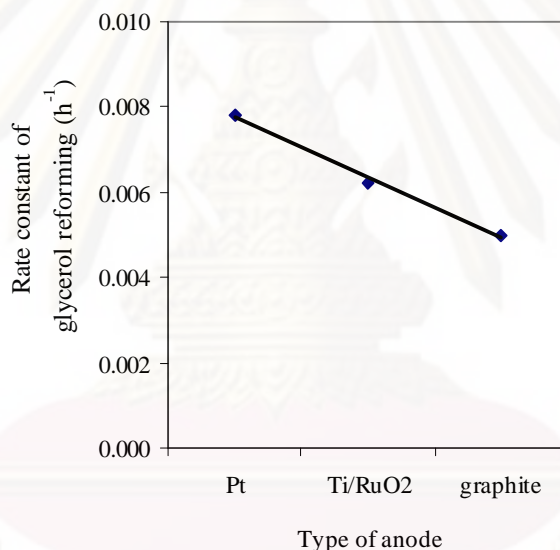


Figure 4.6 Plot of rate constant of pseudo-first-order kinetics of glycerol reforming as a function of type of anode by using synthetic glycerol solution at the concentration of 46.2 g/l and pH of 2.

Regarding the yield of 1,3-propanediol, as displayed in Figure 4.7, the highest yield of 1,3-propanediol was obtained by employing the Pt anode. A graphite anode provided the lowest yield of 1,3-propanediol and it corroded in the presence of electrical charges greater than 32.1 Ah/l (9 h electrolysis time). This behavior was similar to the result of Lissens et al., (2005). The corrosion of graphite electrode might be due to the reaction of graphite with H₂O according to Eq. (4.11).

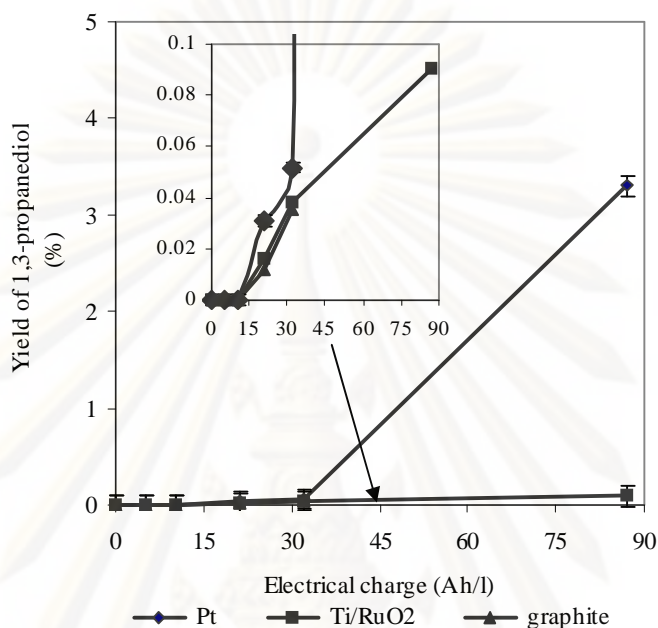
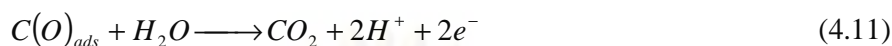


Figure 4.7. The yield of 1,3-propanediol as a function of electrical charges in the presence of different electrodes by using synthetic glycerol solution at the concentration of 46.2 g/l, pH of 2 and current intensity of 1 A.

- Effect of acid type

The effect of the acid type including H_2SO_4 and H_3PO_4 used to set the electrolyte solution pH on the electrochemical reforming of glycerol to 1,3-propanediol was then explored with synthetic glycerol solution at the concentration of 46.2 g/l, pH of 2 and current intensity of 3 A with Pt electrode. Under these conditions, a higher normalized concentration, glycerol reforming and yield of 1,3-propanediol were attained with H_2SO_4 compared with those of H_3PO_4 (Figure 4.8). Namely, in the presence of H_2SO_4 , the maximum glycerol reforming was obtained at around 0.093 mg glycerol/C at 15.25 Ah/l (1.5 h electrolysis time), but it significantly reduced in the presence of a higher electrical charge. With respect to the yield of 1,3-propanediol, it attained in the presence of H_2SO_4 was approximately 2-fold higher than that in the presence of H_3PO_4 for all applied electrical charges. This is because

the dissociation constant (K_a) of H_2SO_4 ($K_a \sim 1000$) is higher than that of H_3PO_4 ($K_a \sim 0.007$) causing the increase of solution conductivity and OH^\bullet activity in the system.

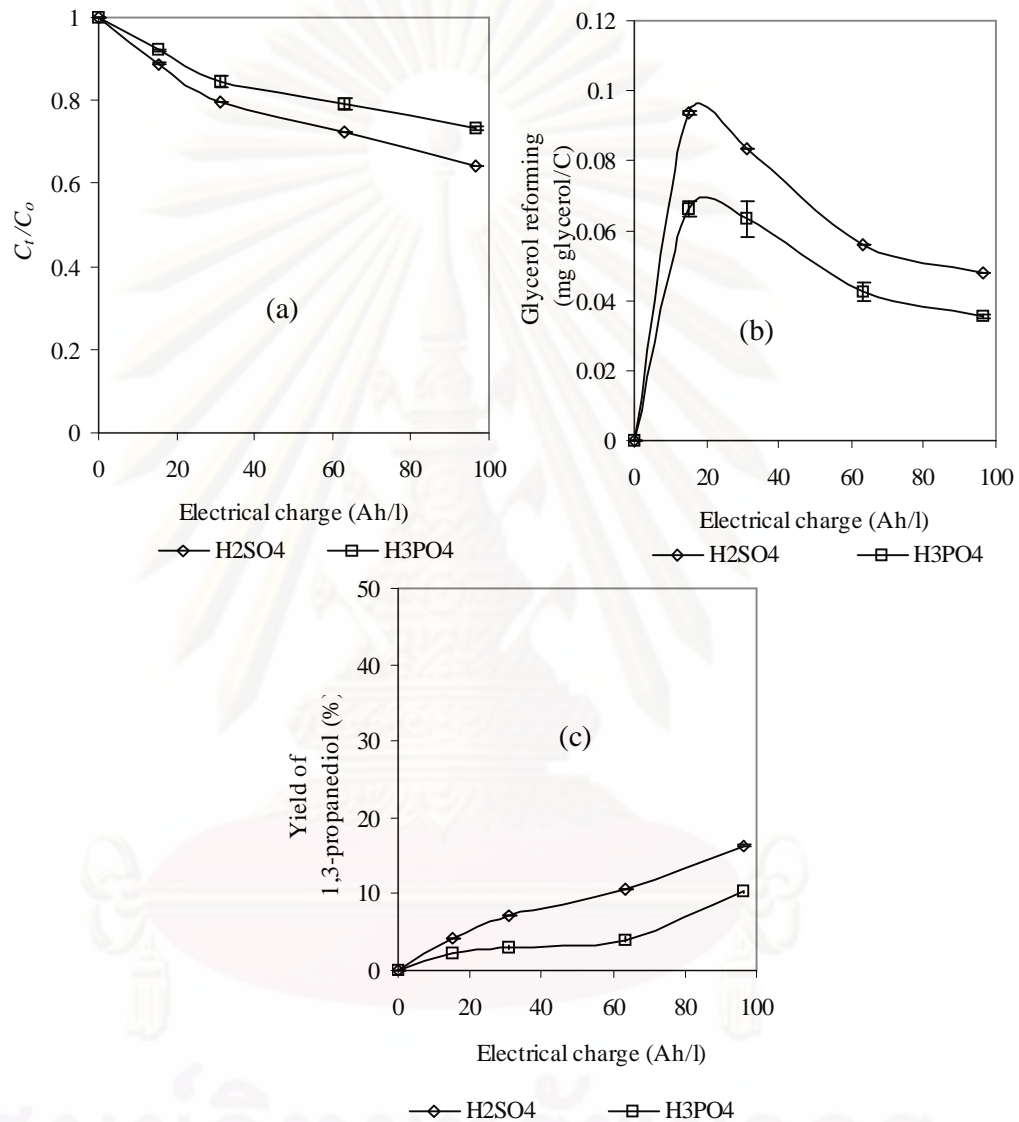


Figure 4.8. Evaluation of the normalized concentration (a), glycerol reforming (b) and yield of 1,3-propanediol (c) as a function of electrical charges with different acid types by using synthetic glycerol solution at the concentration of 46.2 g/l, pH of 2 and current density of 3 A with Pt electrode.

- Effect of current intensity

Effect of applied current intensity on glycerol reforming to 1,3-propanediol was then explored in the range of 3 - 5 A at pH of 2 adjusted by conc. H_2SO_4 with Pt electrode. Increasing the applied current intensity led to an increasing level the normalized concentration and glycerol reforming (Figure 4.9 (a)-(b)), in accordance with Faraday's law. The highest glycerol reforming (0.24 mg glycerol/C) was obtained at an applied current intensity of 5 A. The rate constant of pseudo-first order of glycerol reforming on different applied current intensity was shown in Figure 4.10. The rate constant of glycerol reforming decreased from 0.0529 to 0.2810 h^{-1} when the current intensity was increased from 3 to 5 A. This implies that the rate of glycerol reformation was fast in the presence of a high-applied current intensity. However, at this condition, the yield of 1,3-propanediol dropped rapidly from 26% at an electrical charge of 51.7 Ah/l to around 1.25% at an electrical charge of 160.7 Ah/l (Figure 4.11). This might be due to the reforming of glycerol to other compounds such as formic acid, propanoic acid and propene or it had the complete reforming of glycerol to CO_2 at high current intensity and long electrolysis times (Li et al., 2005).

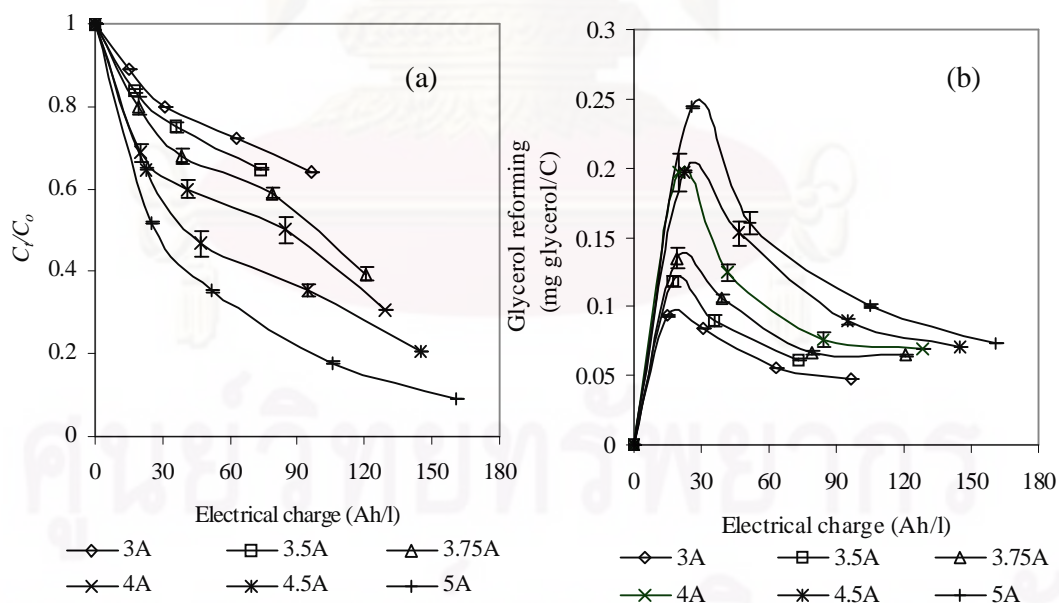


Figure 4.9. Evaluation of the normalized concentration (a) and glycerol reforming (b) as a function of electrical charges at an applied current intensity of 3 - 5 A by using synthetic glycerol solution at the concentration of 46.2 g/l and pH of 2 with Pt electrode.

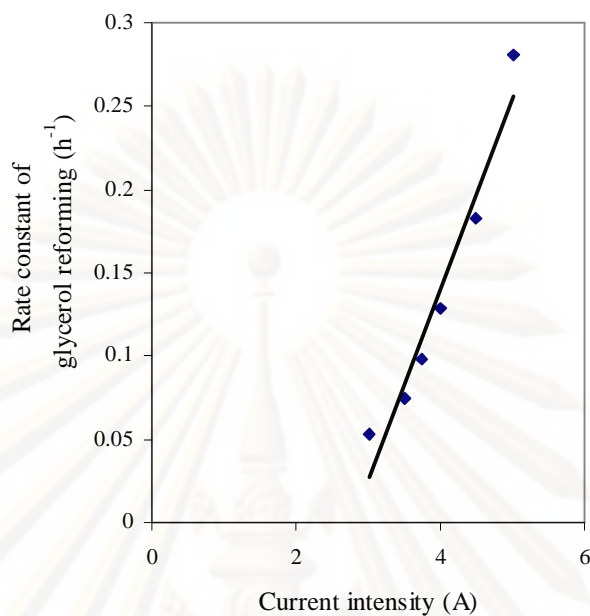


Figure 4.10. Plot of rate constant of pseudo-first-order kinetics of glycerol reforming as a function of current intensity by using synthetic glycerol solution at the concentration of 46.2 g/l and pH of 2 with Pt electrode.

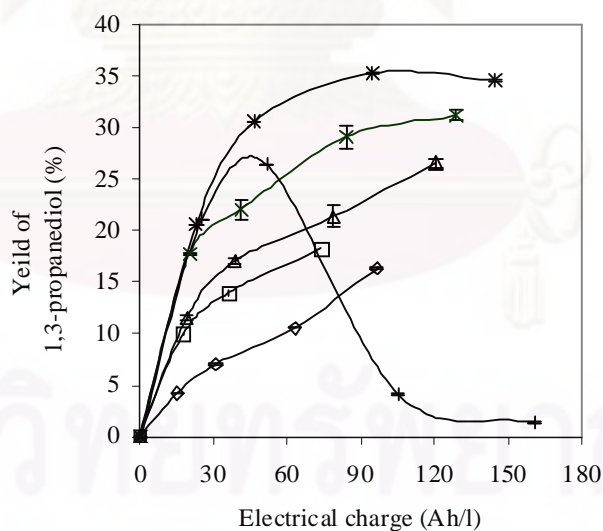


Figure 4.11. The yield of 1,3-propanediol as a function of electrical charges at an applied current intensity of 3 - 5 A by using synthetic glycerol solution at the concentration of 46.2 g/l and pH of 2 with Pt electrode.

According to the results of this part, the optimum current intensity was found at 4.5 A and it can provide the yield of 1,3-propanediol of around 35.34% at an electrical charge of 94.73 Ah/l (6 h electrolysis time).

- Effect of pH

The effect of the initial electrolyte solution pH was then examined in the acidic range of 0.5 - 4 with conc. H_2SO_4 at a constant current intensity of 4.5 A with Pt electrode. The pH of the electrolyte solution had a significant effect upon the normalized concentration and glycerol reforming. Namely, decreasing the initial electrolyte pH led to increasing the normalized concentration and glycerol reforming (Figure 4.12 (a)-(b)). For example, decreasing the initial electrolyte pH from 4 to 0.5 increased the normalized concentration and glycerol reforming around 1.62- and 3.16-fold, respectively at an electrical charge of 22.9 Ah/l. It can be explained that the increase of solution pH decreased the potential oxygen generation obtained from hydroxyl radicals (OH^\bullet) oxidation and consequently increased the transport of oxygen at the electrode surface resulting to lower glycerol diffusion to electrode surface (Samet et al., 2006). This will be discussed again, regarding to the formation mechanism of 1,3-propanediol. According to the results of this part, the maximum glycerol reforming was observed at 0.27 mg glycerol/C at initial electrolyte pH of 0.5 and an electrical charge of 22.9 Ah/l.

The rate constant of pseudo-first order of glycerol reforming on different the initial electrolyte solution pH demonstrated in Figure 4.13. The rate constant of glycerol reforming increased from 0.0878 to 0.3272 h^{-1} as around 3.75-fold when the initial electrolyte pH was decreased from 4 to 0.5. For the yield of 1,3-propanediol, as demonstrated in Figure 4.14, its production yield increased with the increase of solution acidity up to pH 1. However, increasing solution acidity or decreasing initial pH of solution to pH 0.5 cannot promote an increase of the yield of 1,3-propanediol but it decreased significantly at high electrical charge. This is because under strong acid conditions and high electrical charges, a strong oxidation-reduction potential was created that led to the reforming of glycerol to short carbon molecules such as formaldehyde, acetic acid, formic acid (Chbihi et al., 1999) or it had the complete reforming of glycerol to CO_2 .

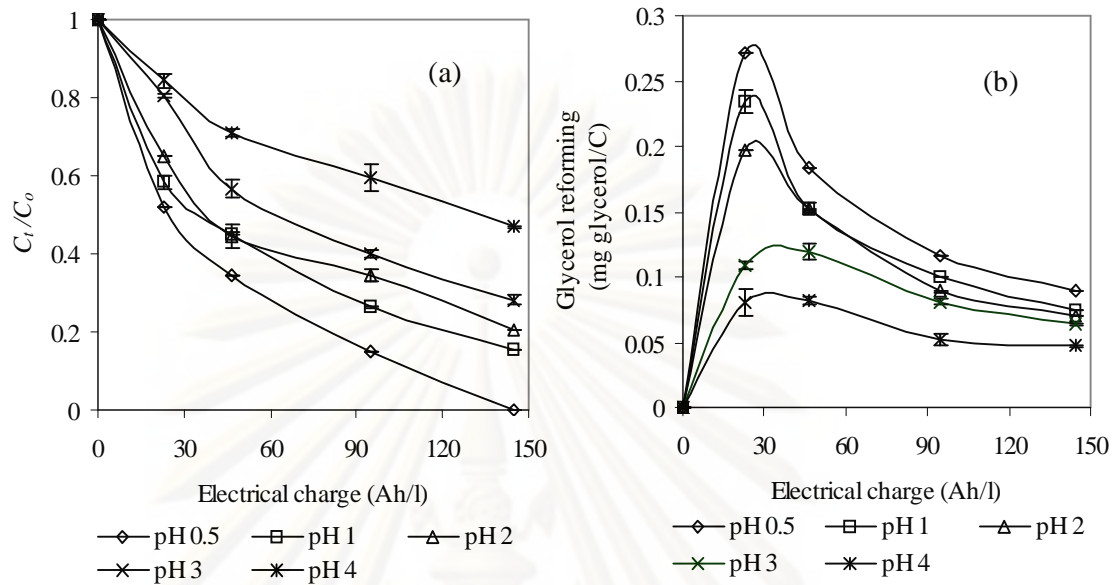


Figure 4.12. Evaluation of the normalized concentration (a) and glycerol reforming (b) as a function of electrical charges at different initial electrolyte pH values by using synthetic glycerol solution at the concentration of 46.2 g/l and current intensity of 4.5 A with Pt electrode.

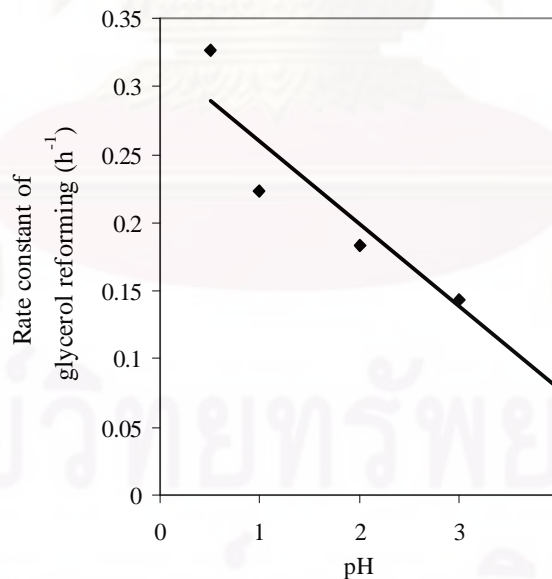


Figure 4.13. Plot of rate constant of pseudo-first-order kinetics of glycerol reforming as different initial electrolyte pH values by using synthetic glycerol solution at the concentration of 46.2 g/l and current intensity of 4.5 A with Pt electrode.

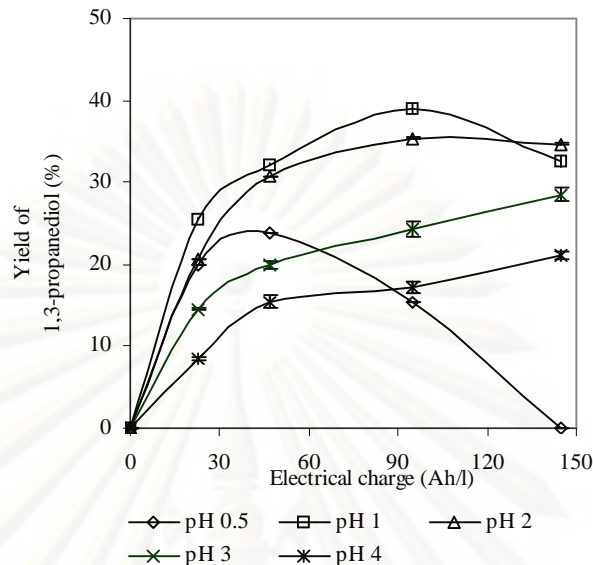


Figure 4.14. The yield of 1,3-propanediol as a function of electrical charges at different initial electrolyte pH values by using synthetic glycerol solution at the concentration of 46.2 g/l and current intensity of 4.5 A with Pt electrode.

- Effect of type additive

The effects of type of additives including NaCl, Na₂SO₄ and (NH₄)₂S₂O₈ at the same dosage (2.93 g/l) were explored at a current intensity of 4.5 A, and an initial pH of 1 with Pt electrode. It was found that the presence of additive can be provided a higher the normalized concentration and glycerol reforming compared with that in the absence of additives. This might be due to fact that, in the presence of additive, large amount of oxidizing agents including OCl⁻, SO₄²⁻ and S₂O₈²⁻ were produced in the system leading to the increase of the transformation rate in the system (Chen, 2004). Nevertheless, the presence of different types of additive provided the similar glycerol evaluation and glycerol reformation efficiency. For example, the presence of additive as (NH₄)₂S₂O₈ and NaCl increased the normalized concentration and glycerol reforming around of 1.08- and 1.26-fold and 1.01- and 1.17-fold, respectively at an electrical charge of 15.25 Ah/l, as demonstrated in Figure 4.15.

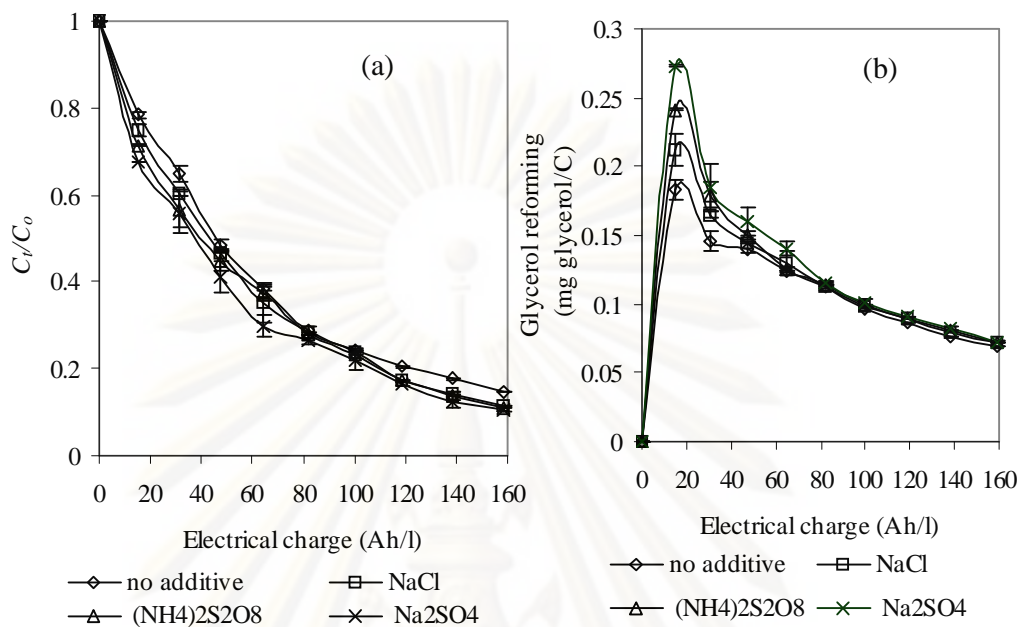


Figure 4.15. Evaluation of the normalized concentration (a) and glycerol reforming (b) at different types of additive by using synthetic glycerol solution at the concentration of 46.2 g/l, current intensity of 4.5 A and pH of 1 with Pt electrode.

With respect to the yield of 1,3-propanediol, as demonstrated in Figure 4.16, the presence of NaCl resulted in a slightly higher yield of 1,3-propanediol, whereas that of the other additives reduced its production yield, particularly at higher levels of electrical charge. This might be attributed to the difference in oxidizing power of each additive. Namely, the oxidizing power exhibits the order for $(NH_4)_2S_2O_8 > Na_2SO_4 > NaCl$ (Chen, 2004). In the presence of too strong oxidizing agent, such as $(NH_4)_2S_2O_8$ or Na_2SO_4 , the complete reforming of glycerol to short carbon molecule or CO_2 occurred leading to lower the yield of 1,3-propanediol.

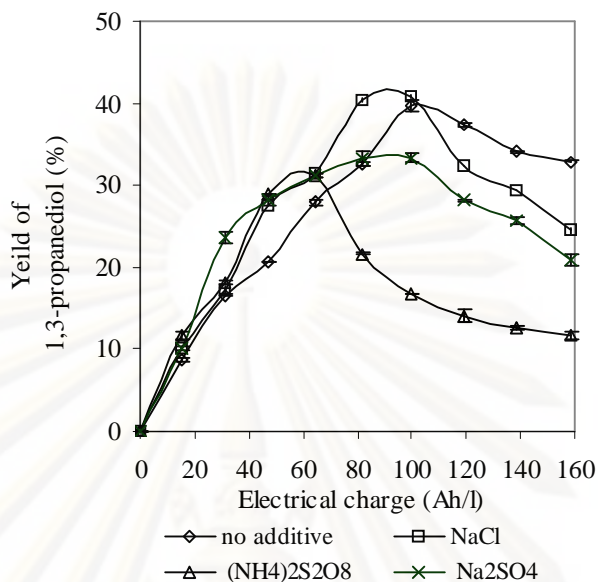


Figure 4.16. The yield of 1,3-propanediol as a function of electrical charges at different type of additive values by using synthetic glycerol solution at the concentration of 46.2 g/l and current density of 4.5 A and pH of 1.

- Effect of concentration of NaCl

The optimum dosage of NaCl was then explored in the range of 0 - 8.78 g/l by employing the current intensity of 4.5 A, and initial pH of 1 by using Pt electrode. It can be seen that increasing the concentration of NaCl can achieve a small increase of the normalized concentration and glycerol reforming (Figure 4.17 (a)-(b)). The maximum glycerol reforming was observed at around 0.27 mg glycerol/C in the presence of 8.78 g/l NaCl at an electrical charge of 15.25 Ah/l (1 h electrolysis time). This is because when the concentration of NaCl increased large amount of OCl^- was produced leading to a higher glycerol reforming (Rajkumar et al., 2005).

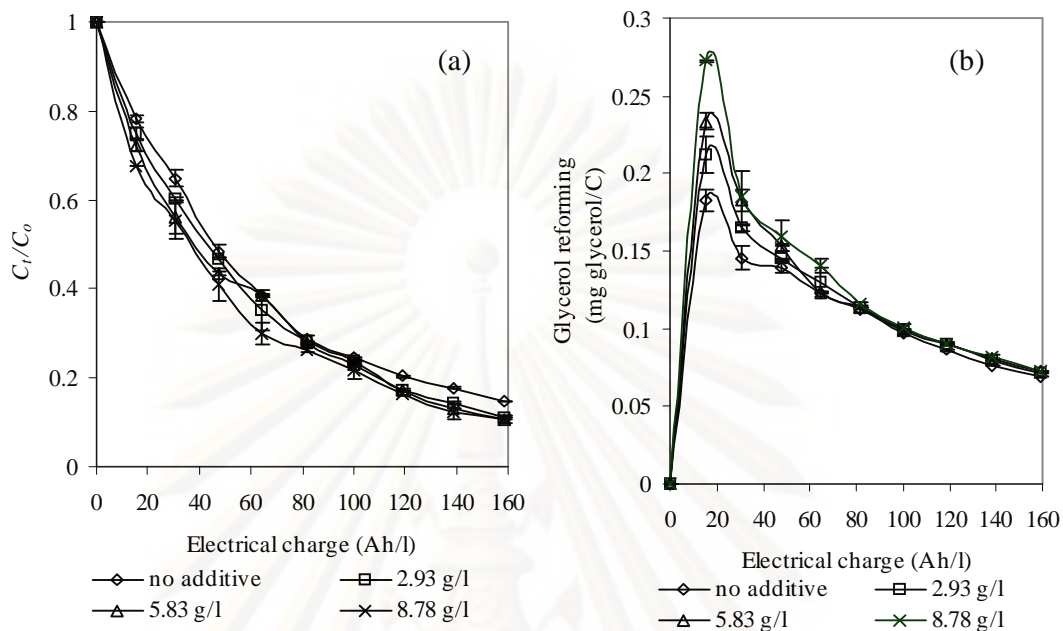


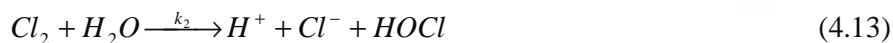
Figure 4.17. Evaluation of the normalized concentration (a) and glycerol reforming (b) as a function of electrical charges at different initial concentrations of NaCl at an applied current intensity of 4.5 A by using synthetic glycerol solution at the concentration of 46.2 g/l and pH of 1 with Pt electrode.

The kinetics rate of glycerol reforming in the presence of NaCl was consequently investigated. Actually, the electrochemical reaction of glycerol reforming to 1,3-propanediol taken place during the electrolysis time was complicated and not exactly known. It was generally involving a coupling of electron transfer reaction with a dissociate chemisorptions step (Mohan et al, 2007).

In the presence of chloride salt, the following reactions assumed to be taken place at the anode.



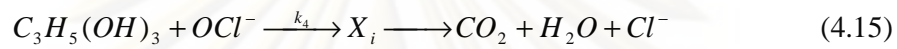
In bulk solution, the liberated chlorine forms hypochlorous acid.



And further dissociated to give hypochlorite ion



The generated hypochlorite ions act as main oxidizing agent in glycerol reforming on as



According to above equations, it can be seen that a cycle of chloride-chlorine-hypochlorite-chloride took place, which produced OCl^- . The pseudo-steady state theory can be applied to each of the intermediate products ($HOCl$ and OCl^-) taking part in the bulk solution. Suppose all other reactions were irreversible processes, the reaction rate r_i specifically for the sequence were.

$$-r_{Cl_2} = k_2[Cl_2] \quad (4.16)$$

$$-r_{HOCl} = k_2[Cl_2] - k_3[HOCl] + k_3'[H^+][OCl^-] \quad (4.17)$$

$$-r_{OCl^-} = k_3[HOCl] - k_3'[H^+][OCl^-] - k_4[C_3H_5(OH)_3][OCl^-] = 0 \quad (4.18)$$

$$-r_{C_3H_5(OH)_3} = k_4[C_3H_5(OH)_3][OCl^-] \quad (4.19)$$

Then using Eqs.(4.16) and (4.17), we can easily deduce the following expression

$$-r_{Cl_2} = -r_{C_3H_5(OH)_3} = k_4[C_3H_5(OH)_3][OCl^-] \quad (4.20)$$

From Eq.(4.12), it can be noted that $-r_{Cl_2} = -r_{Cl^-}$ or

$$-r_{Cl_2} = -r_{Cl^-} = k[Cl_2] = -r_{C_3H_5(OH)_3} = k_4[C_3H_5(OH)_3][OCl^-] \quad (4.21)$$

Where the rate of reaction r_i and the rate constants k_i ($i = 2, 3$ and 4) are defined with respect to the bulk.

The rate expression for main electrode reaction as Eq (4.12) can be written as

$$-r'_{Cl^-} = r'_{Cl_2} = k_1[Cl^-] \quad (4.22)$$

The basic relationship applicable to all electrochemical reaction is Faraday's law that relates to the amount of substance reacted at the surface to charge passed, that is $m_A i_A t / nF$ (assuming 100% efficiency). Thus, the electrochemical reaction rate for the disappearance of reaction A can be expressed as:

$$-\left(\frac{V_R}{A_e}\right) \frac{d[A]}{dt} = \frac{i_A}{nA_e F} \quad (4.23)$$

Then Eq.(4.21) can be rewritten in the another form as

$$\begin{aligned} -r_{Gly} &= -\left(\frac{V_R}{A_e}\right) \frac{d[A]}{dt} = \frac{i_{C_3H_5(OH)_3}}{nA_e F} \\ &= k_4[C_3H_5(OH)_3][OCl^-] \end{aligned} \quad (4.24)$$

During the electrolysis, since the constant current is applied, the rate of OCl^- generation will remain constant under a given set of experimental condition, but it varies as function of the applied current. Then, Eq.(4.24) can expressed in the form of

$$-r_{Gly} = -\left(\frac{V_R}{A_e}\right) \frac{d[A]}{dt} = \frac{i_{C_3H_5(OH)_3}}{nA_e F} = k_{obs}[C_3H_5(OH)_3] \quad (4.25)$$

Integrating Eq.(4.25) provided

$$\ln \frac{[C_3H_5(OH)_3]_i}{[C_3H_5(OH)_3]_t} = k_{obs} t \quad (4.26)$$

According to Eq.(4.26), the rate constant of pseudo-first order of glycerol reforming on different concentrations of NaCl was shown in Figure 4.18. The rate constant of glycerol reforming increased from 0.2238 to 0.2698 h⁻¹ when the concentration of NaCl was increased from 0 to 8.93 g/l

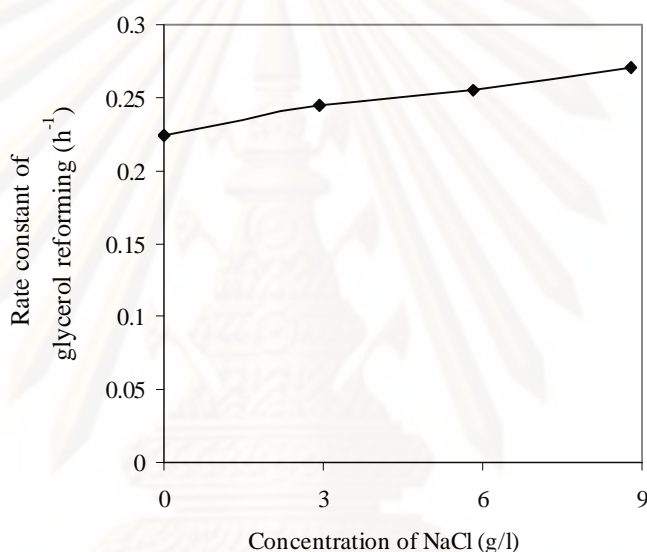


Figure 4.18. Plot of rate constant of pseudo-first-order kinetics of glycerol reforming as different concentrations of NaCl by using synthetic glycerol solution at the concentration of 46.2 g/l and current intensity of 4.5 A with Pt electrode.

For the yield of 1,3-propanediol as shown in Figure 4.19, the different concentrations of NaCl provided the different tendencies of 1,3-propanediol yields. In the presence of NaCl of 2.93 and 5.83 g/l, the yield of 1,3-propanediol was slightly increased but the electrical charge was reduced from 100 to 81.8 Ah/l. This cause by the fact that in the presence of NaCl, the oxidizing agent (OCl) was produced in the system, which can promote the fast reaction rate of 1,3-propanediol production. On the other hand, by employing the NaCl at the dosage of 8.78 g/l, the yield of 1,3-propanediol decreased sharply particularly at long electrolysis time. It was probably

due to glycerol reforming to other intermediates or CO_2 when the concentration of NaCl increase and long electrolysis time.

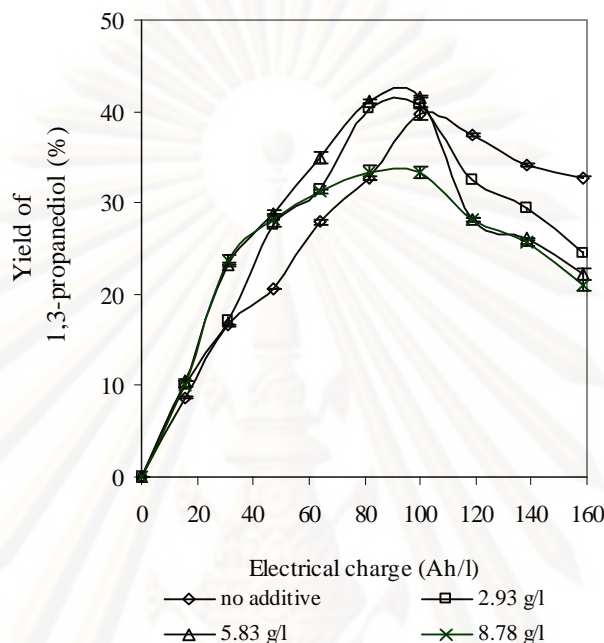


Figure 4.19. The yield of 1,3-propanediol as a function of electrical charges at different initial concentrations of NaCl at an applied current intensity of 4.5 A by using synthetic glycerol solution at the concentration of 46.2 g/l and pH of 1 with Pt electrode.

4.1.3 Mechanisms of synthetic glycerol reforming to 1,3-propanediol

From the GC/MS spectra of glycerol solution at pH of 1 in the absence of NaCl and in the presence of NaCl (2.93 g/l) (Figure 4.20 (a)-(b)) before supplying electricity, it was found that three similar chemical species were detected; 1-hydroxyl-2-propanone (acetol), acrylaldehyde (acrolein) and propene. Figure 4.21 (a)-(b) demonstrates the GC/MS spectra of glycerol solution at pH of 1 in the absence of NaCl or in the presence of NaCl (2.93 g/l) obtained after electrolysis by employing the current intensity of 4.5 A and initial pH of 1 by using Pt electrode at the electrical charge of 100 Ah/l. The detected compounds in both systems were propene, acrylaldehyde, acetaldehydel, propanal, 2-methyl-1,3-dioxane, ethylene glycol, 1-hydroxyl-2-propanone, formic acid, acetic acid, propanoic acid, glycidol, 1,2-

propanediol, 4-hydroxyl-1,3-dioxane, 2-ethyl-4-methanol-1,3-dioxolane, 1,3-propanediol, xylitol and 2,3-dihydroxyl-propanal. However, some transformation compounds in each electrolyte were different. Namely, 2-propenol was produced in system in the absence of NaCl whereas 2-choromethyl-1,3-dioxane was produced in the presence of NaCl.

Figures 4.22-4.23 show the area of glycerol and various compounds generated from glycerol reforming by electrochemical technique as function of electrical charge in the absence of NaCl (Figure 4.22) and in the presence of NaCl (2.93 g/l) (Figure 4.23) after electrolysis by using the current intensity of 4.5 A and initial pH of 1 by using Pt electrode. For both electrolytes, it was found that the quantity of glycerol decreased with the increase of electrical charge. The quantity of the four reforming products, including propanoic acid, acetic acid, 2-ethyl-4-methanol-1,3-dioxolane and propene, increased markedly with the electrical charge indicating that these compounds were the stable products obtained from the reforming process. The quantities of four reforming products, including 1,3-propanediol, 2,3-dihydroxyl-propanal, 1-hydroxyl-2-propanone and 2-methyl-1,3-dioxane, increased within the electrical charge of 100 Ah/l after that they decreased. This might be due to the reforming of those compounds to other compounds in the presence of electrical charges greater than 100 Ah/l. The quantities of other products such as acrylaldehyde, acetaldehydel, propanal, ethylene glycol, formic acid, glycidol, 1,2-propanediol and xylitol, increased within the electrical charge of 32.1Ah/l that they did not change when the electrical charges was greater than 32.1 Ah/l. In the absence of NaCl, the quantity of 2-propenol was increased up to the electrical charge of 100 Ah/l after that it decreased. The maximum of quantity of 2-choromethyl-1,3-dioxane in the presence of NaCl was observed at electrical charge of 118.87 Ah/l (7 h electrolysis time).

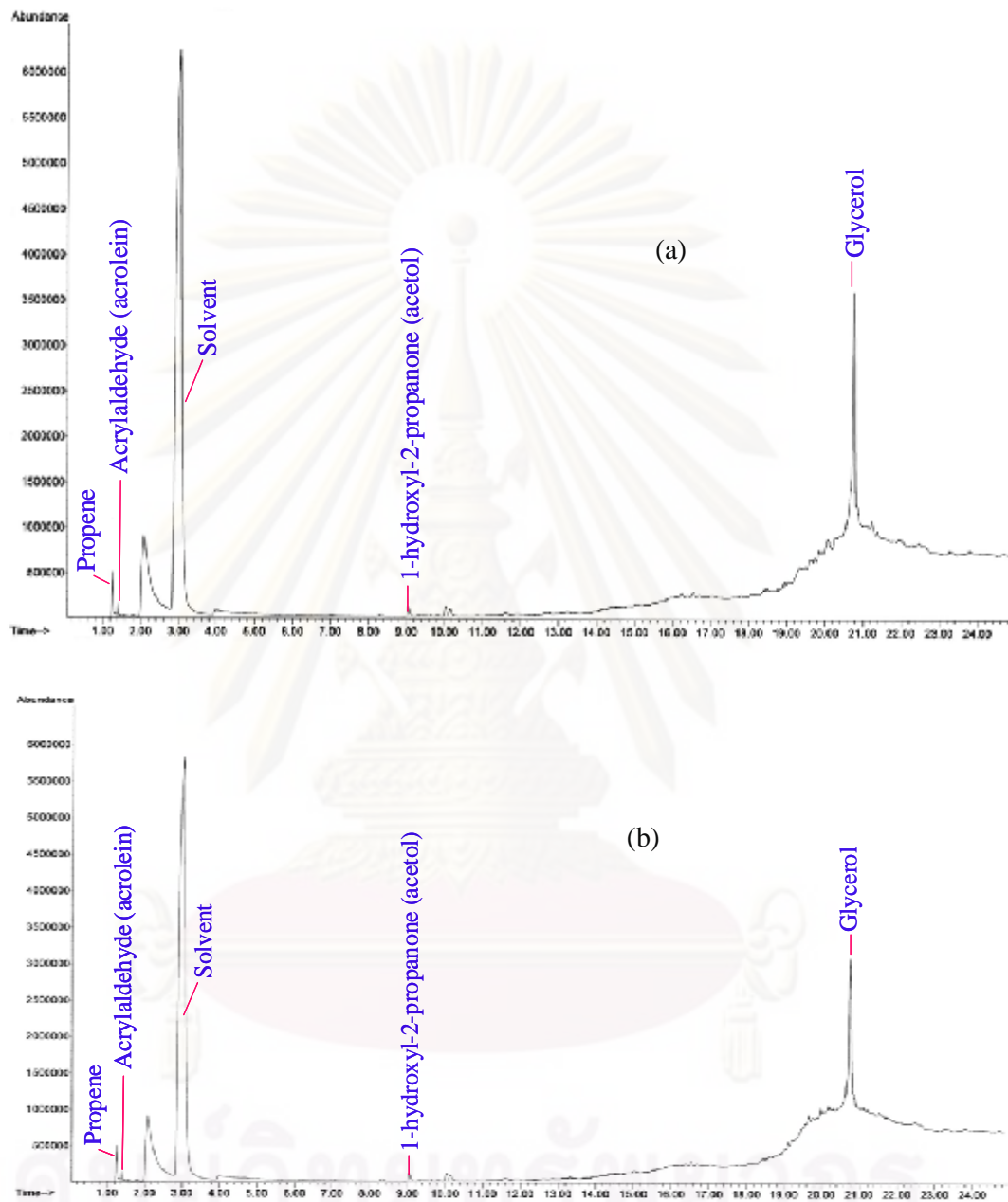


Figure 4.20. Representative GC/MS spectra of glycerol solution at pH of 1 in the absence of NaCl (a) and in the presence of NaCl (b) before supplying electricity.

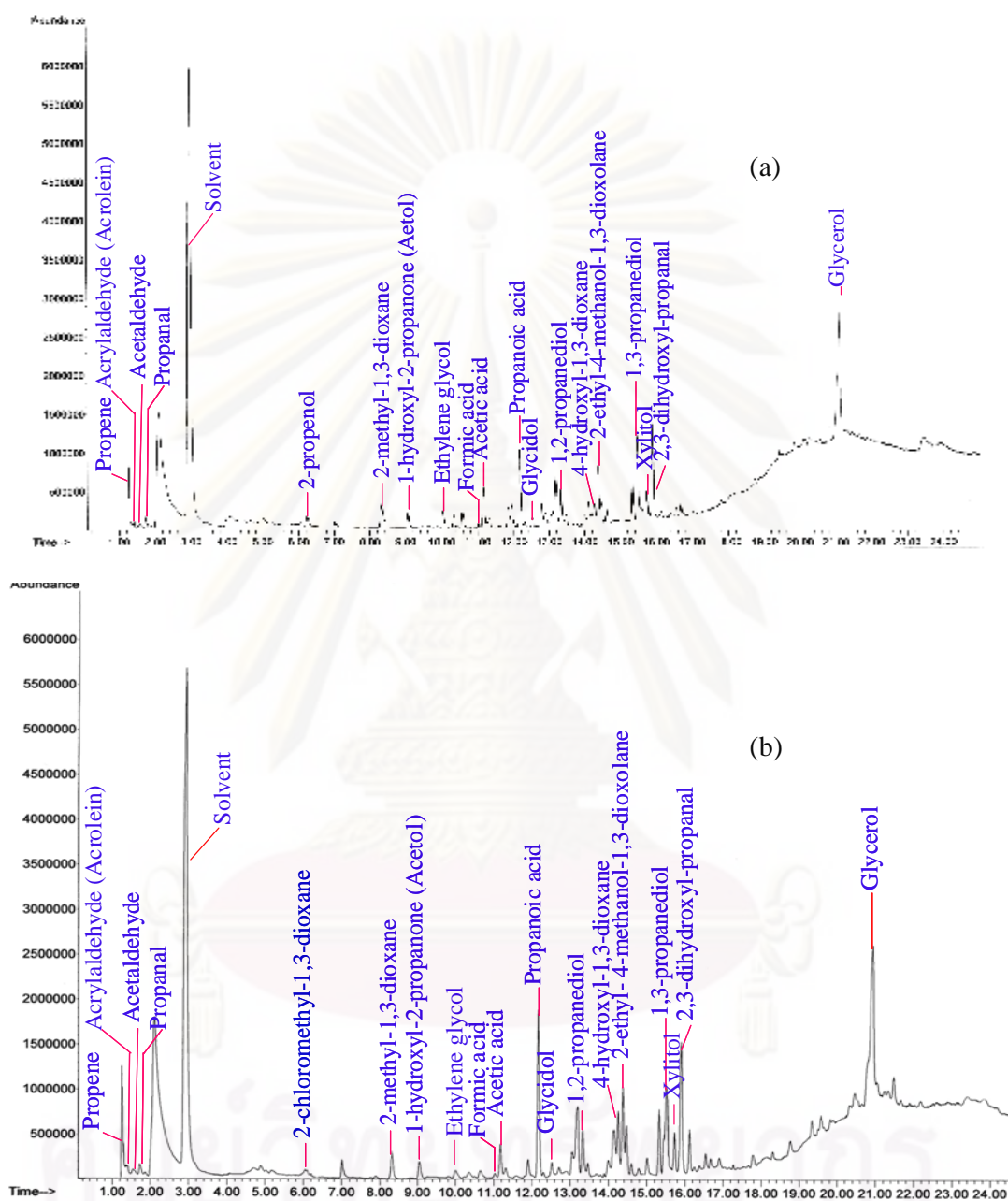


Figure 4.21. Representative GC/MS spectra of glycerol solution at pH of 1 in the absence of NaCl (a) and in the presence of NaCl (b) obtained after electrolysis by employing the current intensity of 4.5 A with Pt electrode at the electrical charge of

100 Ah/l.

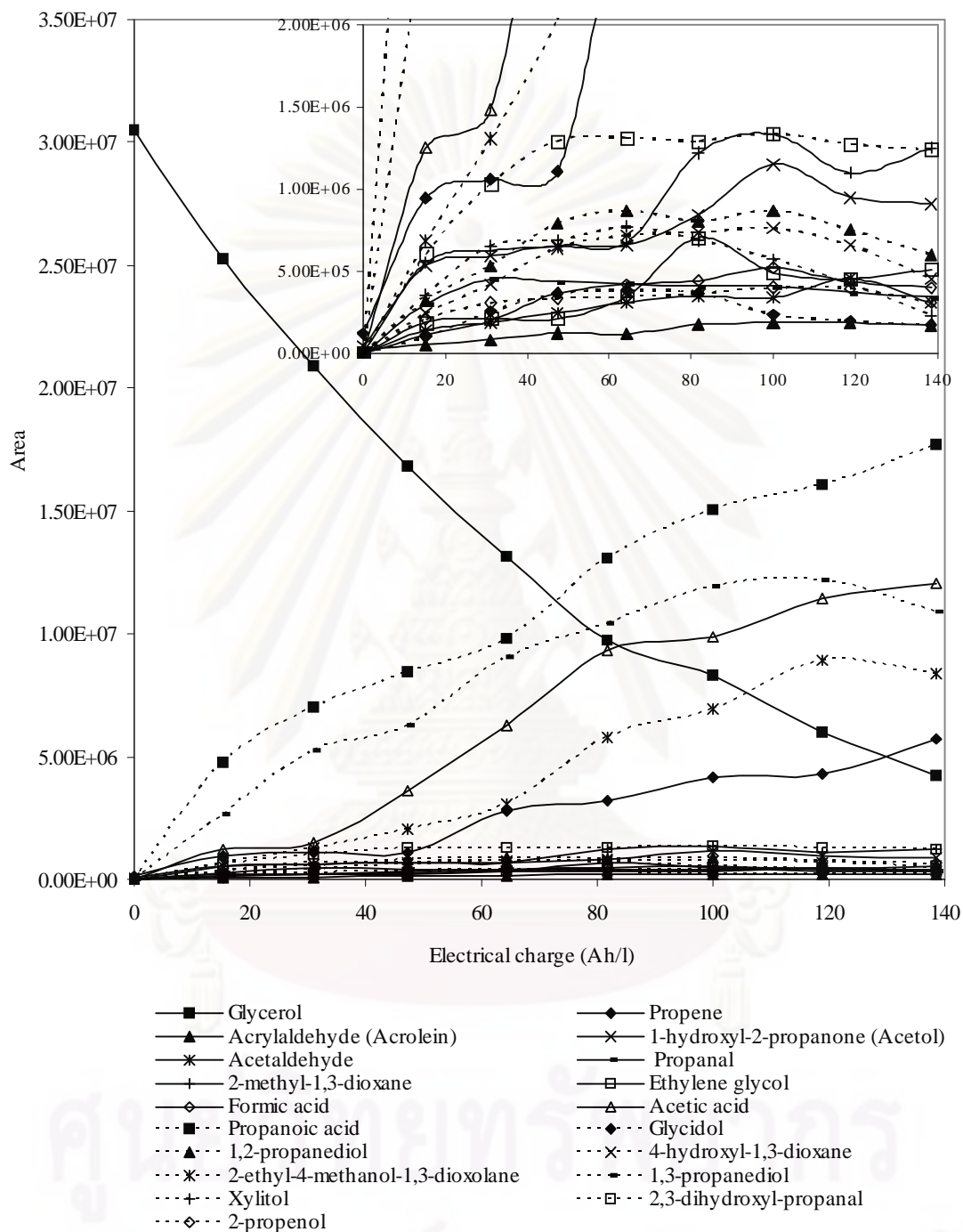


Figure 4.22. Quantity of various compounds generated from glycerol reforming by electrochemical as a function of electrical charge in the absence of NaCl at an applied current intensity of 4.5 A by using synthetic glycerol solution pH of 1 with Pt electrode.

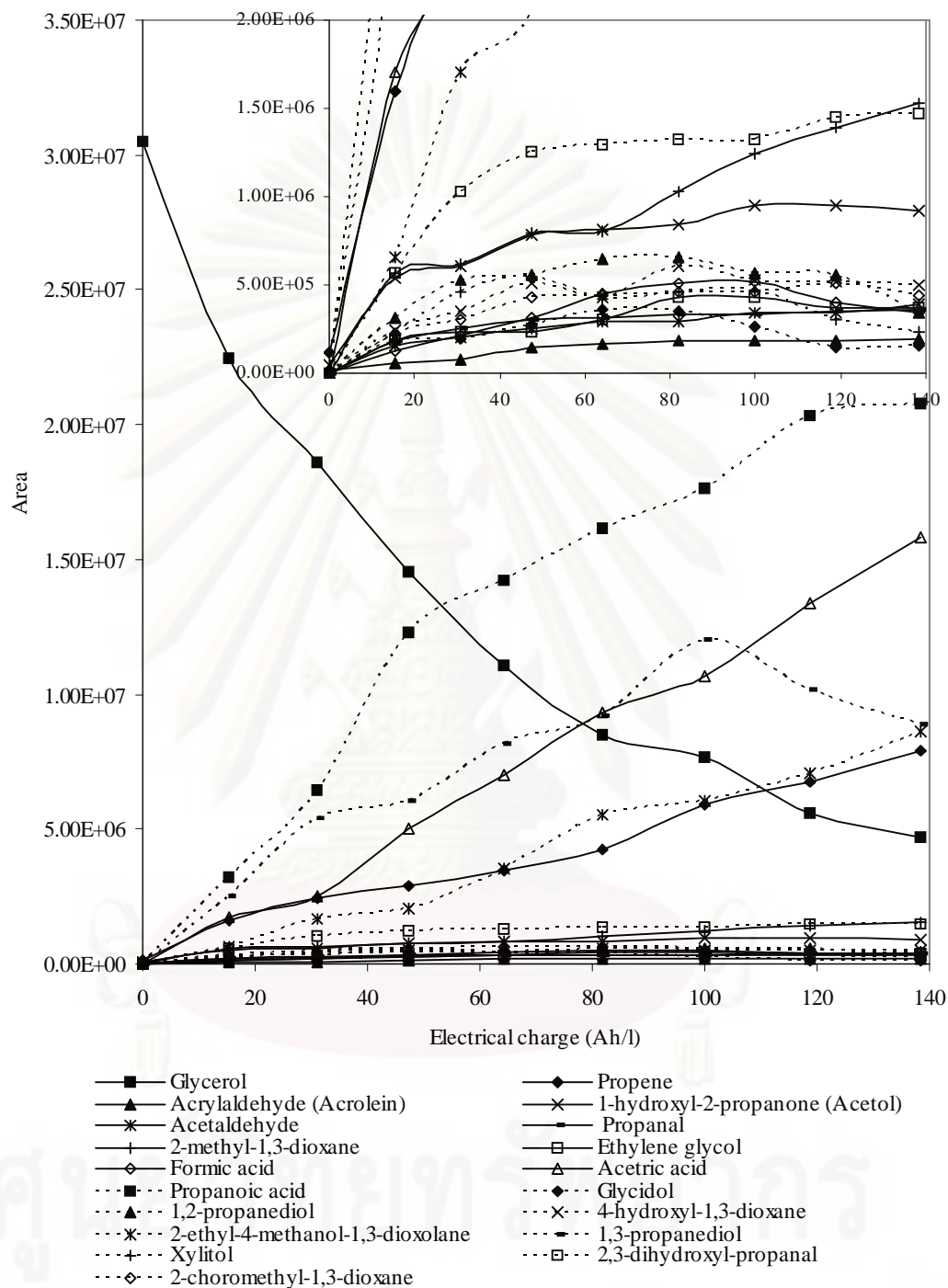


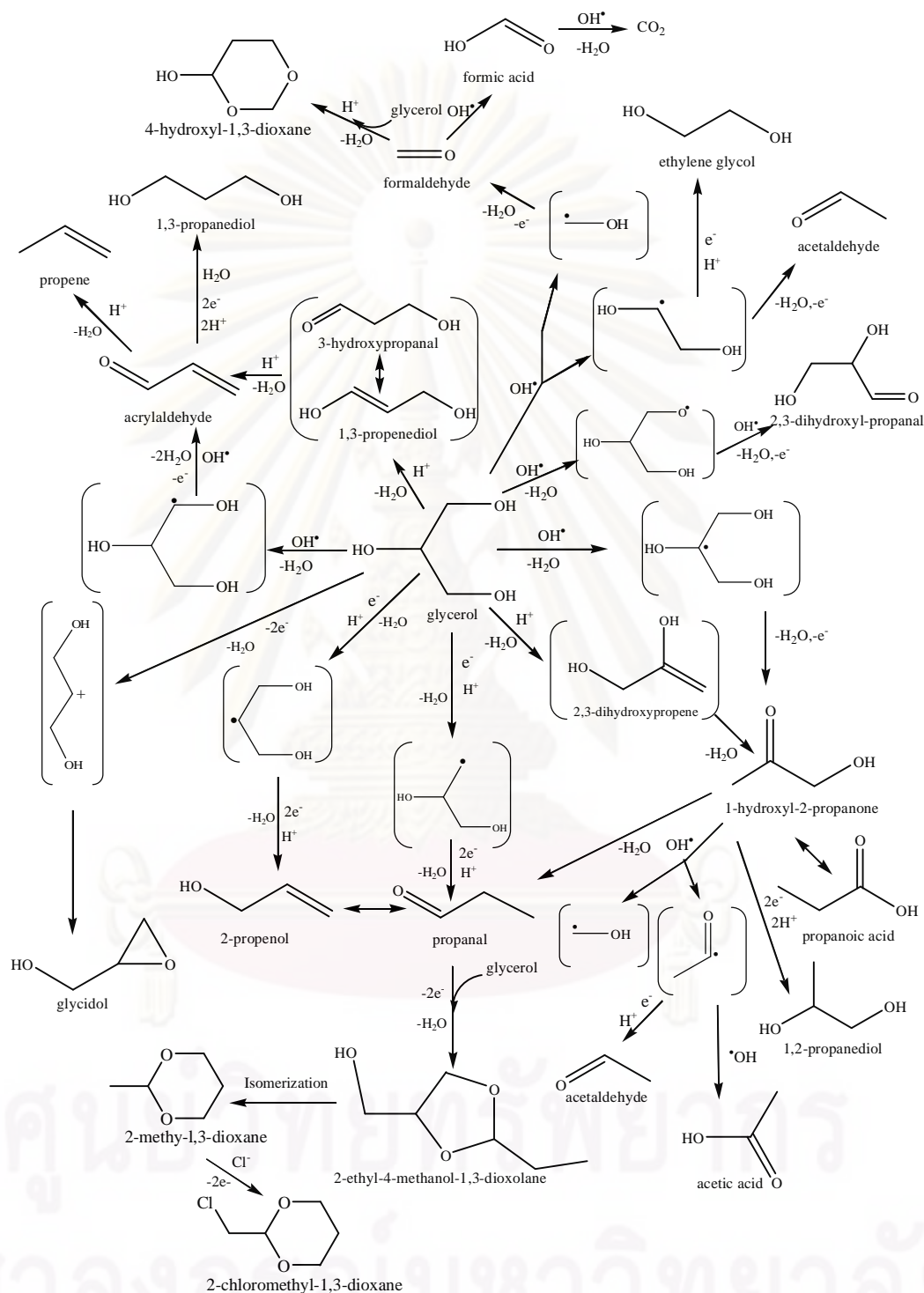
Figure 4.23. Quantity of various compounds generated from glycerol reforming by electrochemical as a function of electrical charge in the presence of NaCl at an applied current intensity of 4.5 A by using synthetic glycerol solution pH of 1 with Pt electrode.

According to the GC/MS results, all generated compounds had many hydrogen and oxygen substitutions with C₂ to C₆ carbon compounds, and some of these compounds had known reaction pathways from glycerol, others do not. In order to provide the fundamental knowledge about the electrochemical reforming of glycerol, it is important to evaluate the mechanisms of synthesis of these valuable compounds from glycerol. However, it is still difficult to deduce an exact mechanism of their syntheses from glycerol by electrolysis in an acid solution. Rather, a hypothetical general scheme (Scheme 4.1) can be proposed with some probable paths for each studied system. According to this scheme, the transformation of glycerol under strong acidic conditions, both in the presence and in the absence of electricity, can be classified into four main reactions; protonation and dehydration, direct oxidation with electricity, oxidation with hydroxyl radicals (OH[•]) and reduction with electricity. All reactions lead to the formation of an identical carbon molecule intermediate species, which subsequently further changes to other chemical compounds, or to smaller carbon compounds by breaking the C-C bond or to higher carbon compounds by coupling reaction.

Under strong acid conditions in the absence of NaCl and electricity, either the 1^o- or 2^o- alcohol group of glycerol could be dehydrated and consequently protonated to form two types of intermediates, 2,3-dihydroxypropene and 1,3-propenediol or 3-hydroxypropanal which rapidly rearranged to 1-hydroxyl-2-propanone and acrylaldehyde, respectively. These two species could be also produced by the electrochemical reforming of glycerol in acid solution. Namely, when the electricity was applied, OH[•] radicals which were produced from the oxidation reaction of H₂O on the Pt electrode could attract the H atom of the -OH group at the C₁ or C₂ of the glycerol molecule and consequently dehydrated leading to the formation of two enol intermediate species, which rapidly rearranged to acrylaldehyde and 1-hydroxyl-2-propanone, respectively. These two species were very active, acrylaldehyde could be dehydrated further to propene or hydrolyzed/protonated/reduced to 1,3-propanediol. For 1-hydroxyl-2-propanone, it could be rearranged to the more stable propanoic acid, dehydrated to propanal, or protonated by the excess protons in solution leading to 1,2-propanediol, a commercially valuable chemical. In addition, 1-hydroxyl-2-propanone could cleave the C₁-C₂ bond leading to the formation of formaldehyde and a C₂ free

radical, which could further reduce or react with OH^\bullet to form acetaldehyde and acetic acid, respectively. With respect to the propanal species, besides the dehydration of 1-hydroxy-2-propanone, it could be produced from the two-step reduction of glycerol. The generated propanal could be considered as an isomer of 2-propenol, which could subsequently react with glycerol to form 2-ethoxy-4-methanol-1,3-dioxolane and further isomerized to form 2-methyl-1,3-dioxane. Besides the above, the OH^\bullet radical could directly attack the unpaired electron of the 1°-OH group of glycerol and then via a dehydration reaction and rearrangement led to the formation of 2,3-dihydroxypropanal. Regarding the reactions with radicals, the $\text{C}_1\text{-C}_2$ bond of glycerol was proposed to be cleaved by the oxidation reaction to form a C_1 alcohol free radical, which was then further dehydrated to formaldehyde, and the C_2 free radical (ethylene free radical) was further dehydrated to acetaldehyde or reduced to ethylene glycol. The generated formaldehyde was unstable but could either react with glycerol to form the stable 5-hydroxy-1,3-dioxolane product, or it could be further oxidized by OH^\bullet radicals to formic acid. One more valuable compound was observed by the electrochemical reforming of glycerol is glycidol. It was believed that the glycerol molecule was protonated by H^+ at the 2°-OH group and consequently dehydrated leading to the formation of the glycerol carbonium ion, which was further rearranged to glycidol. In the presence of NaCl, the main reforming compounds of glycerol before and after supplying electricity were similar to those obtained in the absence of NaCl. Exceptionally, one more compound obtained from glycerol reforming in the presence of NaCl, 2-chloromethyl-1,3-dioxane, was produced from the substitution of Cl^- ions with 2-methyl-1,3-dioxane.

ศูนย์วิจัยทรัพยากร
จุฬาลงกรณ์มหาวิทยาลัย



Scheme 4.1. Possible reaction pathways of synthetic glycerol reforming to 1,3-propanediol and value-added compounds by electrochemical technique.

4.1.4 Preliminary study of electrochemical reforming of crude glycerol

The preliminary study of crude glycerol from biodiesel production reforming to 1,3-propanediol was investigated at the current intensity of 4.5 A, initial pH of 1 and the concentration of NaCl of 2.93 g/l by using Pt electrode. It was found that the normalized concentration (Figure 4.24 (a)), glycerol reforming (Figure 4.24 (b)) and the yield of 1,3-propanediol (Figure 4.25) obtained from crude glycerol reforming were lower than that of synthetic glycerol solution. By using crude glycerol, the yield of 1,3-propanediol was about 4.76 % at 100 Ah/l electrical charge, about 8.57-fold lower than that of synthetic glycerol solution. This might be attributed to the fact that crude glycerol from biodiesel plant was contaminated by various compounds as demonstrated in Figure 4.26. These contaminants might be affected the kinetics of glycerol reforming to 1,3-propanediol. Therefore, to increase the yield of 1,3-propanediol from crude glycerol, the contained contaminants should be removed.

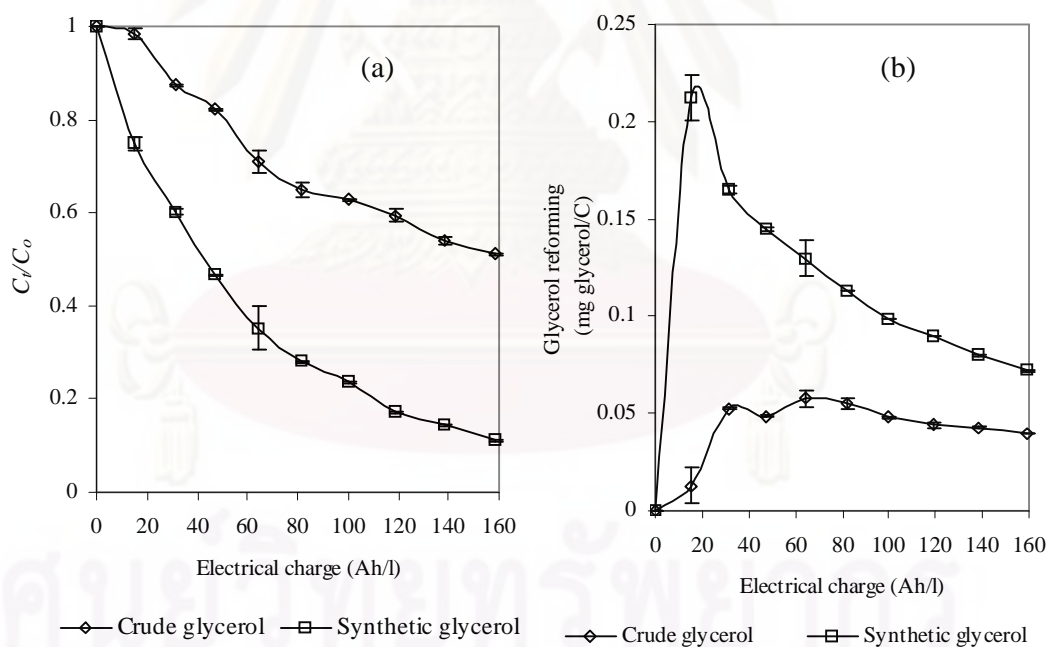


Figure 4.24 Evaluation of the normalized concentration (a) and glycerol reforming (b) as a function of electrical charges by using different glycerol sources including synthetic glycerol solution and crude glycerol solution.

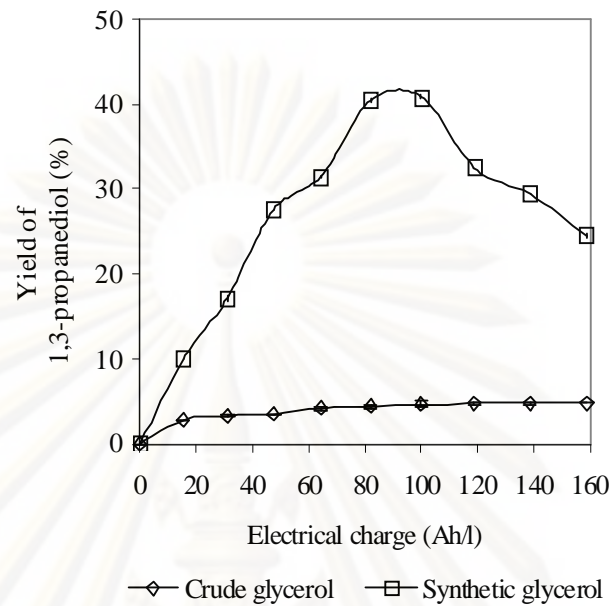


Figure 4.25. The yield of 1,3-propanediol as a function of electrical charges by using different glycerol sources including synthetic glycerol solution and crude glycerol solution.

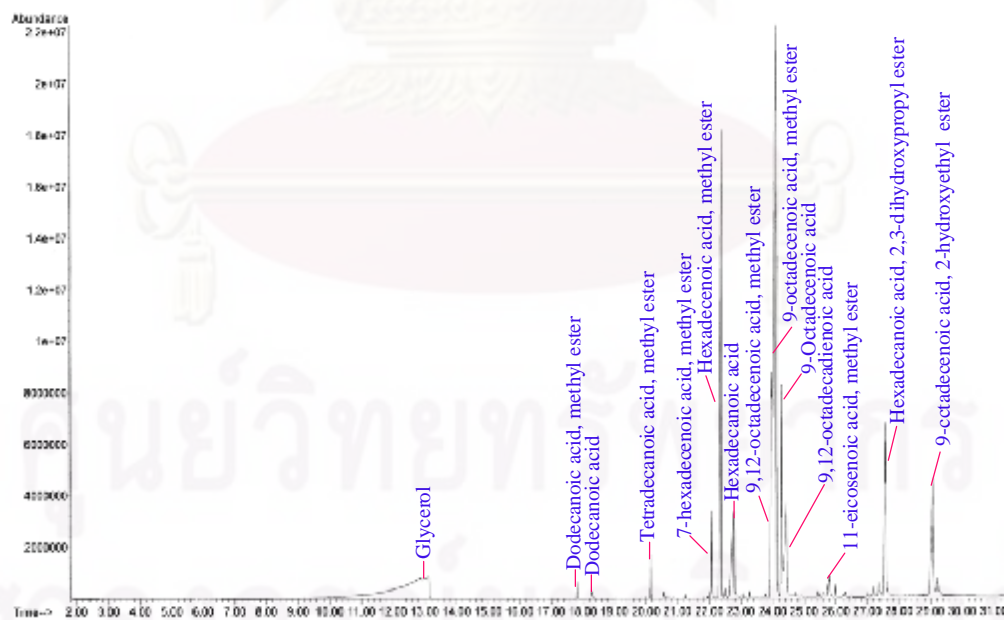


Figure 4.26. Representative GC/MS chromatogram of crude glycerol obtained from the waste used-oil biodiesel production plant.

4.2 Purification of crude glycerol from biodiesel plant

The purification of crude glycerol from waste biodiesel plant was carried out by using chemical treatment. In this work, the purification of crude glycerol consists of two-routes. For the first route, the pH of crude glycerol was adjusted to 1, 2.2, 3.5 and 6 by the addition of 1.19 M H_2SO_4 or H_3PO_4 for phase-separation including glycerol-rich layer. This layer was neutralized with 12.50 M NaOH and KOH, and then evaporated for water elimination. After that, the enriched glycerol was extracted with $\text{C}_2\text{H}_5\text{OH}$. The glycerol-ethanol solution was filtrated to eliminate the crystallized salt, and then evaporated for ethanol elimination. The characteristics of the purified final glycerol were analyzed according to the established ISO and ASTM standards. Finally, the purified crude glycerol as the optimal condition was extracted by $n\text{-C}_6\text{H}_{14}$, and then characterized again.

For second route, the pH of crude glycerol was adjusted pH to 2.2 by the addition of 1.19 M H_3PO_4 for phase-separation including glycerol-rich layer. This layer was extracted by $n\text{-C}_6\text{H}_{14}$ to eliminate MONG. After that, glycerol-rich layer was neutralized with 12.50 M KOH, and then evaporated for water elimination. Next, the enriched glycerol was extracted with $\text{C}_2\text{H}_5\text{OH}$. The glycerol-ethanol solution was filtrated to eliminate the crystallized salt. Finally, the characteristics of the purified glycerol were analyzed according to the established ISO and ASTM standards.

4.2.1 Characteristics of the original crude glycerol from waste used-oil biodiesel plant

The original crude glycerol from the waste used-oil methyl ester plant was a dark brown liquid with a high pH of 10.5, low density and low viscosity compared to the commercial glycerol. Indeed, it contained about 28.56% w/w of glycerol with high contents of ash, water and MONG contaminants, as summarized in Table 4.1. The ash content (3.07% w/w) was largely composed of inorganic matter such as sodium salts, which were originated from the utilized catalyst (NaOH) during the transesterification process, while the water content (5.40% w/w) might be attributed to the water content of raw-materials used for biodiesel production. The largest contaminant was MONG (62.42% w/w), which exactly exceeded the glycerol levels, and was generated by the contamination of soap, methanol, and methyl esters in the glycerol residue from the

biodiesel production process. During the acidification and phase separation based on the purification stage, some of the fatty acids were released as soluble soap, and some of methyl esters dissolved or suspended in the glycerol solution. These free fatty acids and methyl esters reacted with the excess NaOH in the subsequent neutralization stage to re-form soap which remained in the glycerol residue (Yong et al., 2001).

The functional groups of contaminants in crude glycerol were analyzed by FTIR technique and compared to commercial glycerol (Figure 4.27 (a)). The main functional groups of commercial glycerol, including the O-H stretching at 3350 cm^{-1} , C-H stretching at 2880 and 2930 cm^{-1} , C-O stretching at 2100 cm^{-1} , C-O-H bending at 1400 to 1460 cm^{-1} , C-O stretching from 1450 cm^{-1} (primary alcohol) to 1100 cm^{-1} (secondary alcohol), O-H bending at 920 cm^{-1} and also the H_2O blending at 1650 cm^{-1} were apparently observed. However, the spectra of the original crude glycerol obtained from the waste used-oil biodiesel plant (Figure 4.27 (b)) additionally shows a strong FTIR peaks at 1580 cm^{-1} and 1740 cm^{-1} while a small band at 3050 cm^{-1} , indicating the presence of some impurities. The sharp band at 1580 cm^{-1} represented the presence of COO^- function of soap. The small band at 3050 cm^{-1} indicated the presence of unsaturated C=C compound(s), supported by the positive result attained with the Baeyer test by KMnO_4 . The sharp peak at 1740 cm^{-1} indicated the presence of C=O compound(s) of an ester or carboxylic acid of fatty acid.

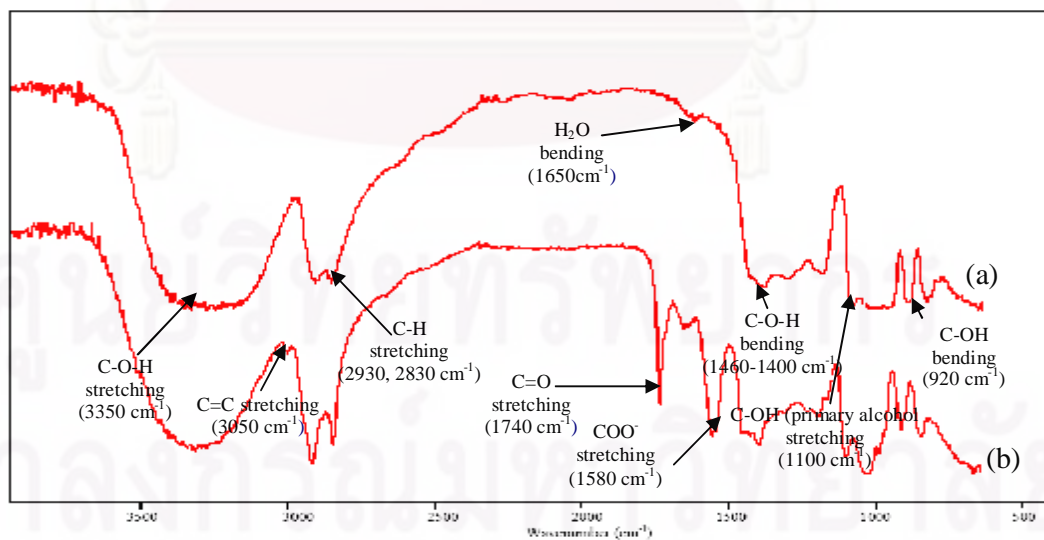


Figure 4.27. Representative FTIR spectra of commercial glycerol (a) and crude glycerol from biodiesel production plant (b).

The composition of original crude glycerol was all characterized by GC/MS, as shown in Figure 4.26. The main compound observed in the original crude glycerol represented the glycerol. Moreover, the main fatty acids and methyl ester contaminated in crude glycerol were saturated aliphatic of fatty acid compounds; hexadecanoic acid or palmitic acid ($\text{CH}_3(\text{CH}_2)_{14}\text{COOH}$), dodecanoic acid or lauric acid ($\text{CH}_3(\text{CH}_2)_{10}\text{COOH}$), methyl-ester, methyl tetradecanoate ($\text{CH}_3(\text{CH}_2)_{12}\text{COOCH}_3$) and unsaturated aliphatic of fatty acid compounds; octadecenoic acid or oleic acid ($\text{CH}_3(\text{CH}_2)_7\text{CH}=\text{CH}(\text{CH}_2)_7\text{COOH}$).

Table 4.1. Characteristics of crude glycerol, commercial glycerol, and purified crude glycerol compared with The BS standard.

Parameters	BS 2622:1979 (Ooi et al., 2001)	Commercial glycerol (Fisher)	Crude glycerol	Purified crude glycerol
pH		6.97	10.5±0.71	7.12±0.71
Glycerol content (%)	>88	99.98	28.56±0.64	97.92±0.16
Ash content (%)	<1.0	0.0002	3.07±0.16	0.01±0.01
Water content (%) (ISO 2097-1972)	No	0.01	5.40±0.42	1.28±0.01
Matter organic non glycerol (MONG) (%) (ISO 2464-1973)	<1.5	0.0008	62.42±0.86	0.79±0.06
Density at 20°C (g/cm^3) (ISO 2099-1972)		1.27	1.03± 0.02	1.26±0.05
Viscosity at 40°C (cSt) (ASTM D 445)		267.70	42.21±0.28	254.82±0.46
1,3-propanediol (%)	<0.5	0	0	0
Color		Clear	Dark brown	Light brown

4.2.2 Composition and characteristics of the purified crude glycerol followed route I

The pH of crude glycerol was varied in various conditions (1, 2.2, 3.5 and 6) by using 1.19 M H_2SO_4 or H_3PO_4 . According to the acidity of different pH values, the original crude glycerol automatically phase-separated into four distinct layers during the purification stage. The upper layer was free fatty acid, the second layer was char and soap layer, the third layer was glycerol-rich layer, and lower layer was alkaline-catalyst. Focusing on the free fatty acid, char and soap and alkaline-catalyst were removed by gravitational decantation and filtration. The remained glycerol layer was contaminated by methanol, free fatty acid, mono-, di-, tri-glycerides and methyl esters formed under the catalytic activity over alkaline-catalyst (NaOH) and the waste used-oil substrate (Ooi et al., 2001 and Chi et al., 2007).

Figure 4.28 shows the weight fraction of all the distinct layers obtained from the H_2SO_4 or H_3PO_4 acidification stage at different pH values. It was found that the increasing of pH stage from 1.0 to 6.0 led to the decrease of glycerol-rich layer, alkaline-catalyst, and free fatty acid layers, whereas char or soap layer was increased. Namely, by using 1.19 M H_2SO_4 , the glycerol, alkaline-catalyst and free fatty acid quantities decreased from 40.73 to 34.96 %, 2.10 to 0.06 % and 38.35 to 10.17 %, respectively in every pH conditions. Conversely, it increased the char and soap quantities from 18.64 to 54.52 %. This might be attributed to the fact that the strong acid condition can neutralize the alkaline catalyst, which will be precipitated out as the bottom layer and converted soap back to free fatty acids as the top layer (Hájek and Skopal, 2010). On the other hand, by using 1.19 M of H_3PO_4 for adjusting the same pH conditions (1.0 – 6.0), the glycerol, catalyst-phosphate and free fatty acid quantities decreased from 41.27 to 29.36 %, 1.97 to 0.05 % and 36.04 to 8.26 % respectively while the char and soap increased from 19.61 to 62.28 %. For the catalyst-phosphate, the conditions with pH of 2.2 exhibited the catalytic activity higher than that at pH 1.0 since the alkaline-catalyst might be dissolved in strong acid solution. This is because the solvent (water) in glycerol-rich layer at pH of 1.0 was higher than that at pH of 2.0 leading to the increase of alkaline-catalyst solubility.

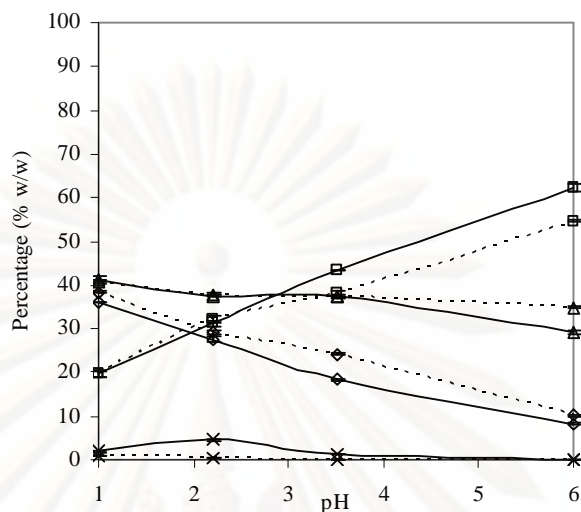


Figure 4.28. Weight fraction of the four distinct layers, free fatty acid layer (\circ), char and soap layer (\blacksquare), glycerol-rich layer (\triangle) and alkaline-catalyst layer (\times) obtained from the H_2SO_4 (---) and H_3PO_4 (—) acidification stage of crude glycerol purification at different pH values.

Certainly, the pH and acid types of the acidification stage during the chemical treatment influenced strongly on the composition of the purified crude glycerol (Figure 4.29). The MONG, ash, and water contents in the purified crude glycerol were lower than the original levels in crude glycerol from the waste used-oil biodiesel plant. Moreover, when the glycerol was treated at low pH, the amount of contaminants was lower than the glycerol treated at high pH. However, the glycerol content decreased with increasing pH during the acidification stage. This might be due to the excess sulphate ions or phosphate ions from H_2SO_4 or H_3PO_4 , which added during the acidification stages, reacted with the sodium ions from the contaminated salts in the crude glycerol to form the relatively insoluble Na_2SO_4 or Na_3PO_4 in an aqueous solution (Hájek and Skopal, 2010). At low pH, it consequently crystallized out during the phase separation and evaporation stages (Israel et al., 2008). Hence, the crude glycerol purified at a low pH value contained less salts, measured in terms of ash content. For MONG, its fraction in the purified crude glycerol, at all pH values by using 1.19 M H_2SO_4 or H_3PO_4 in the acidification mediated phase separation stage, was lower than that in the crude glycerol before treatment. Increasing the pH of the

purification system seemed to enhance the MONG content due to the fact that a large amount of free fatty acid was separated from the crude glycerol under strong acid conditions, leading to a lower amount of MONG in the purified crude glycerol. Nevertheless, it is difficult to completely eliminate MONG contaminated in the purified crude glycerol by this methodology. This cause by the fact that free fatty acids, short (C_{6-8}) and medium chains (C_{10-14}), can dissolve in the polar glycerol phase rather than partition into the upper free fatty acid phase (Chi et al., 2007).

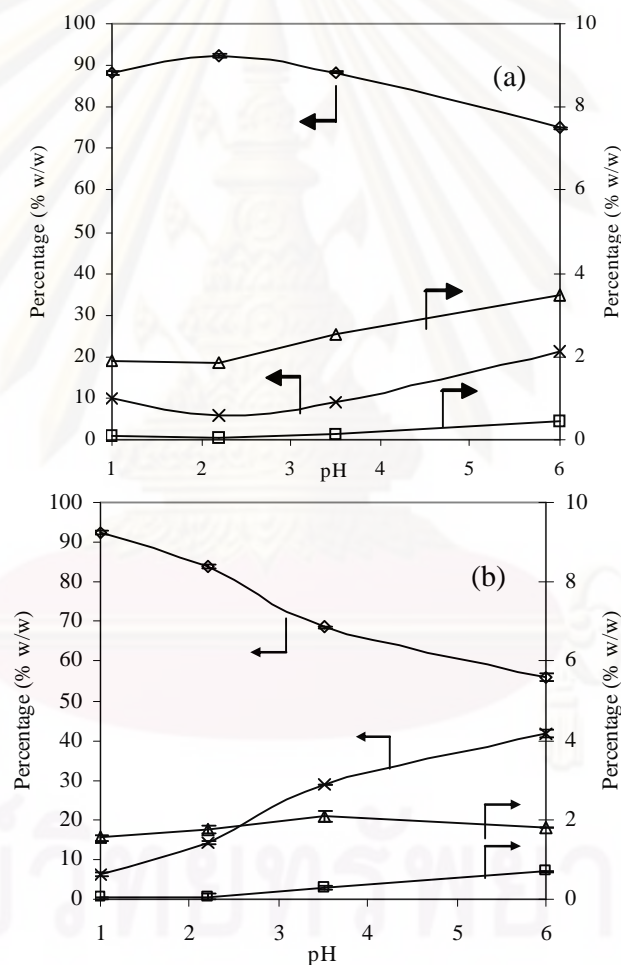


Figure 4.29. Weight fraction of glycerol (\square), ash (\pounds), water (r), and MONG (\bar{I}) contents in glycerol-rich layer obtained from the H_3PO_4 (a) and H_2SO_4 (b) acidification stages of glycerol at different pH values.

As mentioned in the chapter 3, the glycerol-rich layer was then neutralized with NaOH, evaporated, and extracted with C₂H₅OH to obtain high purity glycerol. The FTIR spectrum of the purified crude glycerol in various pH values in the range of 1.0 – 6.0 by addition 1.19 M H₃PO₄ (Figure 4.30 (a')) or H₂SO₄ (Figure 4.30 (b')) was compared with the spectra of the commercial glycerol and the crude glycerol. The principle functional groups of all glycerol solutions were similar to Figure 4.27. Each sample had the peaks of the O-H stretching at 3350 cm⁻¹, C-H stretching at 2880 and 2930 cm⁻¹, C-O stretching at 2100 cm⁻¹, C-O-H bending at 1400 to 1460 cm⁻¹, C-O stretching from 1450 cm⁻¹ (primary alcohol) to 1100 cm⁻¹ (secondary alcohol), O-H bending at 920 cm⁻¹ and also H₂O bending at 1650 cm⁻¹. However, all purified crude glycerol samples acidified at all pH values conditions revealed a much smaller peak than the original crude glycerol at 1580 cm⁻¹, which represented the presence of COO⁻ function of soap. Consequently, this was significantly reduced when the pH in the acidification stage was reduced. The possible explanation might be attributed to the fact that the acidification can reduce and convert the soap bulk to insoluble free fatty acids. For the strong acid condition, large amount of free fatty acid was separated. In addition, strong bands at 1710 and 3050 cm⁻¹ in the original crude glycerol, according to the presence of unsaturated aliphatic of carboxylic acid compound(s), were extremely reduced in strong acid condition and disappeared in the spectra of the purified glycerol at pH of 1.0. It can be emphasized that large amounts of impurities were eliminated at such condition. According to the results of this part, the optimum acidification stage in purification of crude glycerol was found at pH of 2.2 by addition 1.19 M H₃PO₄ and it provided the glycerol content of around 92 wt%.

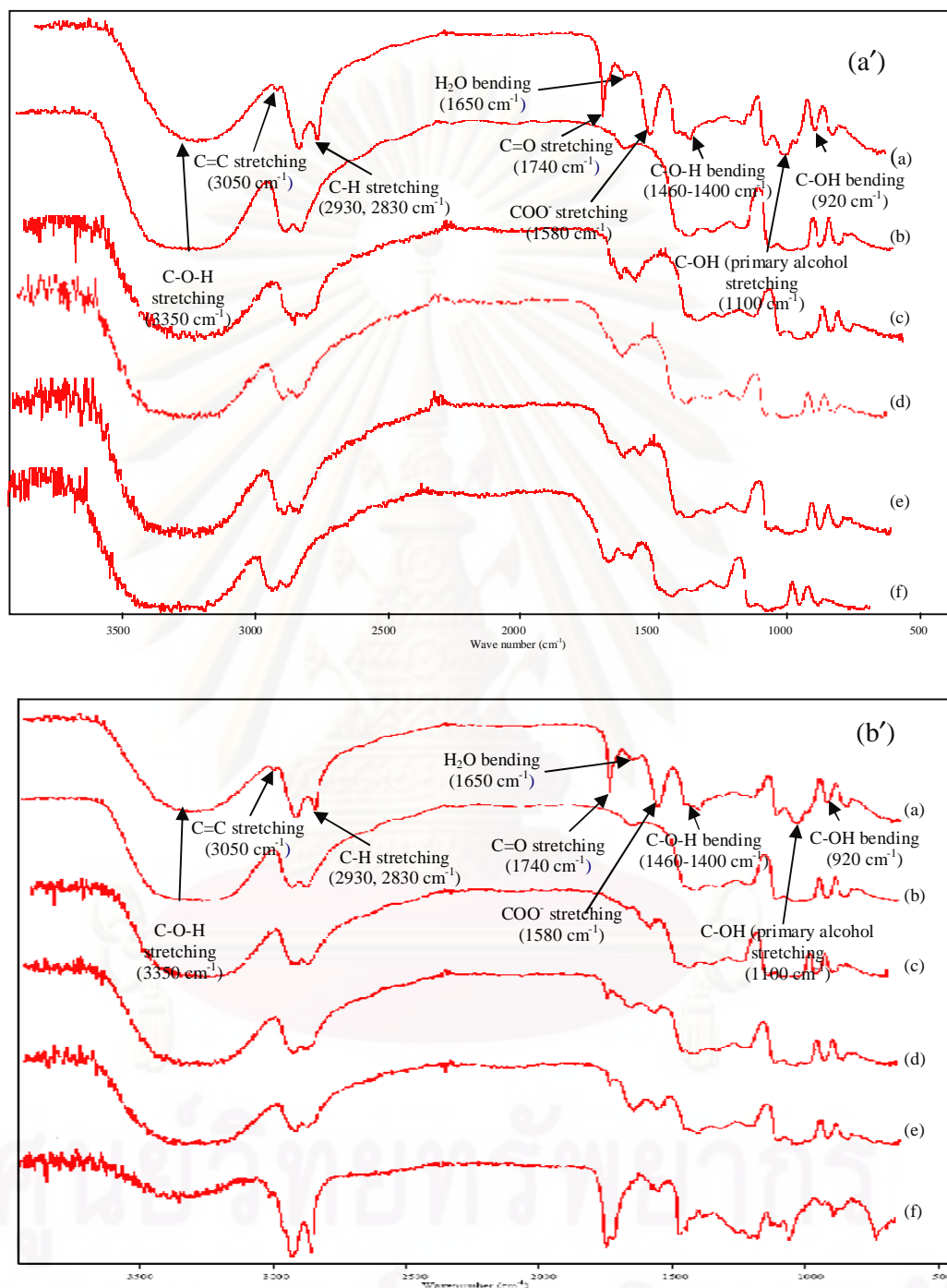


Figure 4.30. Representative FTIR spectra of the crude glycerol (a), a commercial glycerol (b) and purified crude glycerol with the H_3PO_4 (a') and H_2SO_4 (b') performed at a pH of 1.0 (c), 2.2 (d), 3.5 (e) and 6.0 (f).

To investigate the effect of base types during the neutralization stage, two types of base including NaOH and KOH were used to neutralize the pH of glycerol-rich layer pH of 2.2. It was clearly found that the contents of MONG, water, ash and glycerol in the purified crude glycerol were nearly the same by using both types of basic chemicals, as shown in Table 4.2. However, the purified glycerol using NaOH had some black particles and free fatty acid on surface. The glycerol content was decreased after leaving about a week as shown in Figure 4.32 (e). In addition, the neutralized glycerol-rich layer by using NaOH provided more alkali-salt in environment than by using KOH. It may be attributed to the fact that K^+ has larger molecule compared with Na^+ , which can be precipitated with PO_4^{3-} to K_3PO_4 (by-product of neutralization as potash phosphate fertilizer) as shown in the Figure 4.31. This reason can lead to reduce the K^+ content in glycerol-rich layer and purified crude glycerol.

Table 4.2. The contents of glycerol, ash, water, and MONG in purified crude glycerol obtained after base neutralization and extraction.

Sample	Parameters of characterization			
	Glycerol (%wt)	Ash (%wt)	Water (%wt)	MONG (%wt)
A	92.07±0.12	0.06±0.01	1.79±0.01	6.08±0.12
B	93.14±0.18	0.01±0.01	1.74±0.05	5.11±0.13
C	94.04±0.18	0.01±0.01	1.74±0.05	4.21±0.27

Note

A: the purified crude glycerol acidified at pH of 2.2, neutralized with NaOH, evaporated, and extracted with C_2H_5OH .

B: the purified crude glycerol acidified at pH of 2.2, neutralized with KOH, evaporated, and extracted with C_2H_5OH .

C: the purified crude glycerol acidified at pH of 2.2, neutralized with KOH, evaporated, extracted with C_2H_5OH and $n-C_6H_{14}$.

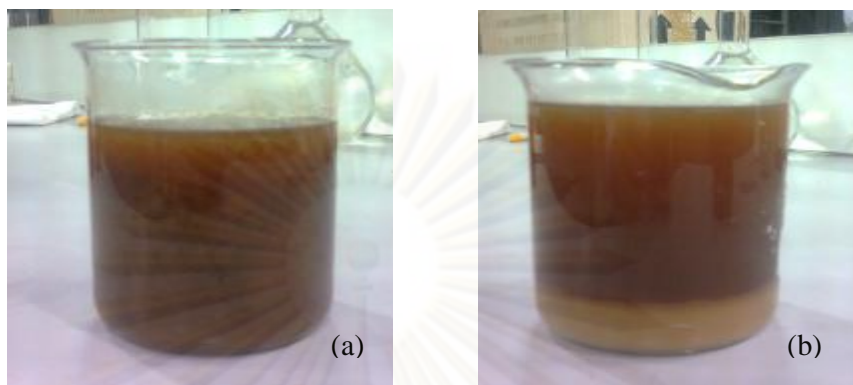


Figure 4.31. The neutralized glycerol-rich layer with NaOH (a) and KOH (b) after leaving for 5 h.

From the effect of pH, types of acid and basic chemical substances, it was observed that the values of MONG, water, ash and glycerol contents in purified crude glycerol were 5.11%, 1.74%, 0.01%, and 93.14%, respectively at pH of 2.2 set by H_3PO_4 , neutralized with KOH and extracted with $\text{C}_2\text{H}_5\text{OH}$. However, the values of MONG in purified crude glycerol was still higher compared with the BS standard of around 3.5-fold. Since the MONG in the origin of crude glycerol and by-products from the side reaction during the purification glycerol stage is difficultly reduced by polar solvent. As mentioned previously, it is necessary to use non-polar solvent such as $n\text{-C}_6\text{H}_{14}$ to extract the MONG content from the purified glycerol. The results showed that the MONG content decreased from 5.11 to 4.21% after extracted with $n\text{-C}_6\text{H}_{14}$, as demonstrated in Table 4.2. In comparison to the purified crude glycerol, the MONG content in the purified glycerol was still higher than the limitation of the BS standard around of 2.8-fold. This cause by the fact that the purified glycerol had high viscosity resulting in difficulty of mixing between glycerol phase and extracting solvent.

4.2.3. Composition and characteristics of the purified crude glycerol followed route II

The pH of crude glycerol was adjusted to 2.2 by 1.19 M H_3PO_4 and then extracted by non-polar solvent ($n\text{-C}_6\text{H}_{14}$). Afterward, the glycerol-rich layer was neutralized with 12.50 M KOH and extracted with excess $\text{C}_2\text{H}_5\text{OH}$. It was found that

all contaminants were markedly reduced to the level of the BS standard. The MONG, water, ash and glycerol contents in the purified glycerol were about 0.79 %, 1.28 %, 0.01 % and 97.92 % w/w, respectively.

Figure 4.32 shows an example of crude glycerol before and after purification with chemical and physical treatments after left for a week at the other conditions compared with the commercial glycerol. At the optimum condition (Figure 4.32 (h)), the color of the purified crude glycerol is light brown with no black particle.

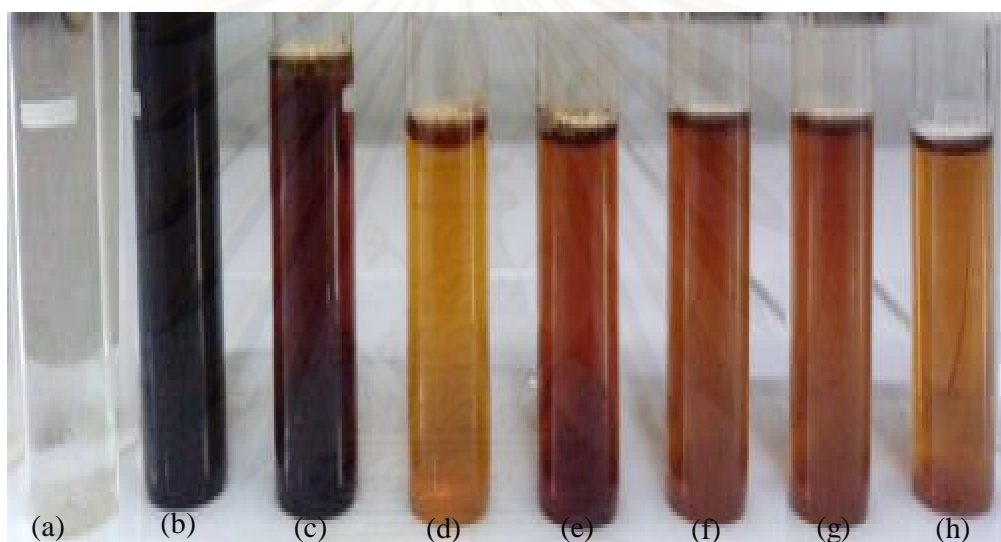


Figure 4. 32. Representation of commercial glycerol (a), crude glycerol (b) and purified crude glycerol with H_2SO_4 (c) and H_3PO_4 (d) at pH of 1, purified crude with H_3PO_4 at pH of 2.2 after neutralization with NaOH (e) and KOH (f) and extraction with $n\text{-C}_6\text{H}_{14}$ (g) and purified crude glycerol with H_3PO_4 at pH of 2.2 after extraction with $n\text{-C}_6\text{H}_{14}$, neutralization with KOH, and extraction with $\text{C}_2\text{H}_5\text{OH}$ (h).

4.2.4 Characteristics of purified crude glycerol

The purified crude glycerol via chemical treatment proposed in this work was characterized by the FTIR spectra (Figure 4.33), the ^{13}C -NMR chromatogram (Figure 4.34), the GC/MS chromatogram (Figure 4.35) and comparison with the BS standard specification for (Table 4.1). From the FTIR spectra, the main function groups of glycerol including the O-H stretching at 3350 cm^{-1} , C-H stretching at 2880 and 2930 cm^{-1} , C-O-H bending at 1400 to 1460 cm^{-1} , C-O-H stretching from 1450 cm^{-1}

(primary alcohol) to 1100 cm^{-1} (secondary alcohol), O-H bending at 920 cm^{-1} and also the H_2O blending at 1650 cm^{-1} were found in the purified crude glycerol (Figure 4.33 (c)). However, the strong FTIR bands of C=O stretching was observed at 1720 cm^{-1} indicating the presence of remained methyl ester compounds.

From the ^{13}C -NMR of glycerol, the spectrum of aliphatic carbon of 1° - and 2° -alcohol of glycerol molecule were demonstrated the signal at 66.4 and 74.3 ppm, respectively (Figure 4.34 (a)). In addition, signals at 184 ppm of carboxyl compounds (-COOH), 131 ppm of unsaturated aliphatic of hydrocarbon (-C=CH-), 49.5 ppm of alpha methyl ester compounds, 39 ppm of alpha aliphatic carbon of carboxyl group (- CH_2COOH), 20-35 ppm of aliphatic carbon in long chain hydrocarbon compounds (- $\text{CH}_2\text{-CH}_2$ -)_{n,n=6-16} and 16 ppm of methyl group (- CH_3) were signification detected indicating the presence of contaminants in crude glycerol (Figure 4.34 (b)). The additional signals related to the structure of contaminants were disappeared indicated that some contaminants in crude glycerol were eliminated by chemical treatment as demonstrated in Figure 4.34 (c).

Figure 4.35 demonstrated the GC/MS spectra of commercial glycerol (Figure 4.35 (a)), crude glycerol (Figure 4.35 (b)) and purified crude glycerol (Figure 4.35 (c)). The main signals of organic compounds observed in crude glycerol were glycerol and contaminants such as hexadecanoic acid or palmitic acid and dodecanoic acid or lauric acid, methyl tetradecanoate and unsaturated aliphatic of fatty acid compounds as 9-octadecenoic acid or oleic acid. After the chemical and physical treatments, some signals of contaminants were disappeared as shown in Figure 4.35 (c). However, the purified crude glycerol was still contaminated by a small quantity of methyl ester such as hexadecenoic acid, methyl ester and 9-octadecenoic acid, methyl ester from initial crude glycerol.

From all results, it can be said that the chemical treatment proposed in this work was effective to purify crude glycerol coming from the waste-used oil biodiesel plant and its properties were closed to that of commercial, as also demonstrated in Table 4.1. Although the amount of glycerol, MONG and ash in the purified crude glycerol were in the acceptable range of the BS standard, the purified crude glycerol was contaminated by water (~1.20 % wt) and the color of the purified crude glycerol

derived from this work was light brown color. Therefore, further purification step such as adsorption process should be carried out to reduce water and color.

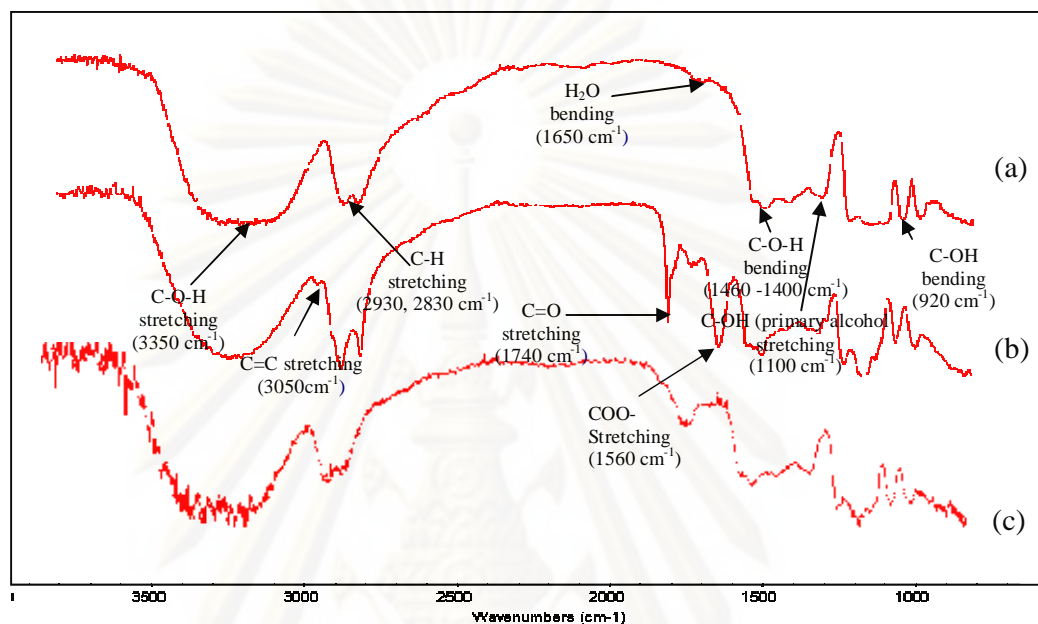


Figure 4.33. Representative FTIR spectra of commercial glycerol (a), crude glycerol (b) and purified crude glycerol (c).

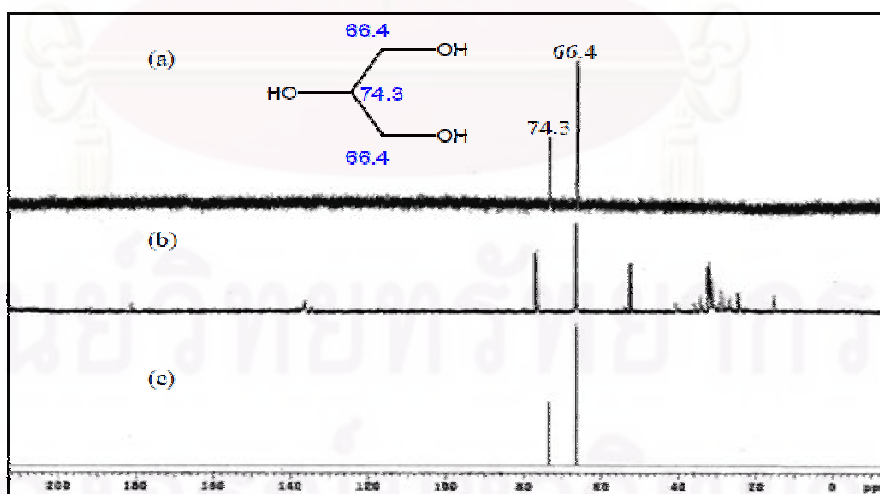


Figure 4.34. Representative ^{13}C -NMR spectra of commercial glycerol (a), crude glycerol (b) and purified crude glycerol (c).

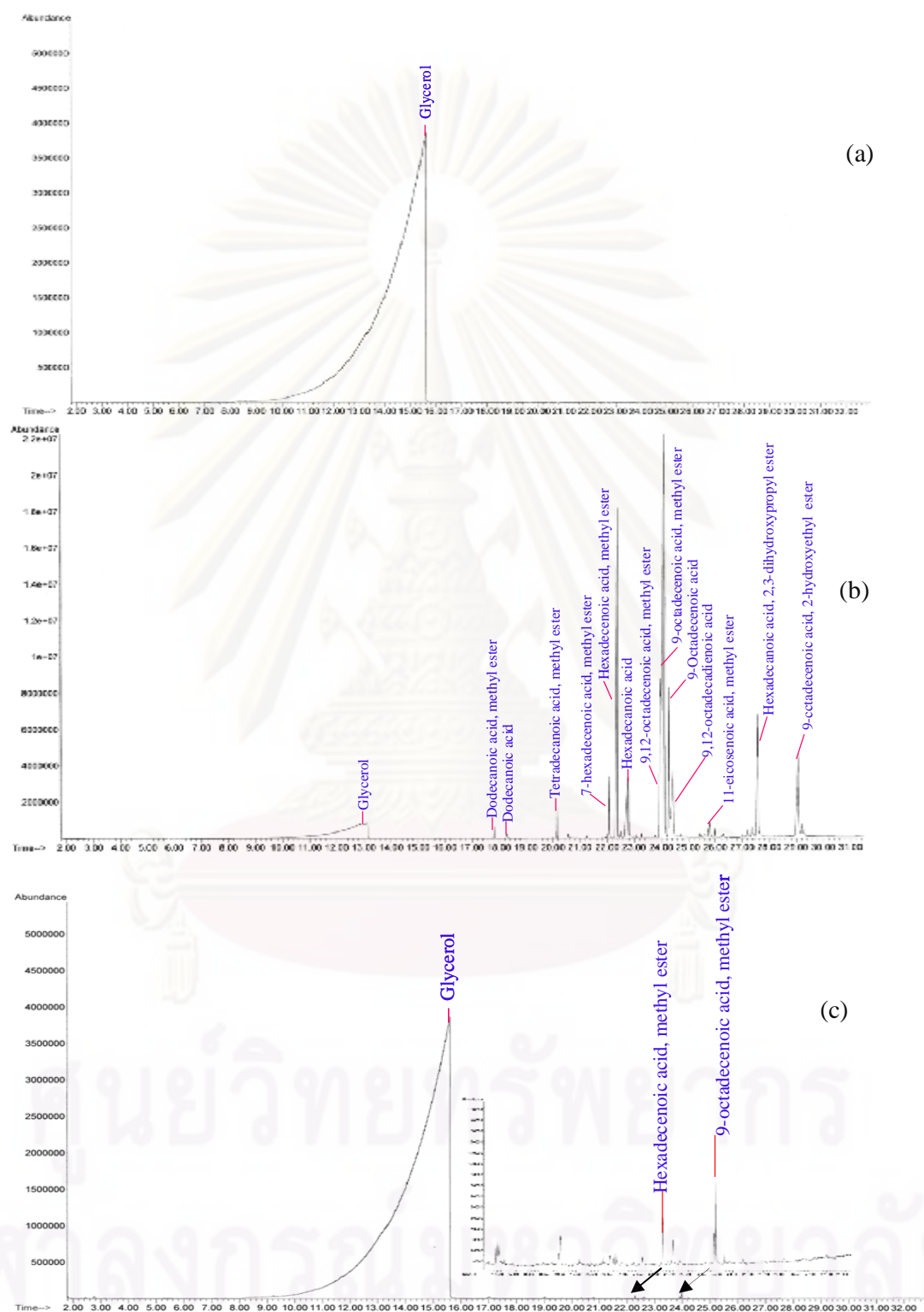


Figure 4.35. Representative GC/MS spectrums of commercial glycerol (a), crude glycerol (b) and purified crude glycerol (c).

Table 4.3 summarized the properties of the purified crude glycerol of this work compared with the previous works. It can be seen that the chemical treatment affected not only for the crude glycerol obtained from the biodiesel plant with the virgin oil such as palm kernel oil but also for the waste used-oil. However, the weight percentage of the purified crude glycerol from this work was higher than that from the work of Ooi et al., (2001) around 1.91-folds. This might be attributed to the operation of different solvent during the extraction stage. With respect to the effect of purification procedure, it can be concluded that our treatment was more effective than the ion exclusion (Asher et al., 1956) and bipolar electro dialysis (Schaffner et al., 2003) but less effective than the chemical and vacuum distillation (Hazimah et al., 2003). However, the former has very low original glycerol content (2.5% w/w) and the later has very high glycerol content (70 and 65% w/w). Furthermore, the chemical and vacuum distillation processes being as the 2-steps purification including chemical method and vacuum distillation, this still technique required high operating temperature (110-120 °C) and low pressure (0.1-3 mbar) which was difficult to control in real situation. For the ion extraction and bi-polar electro dialysis, their performance strongly depended on the concentration of impurities in crude glycerol. In the presence of high impurity contents, some contaminated ions such as Na⁺ and fatty acid could deposit on the membrane surface leading to lower the efficiency of purification.

Table 4.3 Comparison of purified crude glycerol properties obtained from this work with other works.

Author(s)	Source of crude glycerol	Purification procedure	Glycerol (% w/w)		Ash (% w/w)		MONG (% w/w)		Water (% w/w)	
			(a)	(b)	(a)	(b)	(a)	(b)	(a)	(b)
Asher and Simpson (1956)	Soap lye solution	Ion exclusion	7.5	82.5	13	7	-	-	-	-
Ooi et al (2001)	Transesterification of palm kernel oil	Chemical treatment	17.7	51.4	58.7	13.8	17.7	25.9	5.9	8.9
Hazimah et al (2003)	Fatty acid plant	Chemical and vacuum distillation	70	99.3	4	7	-	-	-	-
Schaffner et al (2003)	Synthetic solution	Bipolar electro dialysis	65	95	2	0.054	4	0.56	4	0.45
This work	Transesterification of waste used-oil	Chemical treatment	28.56	97.92	3.07	0.01	62.42	0.79	5.40	1.28

(a) Concentration of glycerol and impurities content in the original crude glycerol

(b) Concentration of glycerol and impurities content in the purified crude glycerol

4.3 Electrochemical reforming of purified crude glycerol

4.3.1 Current density-potential curve

Figure 4.36 illustrated the polarization curve of the purified crude glycerol solution comparison with synthetic glycerol and the crude glycerol from biodiesel plant at initial pH of 1 with the Pt electrode. It was found that the oxidation-reduction peaks of the purified crude glycerol were clearly observed in strong acid solution (pH 1) which was similar to the synthetic glycerol solution. The oxidation-reduction peaks of the purified crude glycerol were presented two oxidation peaks (peaks A and B) during the forward sweep and one reduction peaks (peak C) and one oxidation peak (peak D) during the backward sweep. The principle differences among them were the oxidation peak potential and current density. The maximum oxidation peaks of the purified glycerol solution was observed at -0.19 and 0.85 V/Ag/AgCl, corresponding to a current density of 0.21 and 1.64 mA/cm², respectively. During the backward sweep, the peak shapes were also practically these same with a single reduction (peak C) and oxidation (peak D) peaks. The maximum oxidation peak of the purified crude glycerol was observed at 0.31 V/Ag/AgCl which was corresponding to a current density of 0.58 mA/cm². Also, the reduction peak was observed at a potential of 0.40 V/Ag/AgCl which was relating to the current density of 1.21 mA/cm². According to the polarization curve, it was clear that the oxidation-reduction of purified crude glycerol was principally observed under very strong acid conditions. Therefore, the reforming of purified crude glycerol and product were further explored at pH of 1.

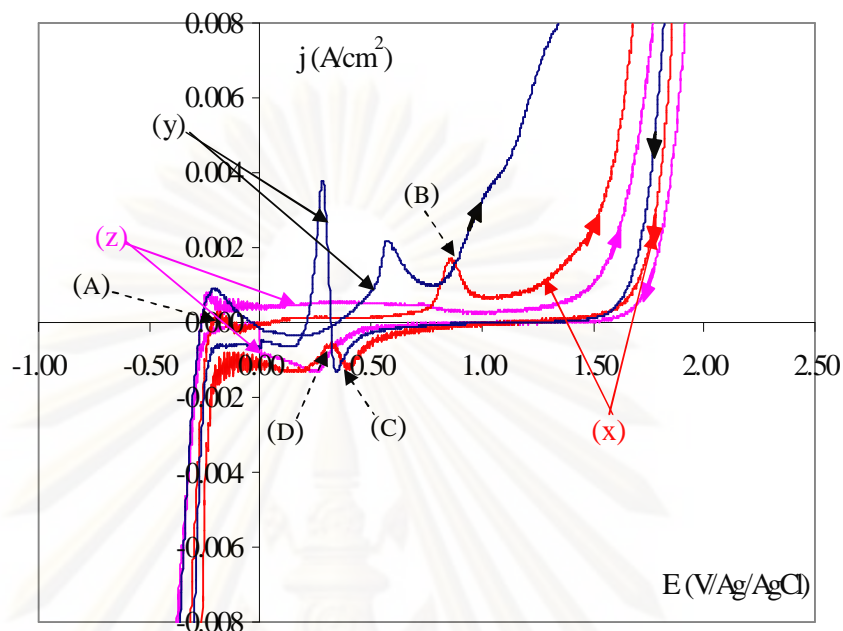


Figure 4.36. Current density-potential curves of the purified crude glycerol (x), synthetic glycerol (y) and the crude glycerol solution (z) at pH of 1 by using the Pt electrodes with a constant magnetic stirring rate of 400 rpm. The scan rate was 5 mV/s with Ag/AgCl reference electrode.

4.3.2 Effect of parameter on purified crude glycerol reforming

- Effect of current intensity

Effect of applied current intensity on the purified crude glycerol reforming to 1,3-propanediol was then explored in the range of 3.75 - 6.5 A at pH of 1 adjusted by H_2SO_4 with Pt electrodes. The change of concentration of glycerol and electrical charge depended strongly on the current intensity. The increasing current density led to the decrease of normalized concentration and increased the glycerol reforming according to Faraday's law. It was found that the highest glycerol reforming was obtained at 0.0964 mg glycerol/C at an applied current intensity of 6.5 A as shown in Figure 4.37. The rate constant of pseudo-first order of glycerol reforming on different applied current intensities was demonstrated in Figure 4.37. The rate constant of glycerol reforming decreased from 0.046 to 0.1955 h^{-1} when the current intensity was increased from 3.75 to 6.5 A. This implies that the rate of glycerol degradation was fast in the presence of a high-applied current intensity. However, at this condition, the

yield of 1,3-propanediol dropped rapidly from 20.35% at an electrical charge of 171.7 Ah/l to around 14.93% at electrical charge of 229.41 Ah/l (Figure 4.39). This might be due to the reforming of glycerol to other compounds such as formic acid and propene or it had the complete reforming of glycerol to CO_2 at high current intensity and long electrolysis times (Li et al., 2005). So, the optimum current intensity for the purified crude glycerol reforming to 1,3-propanediol was selected at 6 A, which provided the yield of 1,3-propanediol of about 26.31 %.

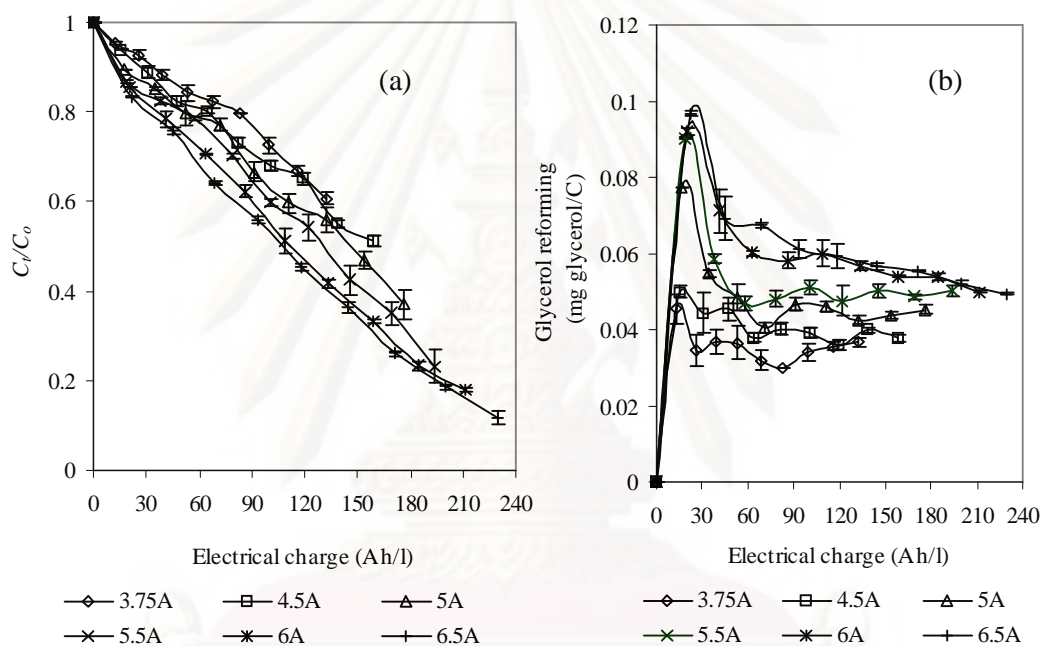


Figure 4.37. Evaluation of the normalized concentration (a) and glycerol reforming (b) as a function of electrical charges at different applied current intensities by using purified crude glycerol solution at the concentration of 46.2 g/l and pH of 1 with Pt electrode.

ศูนย์วิทยาศาสตร์
จุฬาลงกรณ์มหาวิทยาลัย

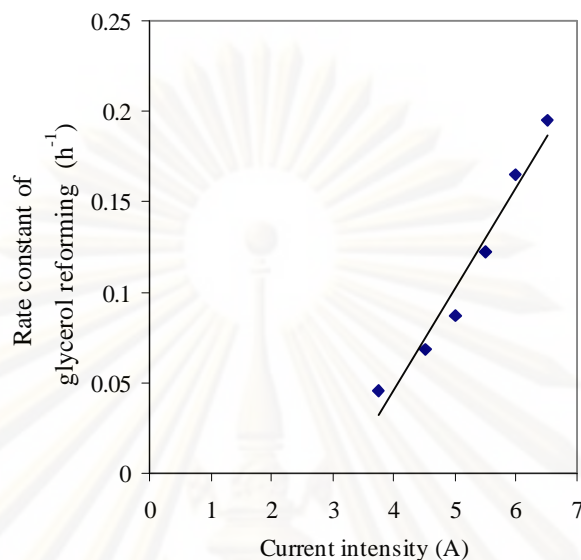


Figure 4.38. Plot of rate constant of pseudo-first-order kinetics of glycerol reforming as a function of current intensity by using purified crude glycerol solution at the concentration of 46.2 g/l and pH of 2 with Pt electrode.

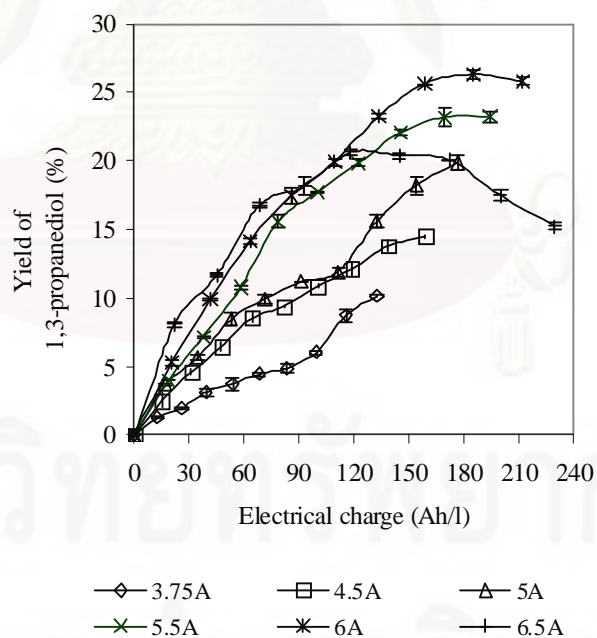


Figure 4.39. The yield of 1,3-propanediol as a function of electrical charges at different applied current intensities by using purified crude glycerol solution at the concentration of 46.2 g/l and pH of 1 with Pt electrode.

- Effect of concentration of NaCl

The effect of NaCl concentration was studied in the range of 0 – 8.78 g/l with the current intensity of 6 A and initial pH of 1 by using Pt electrode as demonstrated in Figure 4.40. It was found that the presence of NaCl can achieve a small increase of the normalized concentration (Figure 4.40 (a)) and glycerol reforming (Figure 4.40 (b)). The maximum glycerol reforming was observed around 0.10 mg glycerol/C in the presence of 8.78 g/l NaCl at electrical charge of 20.34 Ah/l. The rate constant of pseudo-first order of glycerol reformation on different concentration of NaCl shows in Figure 4.41. The rate constant of glycerol reforming increased from 0.1650 to 0.1738 h⁻¹ when the concentration of NaCl was increased from 0 to 8.93 g/l.

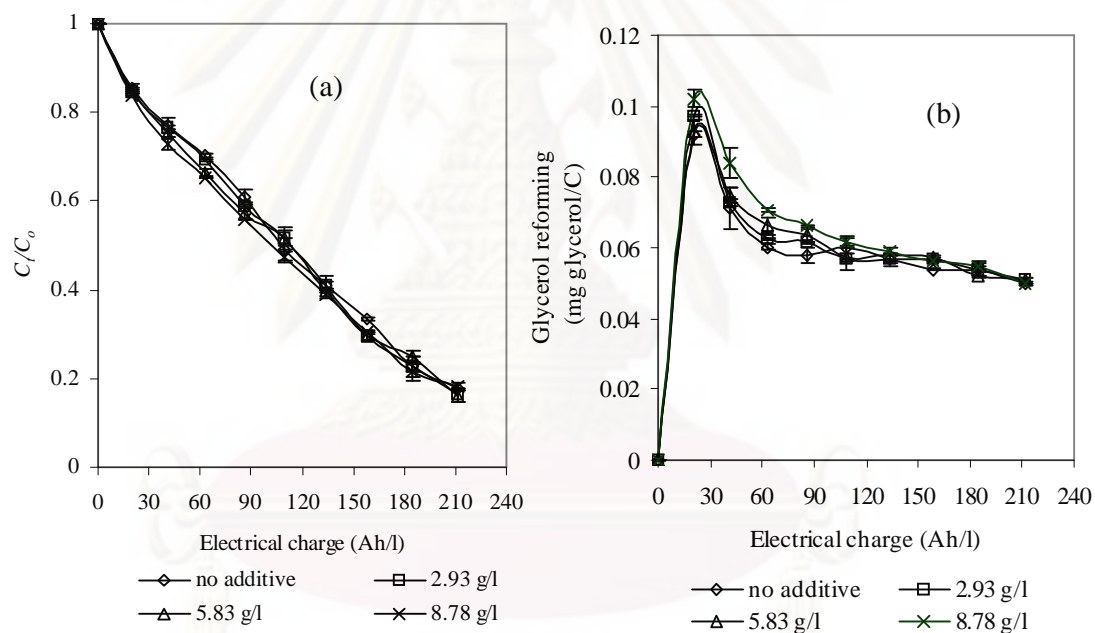


Figure 4.40. Evaluation of the normalized concentration (a) and glycerol reforming (b) as a function of electrical charges at different concentrations of NaCl by using purified crude glycerol solution at the concentration of 46.2 g/l, current intensity of 6 A and pH of 1 with Pt electrode.

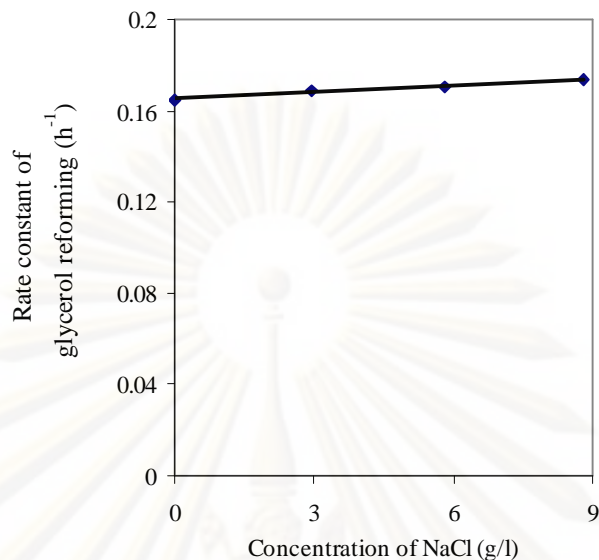


Figure 4.41. Plot of rate constant of pseudo-first-order kinetics of glycerol reforming as a function of different concentration of NaCl by using purified crude glycerol solution at the concentration of 46.2 g/l, current intensity of 6 A and pH of 1 with Pt electrode.

For the yield of 1,3-propanediol as shown in Figure 4.42, the different concentrations of NaCl provided the different yields of 1,3-propanediol. In the presence of NaCl of 2.93 and 5.83 g/l, the yield of 1,3-propanediol was increased small quantity but not significantly. However, increasing of concentration of NaCl from 0 to 2.93 or 5.83 g/l can reduce the electrical charge from 184.61 to 158.49 Ah/l which were corresponding to the reduction of electrolysis time from 8 to 7 h. It can be explained that, in the presence of NaCl, the oxidizing agent (OCl) was produced leading to the fast reaction rate of glycerol reforming. On the other hand, by using the NaCl at the dosage of 8.78 g/l, the yield of 1,3-propanediol decreased sharply particularly at long electrolysis time. It was probably due to the reforming of glycerol to other intermediates or CO₂.

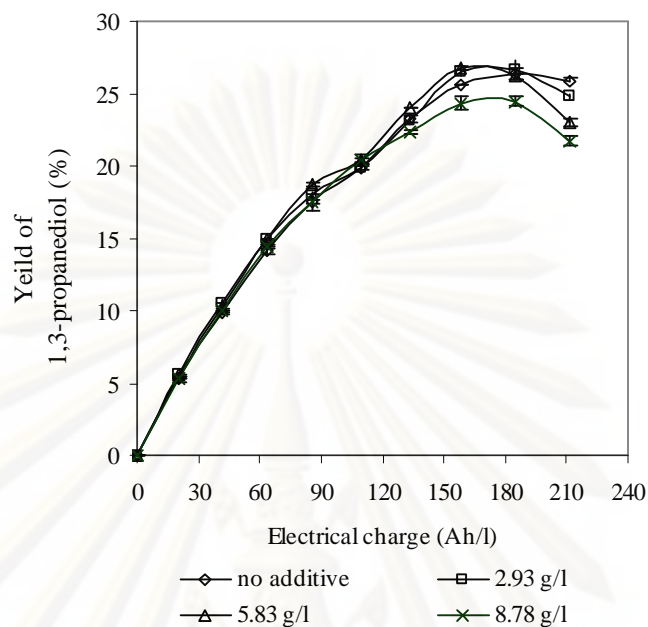


Figure 4.42. The yield of 1,3-propanediol as a function of electrical charges at different concentrations of NaCl by using current intensity of 6 A and initial pH of 1 with Pt electrode.

4.3.3 Mechanisms of purified crude glycerol reforming to 1,3-propanediol

From the GC/MS spectra of the purified crude glycerol solution at pH 1 in the absence of NaCl (Figure 4.43 (a)) or in the presence of NaCl (2.93 g/l) (Figure 4.43 (b)) before supplying electricity, five chemical species were observed; 1-hydroxyl-2-propanone (acetol), acrylaldehyde (acrolein), propene, pentanol and heptanoic acid. The pentanol and heptanoic acid were obtained from the reforming of contaminants in purified crude glycerol. Figure 4.44 demonstrated the GC/MS spectra of glycerol solution at pH of 1 in the absence of NaCl (Figure 4.44 (a)) or in the presence of NaCl (2.93 g/l) (Figure 4.44 (b)) obtained after electrolysis by employing the current intensity of 6 A and initial pH of 1 by using Pt electrode at the electrical charge of 184.61 Ah/l. The detected compounds in both electrolyte were propene, acrylaldehyde, propanal, 1,2-propanediol, 1,3-propanediol, 4-hydroxymethyl-1,3-dioxolane, 5-hydroxyl-1,3-dioxane, pentyl propionate, 2-ethyl-1,3-dioxolane-4-methanol, pentanol, 2,5-dimethyl-1,4-dioxane, heptanoic acid, pentanone,

pentyl acetate, pentanone, 2-methyl-1,3-dioxane, propylene oxide and 5-hydroxyl-2-methyl-1,3-dioxane.

Figure 4.45 shows the area of glycerol and various compounds generated by electrochemical in the absence of NaCl using the current intensity of 6 A and initial pH of 1 by using Pt electrode. It can be seen that the quantity of glycerol, pentanol and heptanic acid decreased with the increase of electrical charge. For 1,3-propanediol, the maximum quantity was found at an the electrical charge of 184.61 Ah/l after that it seemed to be constant. The quantities of the three reforming products, including pentyl propionate, 2-methyl-1,3-dioxane and propene, increased clearly as a function of an electrical charge indicating that those products were the stable parts. For 2-ethyl-4-methanol-1,3-dioxolane, 2,5-dimethyl-1,4-dioxane, pentanone and pentanone, a maximum area was observed at the electrical charge of 133.3 Ah/l. The quantities of other products including 1,2-propanediol, 1-hydroxyl-2-propanone (acetol), acrylaldehyde (acrolein) increased slightly when the electrical charge increased. The maximum area of 4-hydroxymethyl-1,3-dioxolane, 5-hydroxyl-1,3-dioxane and pentyl acetate was obtained at the electrical charge of 85.72, 133.33 and 158.19 Ah/l, respectively. For propylene oxide, it was found that its quantity increased within the electrical charge of 109.09 Ah/l after that it did not significantly change in the presence of electrical charges.

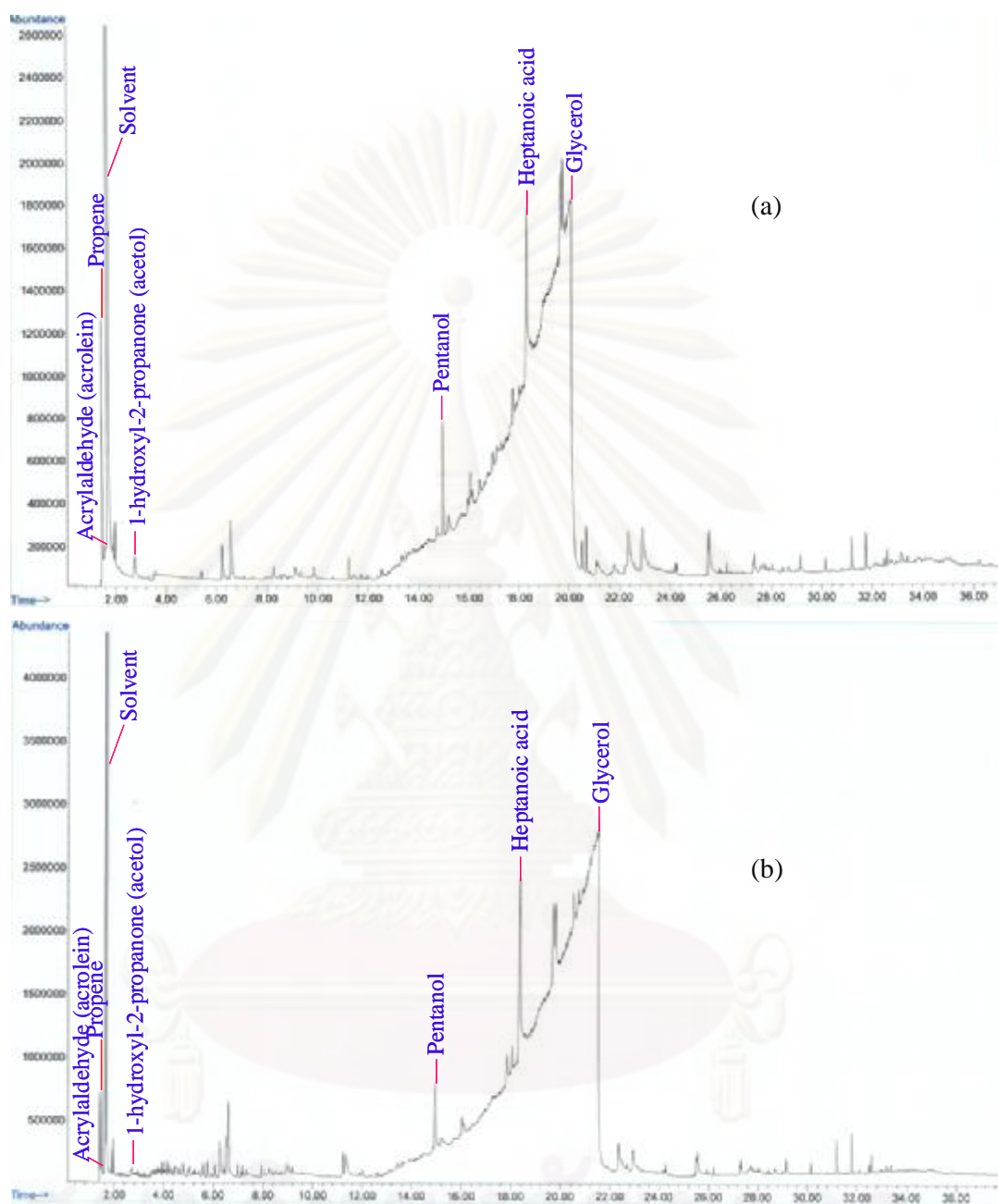


Figure 4.43. Representative GC-MS spectra of purified crude glycerol solution at pH 1 in the absence of NaCl (a) and the presence of NaCl (b) before supplying electricity.

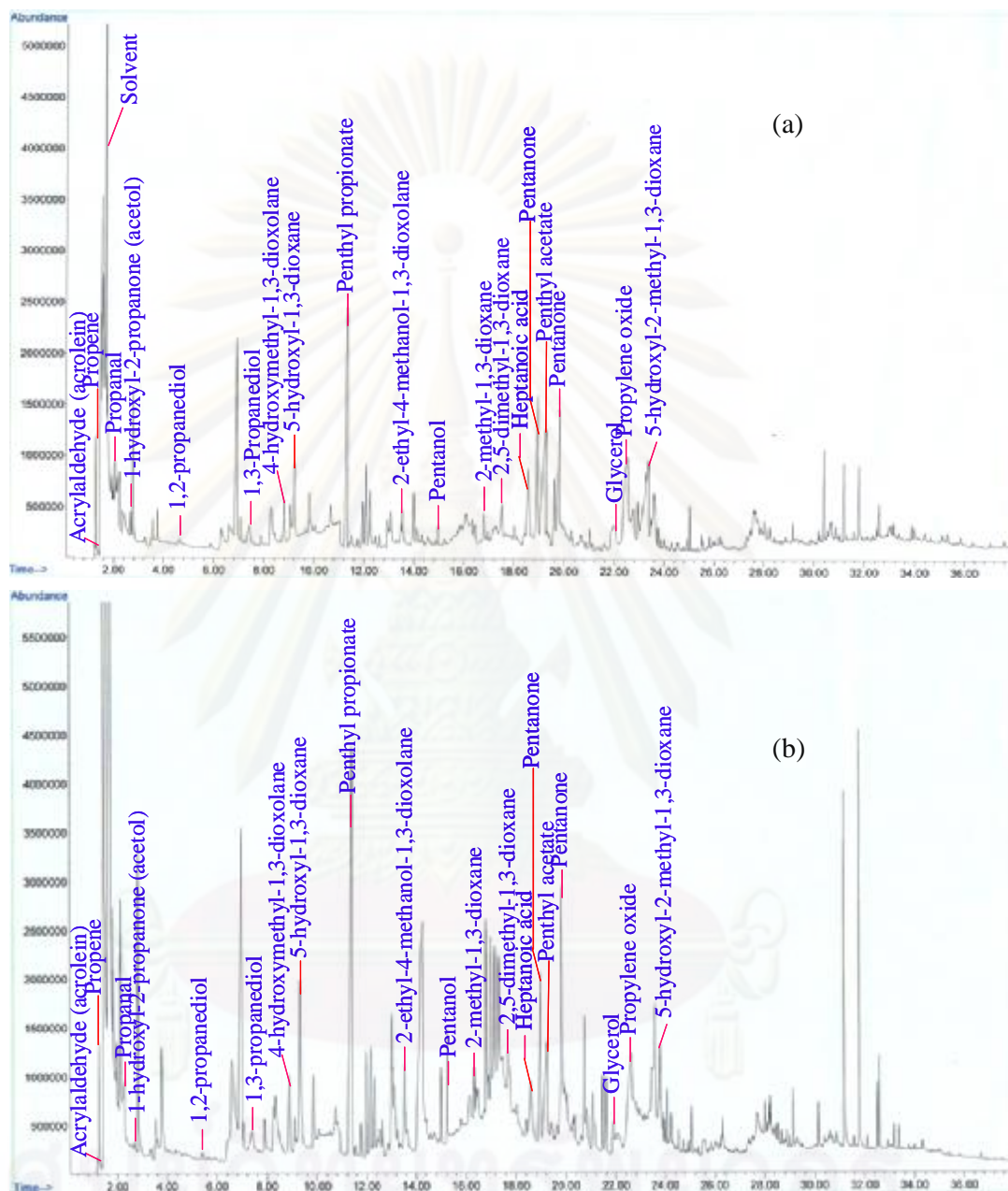


Figure 4.44. Representative GC-MS spectra of purified crude glycerol solution
 glycerol solution at pH of 1 in the absence of NaCl (a) and the presence of NaCl (b)
 obtained after electrolysis by employing the current intensity of 6 A by using Pt
 electrode at the electrical charge of 184.61 Ah/l.

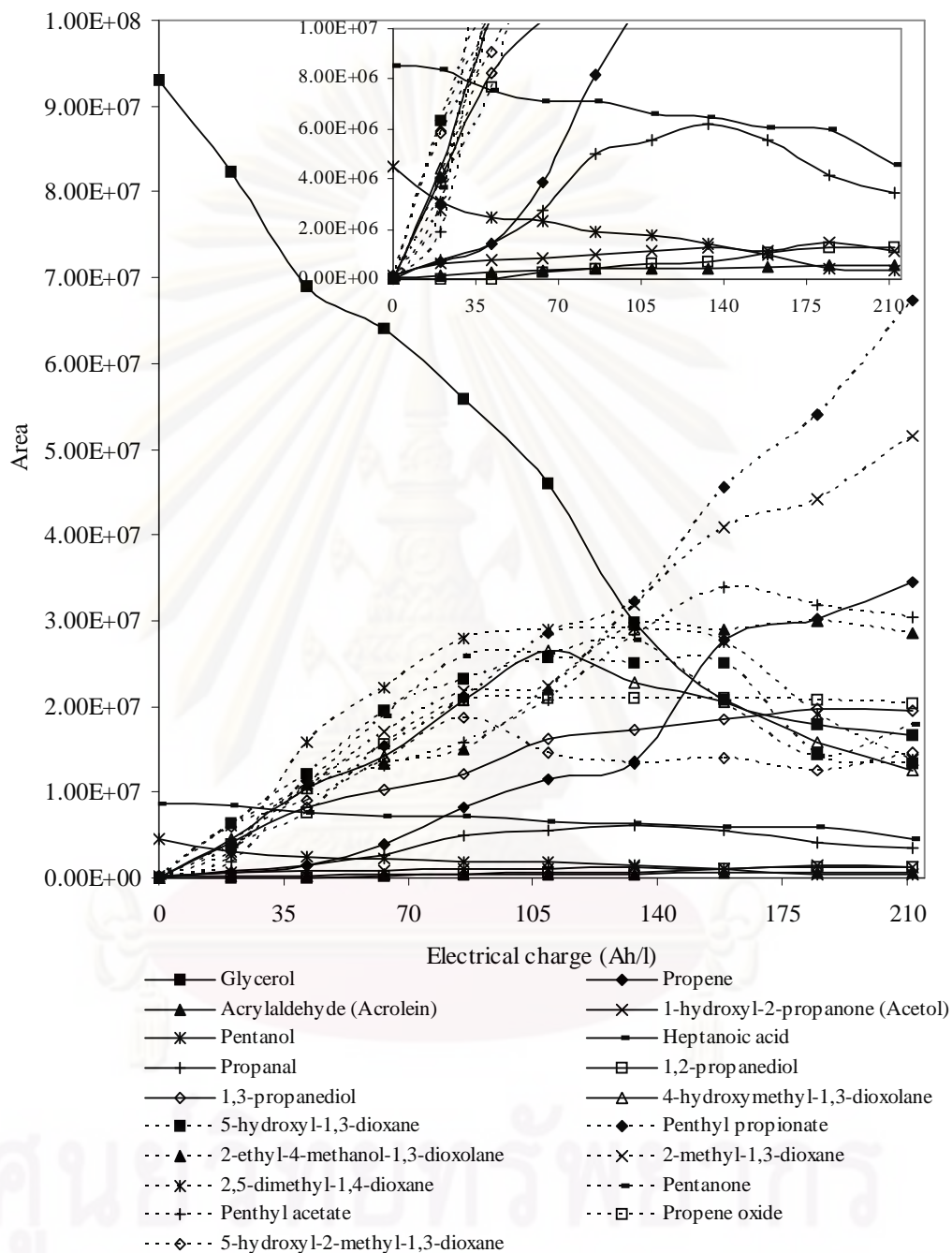


Figure 4.45. Quantity of various compounds generated from purified crude glycerol reforming by electrochemical as a function of electrical charge in the absence of NaCl at an applied current intensity of 6 A by using purified crude glycerol solution pH of 1 with Pt electrode.

All of these compounds had many hydrogen and oxygen substitutions with C₂ to C₁₀ carbon compounds, and whilst some of these compounds had known reaction pathways from purified crude glycerol, others do not. In order to provide the fundamental knowledge about the electrochemical reforming of purified crude glycerol to evaluate the mechanisms of synthesis of these valuable compounds from purified crude glycerol. It is still difficult to realize an exact mechanism of their synthesis compounds from purified crude glycerol by electrolysis in an acid solution because free fatty acid contaminated in purified crude glycerol effects on the pathways of reaction mechanisms. A hypothetical scheme (Scheme 4.2.) can be proposed with some possible paths for each studied system.

According to this scheme, the transformation of purified crude glycerol under strong acidic conditions, both in the presence before supplying electricity, could be classified into three main routes; acid protonation and hydration, direct oxidation with electricity and oxidation with hydroxyl radicals (OH[•]). All routes led to the formation of an identical carbon molecule intermediate species, which subsequently further changed to other chemical compounds, or to smaller carbon compounds by breaking of the C-C bond, or to higher carbon compounds by coupling reaction. Under strong acid conditions in the absence of NaCl and electricity, either the 1^o- or 2^o- alcohol group of glycerol could be dehydrated and consequently protonated to form two types of intermediates, 2,3-dihydroxypropene and 1,3-propenediol or 3-hydroxypropanal which rapidly rearranged to 1-hydroxyl-2-propanone and acrylaldehyde, respectively. These two species could also be produced by the electrochemical reforming of purified crude glycerol in acid solution. Namely, when the electricity was applied, OH[•] radicals which were produced from the oxidation reaction of H₂O on the Pt electrode could attach the H atom of the -OH group at the C₁ or C₂ of the glycerol molecule and consequently dehydrated leading to the formation of two enol intermediate species, which rapidly rearranged to acrylaldehyde and 1-hydroxyl-2-propanone, respectively. These two species were very active, acrylaldehyde could be dehydrated further to propene or hydrolyzed/protonated/reduced to 1,3-propanediol. For 1-hydroxyl-2-propanone, it could be rearranged to propanoic acid and then reacted with pentanol in acid solution to produce the more stable product as penthyl propionate. 1-hydroxyl-2-propanone dehydrated to propanal, or protonated by the

excess protons in solution leading to 1,2-propanediol. Next, 1,2-propanediol could be hydrolyzed to produce propene oxide or 2,5-dimethyl-1,4-dioxane in acid solution. In addition, 1-hydroxyl-2-propanone could cleave the C₁-C₂ bond leading to the formation of formaldehyde and a C₂ free radical, which could further reduce or react with OH• to form acetaldehyde and acetic acid, respectively. Acetic acid reacted with pentanol in acid solution to produce pentyl acetate. With respect to the propanal species, the dehydration of 1-hydroxyl-2-propanone, it could be produced from the two-step reduction of glycerol. The generated propanal could be considered as an isomer of 2-propenol, which can subsequently react with glycerol to form 2-ethyl-4-methanol 1,3-dioxolane and further isomerized to form 2-methyl-1,3-dioxane. The OH• radical could directly attack the C₁-C₂ bond of glycerol leading to the cleavage of C₁-C₂ bond to form a C₁ alcohol free radical, which was then further dehydrated to formaldehyde, and the C₂ free radical (ethylene free radical) which could further dehydrate to acetaldehyde. The generated formaldehyde was unstable but it can react with glycerol to form the stable 5-hydroxy-1,3-dioxolane and 4-hydroxymethyl-1,3-dioxolane products.

4.4 Comparison of yield of 1,3-propanediol from synthetic glycerol solution, crude glycerol and purified crude glycerol by electrochemical technique

For the synthetic and crude glycerol reforming to 1,3-propanediol by the electrochemical technique, the optimum operating conditions; an applied current intensity of 4.5 A, an initial pH of 1 set by H₂SO₄, 2.93 g/l NaCl and an electrical charge of 100 Ah/l with Pt electrodes; could be suggested to provide the yield of 1,3-propanediol by using synthetic and crude glycerol around 40.81% and 4.76%, respectively. For the purified crude glycerol reforming to 1,3-propanediol, the optimum conditions; an applied current intensity of 6 A, an initial pH of 1, and an electrical charge of 184.61 Ah/l with Pt electrodes; exhibited the yield of 1,3-propanediol around 26.31%. It was clearly seen that the yield of 1,3-propanediol by using crude glycerol from biodiesel production and purified crude glycerol was lower than that of synthetic glycerol around 8.75- and 1.55-fold, respectively. This might be attributed to the fact that the crude glycerol from biodiesel production had high contents of fatty acids, methyl ester (Figure 4.26) and water (Table 4.1) while the purified crude glycerol was still contaminated by a small quantity of methyl ester from initial crude glycerol (Figure 4.35 (c)) and water. As the results, the contaminants in crude and the purified crude glycerol had considerably affected on the yield of 1,3-propanediol because they can firstly react with OH[•] radical generated by electricity to produce some intermediates in system leading to a decrease of the production yield of 1,3-propanediol compared with synthetic glycerol.

4.5 Comparison of concentration and production yield of 1,3-propanediol between this work and some previous works.

Table 4.4 displays the comparison of the yield of 1,3-propanediol obtained from this work by electrochemical technique with other works. It can be seen that the yield of 1,3-propanediol obtained by this technique at the optimum condition was higher than that of hydrogenolysis reaction with Rh/C or with Pt/WO₃/ZrO₂ catalysts of around 1.56-fold and 1.72-fold, respectively by using synthetic glycerol. Although, the fermentation process with *K. pneumoniae* can provide a higher production yield of around 1.68-fold compared with the electroreforming process, it required special fermentation condition such as high cultivation temperature (40°C) and high pH (8.0).

In addition, it provided slowly reaction rate of 1,3-propanediol production due to its 2-step reaction.

Table 4.4. Comparison of concentration and production yield of 1,3-propanediol between this work and some previous works.

Authors	Processes	Initial concentration of glycerol (g/l)	Yield of 1,3-propanediol (%)
Chaminand et al., (2004)	Hydrogenolysis with Rh/C catalyst	15	26.67
Kurosaka et al., (2008)	Hydrogenolysis with Pt/WO ₃ /ZrO ₂ catalyst	0.1386	24.2
Zhang et al., (2007)	Fermentation by <i>K. pneumoniae</i> XJ-Li	66.4	70.0
This work	Electrochemical reforming of synthetic glycerol	46.2	40.56
	Electrochemical reforming of purified crude glycerol	46.2	26.31

CHAPTER V

CONCLUSIONS AND RECOMMENDATIONS

This work was carried out to determine the optimum conditions for reforming of glycerol to 1,3-propanediol by an electrochemical technique. The experiment of glycerol reforming was separated into three parts including the synthetic and crude glycerol reforming to 1,3-propanediol by an electrochemical technique, the purification of crude glycerol by chemical treatment, and the purified crude glycerol reforming to 1,3-propanediol by electrochemical technique.

The first part studied the synthetic and crude glycerol reforming to 1,3-propanediol by the electrochemical technique. Effects of various parameters including types of electrode, types of acid, current intensities, initial pH of glycerol solution, types of additives and their concentrations were determined. At the end of this part, mechanism of synthetic glycerol reforming was also explained. Optimum operating conditions; applied current intensity of 4.5 A, an initial pH of 1 set by H_2SO_4 , 2.93 g/l NaCl and an electrical charge of 100 Ah/l with Pt electrode; could be suggested to provide the yield of 1,3-propanediol by using synthetic and crude glycerol about 40.81% and 4.76%, respectively. The yield of 1,3-propanediol by using crude glycerol from biodiesel production was around 8.75-fold lower than that of synthetic glycerol since crude glycerol from biodiesel production has high contents of MONG, water and ash.

In the part of crude glycerol purification, the influences of the main parameters including pH condition, types of base and acid chemical substances, and solvent extraction were explored. The optimum condition was found at pH of 2.2 by the addition of 1.19 M H_3PO_4 , and by the extraction of glycerol-rich layer with n- C_6H_{14} , neutralization with KOH, and also extraction by excess $\text{C}_2\text{H}_5\text{OH}$. At this condition, greater than 97.92% glycerol was obtained, with low contaminant levels.

For the last part, reforming of purified crude glycerol to 1,3-propanediol, the optimum conditions; applied current intensity of 6 A, an initial pH of 1, and an electrical charge of 184.61 Ah/l with Pt electrode; exhibited the yield of

1,3-propanediol about 26.31%. The presence of NaCl during the glycerol reforming had no significant improvement in the yield of 1,3-propanediol.

Recommendations

To achieve a higher yield of 1,3-propanediol, the new types of electrode were suggested for further study such as Pt/WO₃/ZrO₂.

To develop the glycerol value-added, the production of more valuable compounds such as 1,2-propanediol, glycidol, and 2,3-dihydroxyl-propanal by electrochemical technique should be paid more attention.

From the results of the purification of crude glycerol, it can be further studied for industrial application.

The environmental costs of the disposal of the waste components and costs of used chemical (acid-alkali and extracting solvent) need to be evaluated. With respect to the color and water content of the purified crude glycerol derived from this work, the adsorption process seems to be the suitable option for reducing color and water.

REFERENCES

- A glycerin factor Biodiesel Magazine August/September. 2005. [Online] Available from:
http://biodieselmagazine.com/article.jsp?article_id=377&q=glycerol&page=1
[2009, 08 15].
- Alhanash A., Kozhevnikova E.F. and Kozhevnikov I.V. 2008. Hydrogenolysis of glycerol to propanediol over Ru: polyoxometalate bifunctional catalyst. Catalysis Letters 120: 307 - 311.
- Asher D.R. and Simpson D.W. 1956. Glycerol purification by ion exclusion. Journal of Physical Chemistry.60(5):518 - 521.
- Bard A.J. and Faulkner L.R. 2001. Electrochemical Methods: Fundamental and Application 2nd edition (n.p.): John Wiley & Sons.
- Besson M., Gallezot P., Pigamo A. and Reifsnnyder S. 2003 Development of an improved continuous hydrogenation process for the production of 1,3-propanediol using titania supported ruthenium catalysts. Applied Catalysis A: General 250: 117 - 124.
- Biodiesel. 2009. [Online] Available from:
<http://www.energy.go.th/moen/Index.aspx?MenuID=60>. [2009, 09 12].
- Bard A.J. and Stratmann M. 2007. Encyclopedia of electrochemistry electrochemical engineering. Volume 5: Wiley - VCH.
- Cameron D.C., Altaras N.E., Hoffman M.L. and Shaw A.J. 1998. Metabolic engineering of propanediol pathways. Biotechnology Progress 14: 116 - 125.
- Cerrate S., Yan F., Wang Z., Coto C., Sacakli P. and Waldroup P.W. 2006. Evaluation of glycerine from biodiesel production as a feed ingredient for broilers. International Journal of Poultry Science 5(11): 1001 - 1007.
- Chaminand J., Djakovitch L.a., Gallezot P., Marion P., Pinel C. and Rosier C. 2004. Glycerol hydrogenolysis on heterogeneous catalysts. Green Chemistry 6: 359 - 361.
- Chbihi M.E.M., Takky D., Hahn F., Huser H., Léger J.M. and Lamy C., 1999. In-situ infrared reflectance spectroscopic study of propanediol electrooxidation at

- platinum and gold: Part 1. 1,3-propanediol. Journal of Applied Electrochemistry. 463: 63 - 71.
- Chen G. 2004. Electrochemical technologies in wastewater treatment. Separation and Purification Technology 38: 11 - 44.
- Chen H.W., Wang W., Fang B.S. and Hu Z.D. 2004. Studies on fermentation conditions for key enzymes in 1,3-propanediol production with *Klebsiella Pneumoniae*. Journal of Chemical Engineering of Chinese Universities 18(5): 621 - 627.
- Chen X., Xiu Z., Wang J., Zhang D. and Xu P. 2003. Stoichiometric analysis and experimental investigation of glycerol bioconversion to 1,3-propanediol by *Klebsiella Pneumoniae* under microaerobic conditions. Enzyme and Microbial Technology 33(4): 386-394.
- Chi Z.P., Pyle D., Wen Z., Frear C. and Chen S. 2007. A laboratory study of producing docosahexaenoic acid from biodiesel-waste glycerol by microalgal fermentation. Process Biochemistry. 42:1537 - 1545.
- Ciriminna R., Palmisano G., Pina C.D., Rossi M. and Pagliar M. 2006. One-pot electrocatalytic oxidation of glycerol to DHA. Tetrahedron Letters 47: 6993 - 6995.
- Cortright R.D., Davda R.R. and Dumesic J.A. 2002. Hydrogen from catalytic reforming of biomass-derived hydrocarbons in liquid water. Nature 418: 964 - 967.
- Cyclic voltammetry. 2004. [Online] Available from: http://www.earlham.edu/~chem/chem341/c341_labs_web/cyclic_voltammetry.pdf. [2009, 05 13].
- Da Silva G.P., Mack M. and Contiero J. 2009. Glycerol: A promising and abundant carbon source for industrial microbiology. Biotechnology Advances 27: 30 - 39.
- Demirel-Gülen S., Lucas M. and Claus P. 2005. Liquid phase oxidation of glycerol over carbon supported gold catalysts. Catalysis Today 102 - 103: 166 - 172.
- Gerger I. and Haubner R. (2005). Cyclic voltammetry measurement on boron-and nitrogen-doped diamond layers. Diamond and Related Materials 14:369 - 374.
- Glycerin market analysis. 2009. [Online] Available from: http://www.asasea.com/download_doc.php [2009, 09 10].

- González-Pajuelo M., Meynial-Salles I., F. Mendes, Andrade J.C., Vasconcelos I. and Soucaille P. 2005. Metabolic engineering of *Clostridium acetobutylicum* for the industrial production of 1,3-propanediol from glycerol. Metabolic Engineering 7: 329 - 336.
- Grimshaw J. 2000. Electrochemical reactions and mechanisms in organic chemistry. Elsevier.
- Gui M.M., Lee K.T. and Bhatia S. 2008. Feasibility of edible oil vs. non-edible oil vs. waste edible oil as biodiesel feedstock. Energy 33:1646 – 53.
- Haas M.J. 2005. Improving the economics of biodiesel production through the use of low value lipids as feedstocks: vegetable oil soapstock. Fuel Processing Technology 86:1087 - 1096.
- Haas T., Jaeger B., Weber R., Mitchell S.F. and King C.F. 2005. New diol processes: 1,3-propanediol and 1,4-butanediol. Applied Catalysis A: General 280: 83 - 88.
- Hájek M and Skopal F. 2010. Treatment of glycerol phase formed by biodiesel production. Bioresource Technology 101: 3242 - 3245.
- Hazimah A. H.; Ooi T. L. and Salmiah A. 2003. Recovery of Glycerol and diglycerol from glycerol pitch. Journal of Oil Palm Research. 15(1):1 - 5.
- Himmi E.H., Bories A. and Barbirato F. 1999. Nutrient requirements for glycerol conversion to 1,3-propanediol by *Clostridium butyricum*. Bioresource Technology. 67: 123-128.
- Hongwen C., Baishan F. and Zongding H. 2005 Optimization of process parameters for key enzymes accumulation of 1,3-propanediol production from *Klebsiella pneumoniae*. Biochemical Engineering Journal 25: 47 - 53.
- Huber A.G.W., Sauvinaud L. and O'Connor P. 2008 Biomass to chemicals: Catalytic conversion of glycerol/water mixtures into acrolein, reaction network. Journal of Catalysis 257(1): 163 - 171.
- Icis.com, [Online] Available from: <http://www.icis.com/staticpages/prices.htm>. [2009, 10 15].
- International Energy Outlook. 2009. [Online] Available from: [http://www.eia.doe.gov/oiaf/ieo/pdf/0484\(2009\).pdf](http://www.eia.doe.gov/oiaf/ieo/pdf/0484(2009).pdf). [2009, 11 12].
- Israel A.U., Obot I.B. and J.E Asuque. 2008. Recovery of glycerol from spent soap lye by-product of soap manufacture. E-Journal of Chemistry. 5(4): 940 - 940.

- Kansedo J., Lee K.T. and Bhatia S. 2009. Cerbera odollam (sea mango) oil as a promising non-edible feedstock for biodiesel production. Fuel 88:1148 - 1150.
- Kurosaka T., Maruyama H., Naribayashi I. and Sasaki Y. 2008. Production of 1, 3-propanediol by hydrogenolysis of glycerol catalyzed by Pt/WO₃/ZrO₂. Catalysis Communications 9: 1360 - 1363.
- Kusunoki Y., Miyazawa T., Kunimori K. and Tomishige K. 2005. Highly active metal–acid bifunctional catalyst system for hydrogenolysis of glycerol under mild reaction conditions. Catalysis Communications 6: 645 - 649.
- Lahr D.G. and Shanks B.H. 2005. Effect of sulfur and temperature on ruthenium - catalyzed glycerol hydrogenolysis to glycols. Journal of Catalysis 232: 386 - 394.
- Lammers P.J., Kerr B.J., Weber T.E., Dozier W.A., Kidd M.T., Bregendahl K. and Honeyman M.S. 2008. Digestible and metabolizable energy of crude glycerol for growing pigs. Journal of Animal Science 86(3): 602 - 608.
- Lee P.C., Lee W.G., Lee S.Y. and Chang H.N. 2000. Succinic acid production with reduced by-product formation in the fermentation of *Anaerobiospirillum succiniciproducens* using glycerol as a carbon source. Biotechnology and Bioengineering 72(1): 41 - 48.
- Leifeng G., Yuan L., Yunjie D., Ronghe L., Jingwei L., Wenda D., Tao W. and Weimiao C. 2009. Solvent effect on selective dehydroxylation of glycerol to 1,3-propanediol over a Pt/WO₃/ZrO₂ catalyst. Chinese Journal of Catalysis 30(12): 1189 - 1191.
- Leung D.Y.C and Guo Y. 2006. Transesterification of neat and used frying oil: optimization for biodiesel production. Fuel Processing Technology 87: 883 - 890.
- Leung D.Y.C., Wu X. and Leung M.K.H. 2010. A review on biodiesel production using catalyzed transesterification. Applied Energy 87: 1083 - 1095.
- Li X.Y., Cui Y.H., Feng Y.J., Xie Z.M. and Gu J.D. 2005. Reaction pathways and mechanisms of the electrochemical degradation of phenol on different electrodes. Water Research. 39: 1972 - 1981.
- Lin R., Liu H., Hao J., Cheng K. and Liu D. 2005. Enhancement of 1,3-propanediol production by *Klebsiella Pneumoniae* with fumarate addition. Biotechnology Letters 27(22): 1755 - 1759.

- Lissens G., Pieters J., Verhaege M., Pinoy L. and Verstraete W. 2003. Electrochemical degradation of surfactants by intermediates of water discharge at carbon-based electrodes. Electrochimica Acta 48 (2003): 1655 - 1663.
- Ma F. And Hanna M.A. 1999. Biodiesel production: a review. Bioresource Technology 70:1 - 15.
- Macdonald D.D. and Schmuki P. 2007. Electrochemical engineering. Wiley-VCH.
- Marinoiu A., Ionita G., Gáspár C.L, Cobzaru C. and Oprea S. 2009. Glycerol hydrogenolysis to propylene glycol. Reaction Kinetics and Catalysis Letters 97: 315 - 320.
- Marshall A.T. and Haverkamp R.G. 2008. Production of hydrogen by the electrochemical reforming of glycerol–water solutions in a PEM electrolysis cell. International Journal of Hydrogen Energy 33(17): 4649 - 4654.
- Melero J.A., Vicente G., Morales G., Paniagua M., Moreno J.M., Roldán R., Ezquerro A. and Pérez C. 2008 Acid-catalyzed etherification of bio-glycerol and isobutylene over sulfonic mesostructured silicas. Applied Catalysis A: General 346 (1-2): 44 - 51.
- Menzel K., Zeng A.P. and Deckwer W.D. 1997. High concentration and productivity of 1,3-propanediol from continuous fermentation of glycerol by *Klebsiella pneumoniae*. Enzyme and Microbial Technology 20: 82 - 86.
- Miyazawa T., Kusunoki Y., Kunimori K. and Tomishige K. 2006. Glycerol conversion in the aqueous solution under hydrogen over Ru/C + an ion-exchange resin and its reaction mechanism. Journal of Catalysis. 240: 213 - 221.
- Mohan N., Balasubramanian N. and Basha C.A. 2007. Electrochemical oxidation of textile wastewater and its reuse. Journal of Hazardous Materials 147: 644 - 651.
- Naresh P. and Brian H. 2006. Value-added Utilization of Crude Glycerol from biodiesel production: A Survey of Current Research Activities, American Society of Agricultural and Biological Engineers (ASABE) Paper Number: 066223.
- National Biodiesel Board. 2009. [Online] Available form: http://biodiesel.org/pdf_files/emissions.pdf. [2009, 09 10]
- Ooi T.L., Yong K.L, Dzulkefly K., Wan Yunus W.M.Z and Hazimah A.H. 2001. Crude glycerol recovery from glycerol residue waste from a palm kenel oil methyl ester plant. Journal of Oil Palm Reseach. 13(2): 1 - 6.

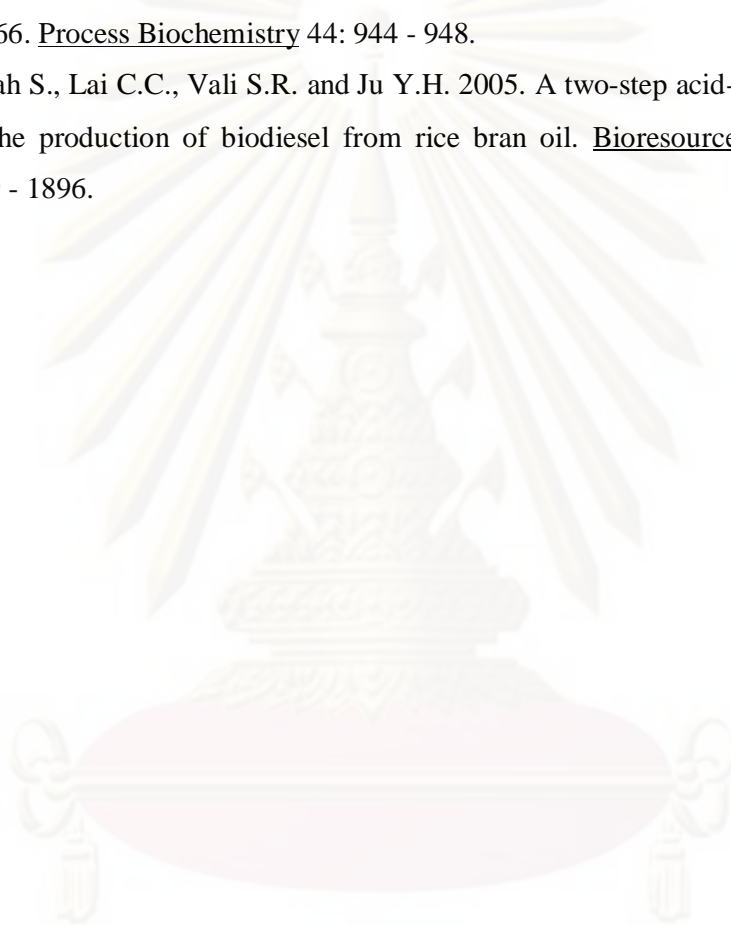
- Papanikolaou S., Ruiz-Sanchez P., Pariset B., Blanchard F. and Fick M. 2000. High production of 1,3-propanediol from industrial glycerol by a newly isolated *Clostridium butyricum* strain. Journal of Biotechnology 77: 191 - 208.
- Patil P.D and Deng S. 2009. Optimization of biodiesel production from edible and nonedible vegetable oils. Fuel 88:1302 - 1306.
- Piya-areetham P., Shenchunthichai K. and Hunsom M. 2006. Application of electrooxidation process for treating concentrated wastewater from distillery industry with a voluminous electrode. Water Research 40: 2857 - 2864.
- Pleteher D. and Weinberg F. 1990. Industrial Electrochemical. Chapman and Hill.
- Prentice G. 1991. Electrochemical Engineering Principles (n.p.): Prentice - Hall.
- Rajeshwar K., Ibanez J.G. and Swain G.M. 1994. Electrochemistry and the environment. Journal of Applied Electrochemistry 24:1077 - 1091.
- Rajkumar D., Kim J.G. and Palanivelu K. 2005. Indirect electrochemical oxidation of phenol in the presence of chloride for wastewater treatment. Chemical engineering & technology. 28: 98 - 105.
- Sabourin-Provost G. and Hallenbeck P. C. 2009. High yield conversion of a crude glycerol fraction from biodiesel production to hydrogen by photofermentation. Bioresource Technology 100: 3513 - 3517.
- Samet Y., Elaoud S. C., Ammar S. and Abdelhedi R. 2006. Electrochemical degradation of 4-chloroguaiacol for wastewater treatment using PbO₂ anodes. Journal of Hazardous Materials B138: 614 - 619.
- Schaffner F., Pontalier P.Y., Sanchez V. and Lutin F. 2003. Bipolar electro dialysis for glycerin production from diester wastes. Filtration and Separation 30(10): 35 - 39.
- Sciencelab.com, Inc [Online] Available from: <http://www.sciencelab.com>. [2009, 10 15].
- Simod O., Schaller V. and Comninellis C. 1997. Theoretical model for the anodic oxidation of organics on metal oxide electrodes. Electrochimica Acta 42: 2009 - 2012.
- Srivastava A. and Prasad R. 2000. Triglycerides-based diesel fuels. Renewable and Sustainable Energy Reviews 4: 111 - 133.
- Sunivo, [Online] Available from: <http://www.sunivo.com>. [2009, 10 15].

- Tanaka S., Nakata Y., Kimura T., Yusiawati M., Kawasaki M. and Kuramitz H. 2002. Electrochemical decomposition of bisphenol A using Pt/Ti and SnO₂/Ti anodes. Journal of Applied Electrochemistry 32: 197 - 201.
- Tang S., Boehme L., Lam H. and Zhang Z. 2009. *Pichia pastoris* fermentation for phytase production using crude glycerol from biodiesel production as the sole carbon source. Biochemical Engineering Journal 43: 157 - 162.
- Thompson J.C. and He B.B. 2006. Characterization of crude glycerol from biodiesel production from multiple feedstocks. Applied Engineering in Agriculture 22(2): 261 - 265.
- Valliyappan T., Bakhshi N.N. and Dalai A.K. 2008. Pyrolysis of glycerol for the production of hydrogen or syn gas, Bioresource Technology 99(10): 4476 - 4483.
- Wang J.F., Xiu Z.L., Liu H.J. and Fan S.D. 2001. Study on microaerobic conversion of glycerin to 1,3-propanediol by *Klebsiella pneumoniae*. Modern Chemical Industry 21(5): 28 - 31.
- Wang K., Hawley M.C. and DeAthos S.J. 2003. Conversion of glycerol to 1,3-propanediol via selective dehydroxylation. Industrial and Engineering Chemistry Research 42(13): 2913 - 2923.
- Xiu Z.L., Chen X., Wang J.F. Zhang D.J. and Xu P. 2003. Stoichiometric analysis and experimental investigation of glycerol bioconversion to 1,3-propanediol by *Klebsiella pneumoniae* under microaerobic conditions Enzyme and Microbial Technology. 33: 386 - 394.
- Xiu Z.L., Song B.H., Wang Z.T., Sun L.H., Feng E.M. and Zeng A.P. 2004. Optimization of dissimilation of glycerol to 1,3-propanediol by *Klebsiella Pneumoniae* in one- and two-stage anaerobic cultures. Biochemical Engineering Journal 19(3): 189 - 197.
- Zeng A.P., Biebl H., Schlieker H. and Deckwer W.D. 1993. Pathway analysis of glycerol fermentation by *Klebsiella Pneumoniae*: Regulation of reducing equivalent balance and product formation. Enzyme and Microbial Technology 15(9): 770 - 779.
- Zhang G., Ma B., Xu X., Li C and Wang L. 2007. Fast conversion of glycerol to 1,3-propanediol by new stain of *Klebsiella pneumoniae* Biochemical Engineering Journal 37: 256 - 260.

Zheng Z.M., Hu Q.L., Hao J., Xu F., Guo N.N., Sun Y. and Liu D.M. 2008. Statistical optimization of culture conditions for 1,3-propanediol by *Klebsiella pneumoniae* AC 15 via central composite design. Bioresource Technology 99: 1052 - 1056.

Zheng Z.M., Hu Q.L., Hao J., Xu F., Guo N.N., Sun Y. and Liu D.M. 2009. Scale-up of micro-aerobic 1,3-propanediol production with *Klebsiella pneumoniae* CGMCC 1.6366. Process Biochemistry 44: 944 - 948.

Zullaikah S., Lai C.C., Vali S.R. and Ju Y.H. 2005. A two-step acid-catalyzed process for the production of biodiesel from rice bran oil. Bioresource Technology 96: 1889 - 1896.



ศูนย์วิทยทรัพยากร
จุฬาลงกรณ์มหาวิทยาลัย



APPENDICES

ศูนย์วิทยทรัพยากร
จุฬาลงกรณ์มหาวิทยาลัย

APPENDIX A

CACULATION EXAMPLE

A.1 Calculation of the normalization of glycerol concentration, glycerol reforming and yield of 1,3-propanediol

Example: Data from the optimum condition for synthetic glycerol solution reforming to 1,3-propanediol (Section effect of concentration of NaCl).

Given,

Current intensity	4.5A
Initial concentration of glycerol ($[C_3H_5(OH)_3]_i$)	46.35 g/l
Initial of pH	1
Concentration of NaCl	2.93 g/l
Concentration of glycerol at 6 h ($[C_3H_5(OH)_3]_t$)	11.04 g/l
Concentration of 1,3-propanediol at 6h ($[C_3H_6(OH)_2]_t$)	18.92 g/l
Electrolyte volume (V)	0.27 l
Electrolysis time (t)	6 h
Voltage	5.1 V

$$\begin{aligned}
 \text{Normalized concentration} &= \frac{(C_3H_5(OH)_3)_t}{(C_3H_5(OH)_3)_i} \\
 &= \frac{11.04}{46.35} \\
 &= 0.24
 \end{aligned}$$

$$\begin{aligned}
 \text{Charge passed (C)} &= i \times t \times 3600 \\
 &= 4.5 \times 6 \times 3600 \\
 &= 97,200 \text{ C}
 \end{aligned}$$

$$\text{Electrical charge per volume (Ah/l)} = \frac{i \times t}{V}$$

$$\begin{aligned}
 &= \frac{4.5 \times 6}{0.27} \\
 &= 100 \text{ Ah/l} \\
 \text{Glycerol reforming (mg glycerol/C)} &= \frac{([C_3H_5(OH)_3]_i - [C_3H_5(OH)_5]_i) V}{C} \\
 &= \frac{(46.33 - 11.04) \times 0.27}{97,200} \\
 &= 0.000098 \text{ g glycerol/C} \\
 &= 0.098 \text{ mg glycerol/C} \\
 \text{Yield of 1,3-propanediol (\%)} &= \frac{[C_3H_5(OH)_2]_i \times 100}{[C_3H_5(OH)_3]_i} \\
 &= \frac{18.92 \times 100}{46.33} \\
 &= 40.81\%
 \end{aligned}$$

A.2 Calculation of compositions in purified crude glycerol

Example: Data from the optimum for purified crude glycerol (Section 4.2.3).

Given;

$$\text{Mass of crude glycerol} = 100.05 \text{ g}$$

$$\text{Mass of glycerol content in purified crude glycerol} = 97.97 \text{ g}$$

$$\text{Mass of ash content in purified crude glycerol} = 0.0112 \text{ g}$$

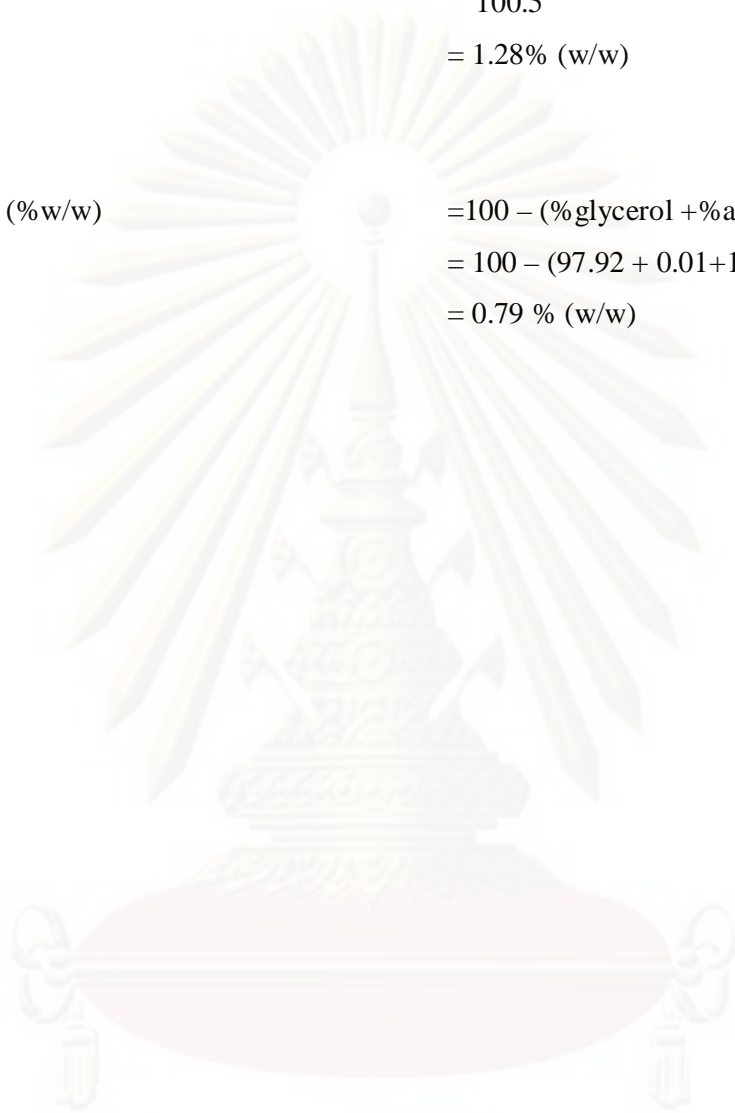
$$\text{Mass of water content in purified crude glycerol} = 1.28 \text{ g}$$

$$\begin{aligned}
 \text{Glycerol content (\% w/w)} &= \frac{97.97}{100.05} \times 100 \\
 &= 97.92 \text{ \% (w/w)}
 \end{aligned}$$

$$\begin{aligned}
 \text{Ash content (\% w/w)} &= \frac{0.0112}{100.5} \times 100 \\
 &= 0.01 \text{ \% (w/w)}
 \end{aligned}$$

$$\begin{aligned}\text{Water content (\%w/w)} &= \frac{1.28}{100.5} \times 100 \\ &= 1.28\% \text{ (w/w)}\end{aligned}$$

$$\begin{aligned}\text{MONG (\%w/w)} &= 100 - (\% \text{glycerol} + \% \text{ash} + \% \text{water}) \\ &= 100 - (97.92 + 0.01 + 1.28) \\ &= 0.79\% \text{ (w/w)}\end{aligned}$$



ศูนย์วิทยทรัพยากร
จุฬาลงกรณ์มหาวิทยาลัย

APPENDIX B

ANALYTICAL METHODS

B.1 Explanation of characterization method to determine quantities of cure glycerol

Glycerol was analyzed by High Performance Liquid Chromatography (HPLC: Shimadzu LC-10ADvp) with a RID-10A refractive index detector, and by FTIR. For the HPLC analysis, the stationary phase was a Pinnacle II C18 column (240 x 4.6 mm) and the mobile phase was a 96.7: 3.3 (v/v) ratio of 5 mM H₂SO₄: pure methanol, passed through the column at 0.6 ml/min.

Water content (Standard method ISO 2097-1972) determined using volumetric Karl Fisher titration.

Ash content is under the standard method ISO 2098-1972.

Procedure

- Oven-dried sample of ash at 105°C
- Burned in muffle furnace at 750°C for 3h (Alsertenok, Prothern).

Calculate the ash content as follows

$$\text{Ash content (\%)} = \frac{[A'' - B']}{B'} \times 100 \quad (\text{B.2})$$

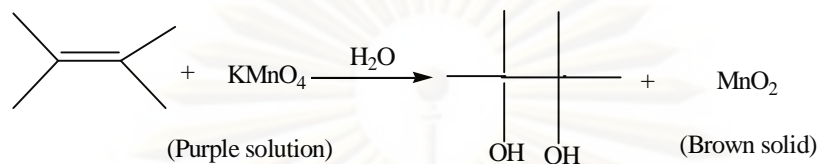
MOMG (Standard method ISO 2464-1973) defined as 100 - (% glycerol content + % water content + % ash content).

pH of a solution of 20% glycerol residue in 100.0 ml distilled water was measured with a pH meter (Mettler Toledo, MP220).

B.2 Chemical test of chemical function group

B.2.1 Baeyer Test for Multiple Bonds (Potassium Permanganate Solution)

Alkene



(B.3)

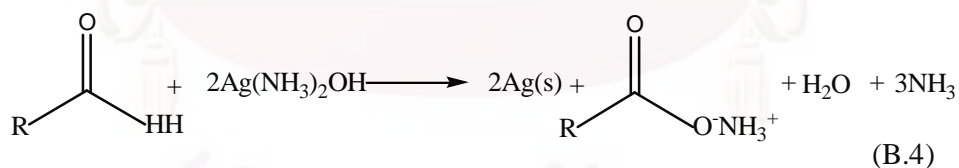
Procedure

- Dissolve 1 drop or 0.02 g of the unknown in 0.5 ml reagent grade acetone
- Add a 1% aqueous solution of potassium permanganate drop-wise with shaking
- If more than one drop of reagent is required to give a purple color to the solution, unsaturation or an easily oxidized functional group is present
- Run parallel tests on pure acetone and, as usual, the standards listed above

Positive Test, the disappearance of the KMnO_4 's purple color and the appearance of a brown suspension of MnO_2 is a positive test

B.2.2 Tollen's Test for Aldehydes

Aldehyde standards



Procedure

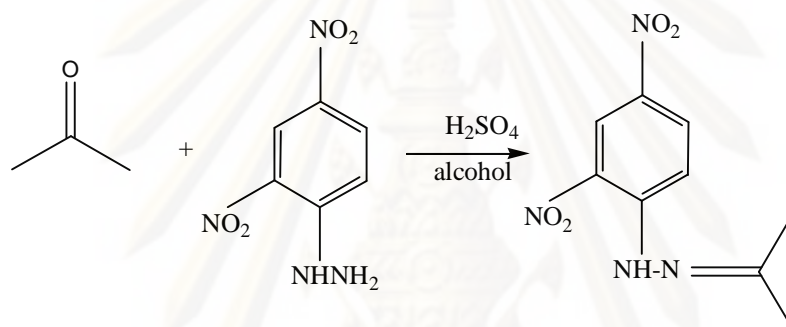
- Add one drop or a few crystals of unknown to 1 ml of the freshly prepared Tollens reagent
- Gentle heating can be employed if no reaction is immediately observed
- Add Tollens reagent into a test tube which has been cleaned with 3 M sodium hydroxide, place 2 ml of 0.2 M silver nitrate solution, and add a drop of 3 M sodium hydroxide

- Add 2.8% ammonia solution, drop by drop, with constant shaking, until almost all of the precipitate of silver oxide dissolves
- Don't use more than 3 ml of ammonia. Then dilute the entire solution to a final volume of 10 ml with water

Positive Test; formation of silver mirror or a black precipitate is a positive test.

B.2.3 2,4-DNP Test for Aldehydes and Ketones

Ketones standards



(B.5)

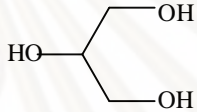
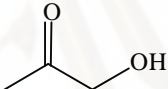
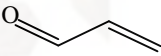
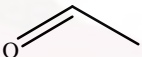
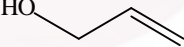
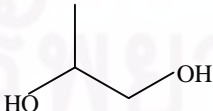
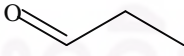
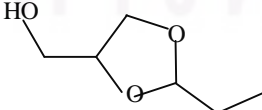
Aldehyde or Ketone Procedure

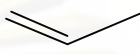
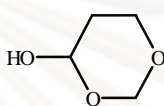
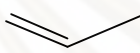

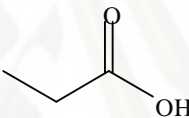
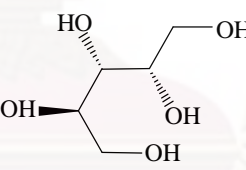

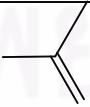
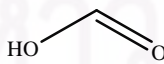
- Add a solution of 1 or 2 drops or 30 mg of unknown in 2 mL of 95% ethanol to 3 mL of 2,4-dinitrophenylhydrazine reagent
- Shake vigorously, and, if no precipitate forms immediately, allow the solution to stand for 15 minutes
- The 2,4-dinitrophenylhydrazine reagent will already be prepared

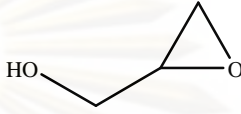
Positive test, formation of a precipitate is a positive test.

APPENDIX C

Table C.1 List of compounds generated from glycerol reforming by the electrochemical technique under strong acidic conditions.

IUPAC name	Other names (Molecular formula)	Chemical structure	Prices (\$/lb)(Purity (%)) (Sunivo, 2009 and Icis.com,2009) [CAS No.]
Propane-1,2,3-triol (C ₃ H ₈ O ₃)	1,2,3-propanetriol or Glycerol		3.95 (>99.5 %) ^a 0.36 (99.5%) ^b 5.47 (>99.5%) ^c [56-81-5]
1-hydroxypropan-2-one (C ₃ H ₆ O ₂)	1-hydroxyl-2-propanone or Acetol		N/A [111-09-6]
Prop-2-enal (C ₃ H ₄ O)	Acrylaldehyde or Acrolein		393.57 (>95 %) ^a [107-02-8]
Acetaldehyde (C ₂ H ₄ O)	Ethanal		222.85 (>99%) ^c [75-07-0]
Prop-2-en-1-ol or Allyl alcohol (C ₃ H ₅ O)	2-propenol		1.37 (99.5%) ^b [107-18-6]
propane-1,2-diol (C ₃ H ₈ O ₂)	Propylene glycol or 1,2-propanediol		4.77(>99.5 %) ^a 0.52 (99.5%) ^b [57-55-6]
Propionaldehyde (C ₃ H ₆ O)	Propanal		161.24 (>97 %) ^a [123-38-6]
2-ethyl-1,3-dioxolan-4-yl) methanol (C ₆ H ₁₂ O ₃)	2-ethyl-1,3-dioxolane-4-methanol		N/A N/A

IUPAC name	Other names (Molecular formula)	Chemical structure	Prices (\$/lb)(Purity (%)) (Sunivo, 2009 and Icis.com,2009) [CAS No.]
Propene (C ₃ H ₆)	Propylene		0.46 ^d [115-07-1]
1,3-dioxan-4-ol (C ₅ H ₈ O ₃)	4-Hydroxy-1,3-dioxane		N/A N/A
Propene (C ₃ H ₆)	Propylene		0.46 ^d [115-07-1]
Propane-1,3-diol (C ₃ H ₈ O ₂)	Trimethylene glycol or 1,3-propanediol		102.34 (>98%) ^a [504-63-2]
Propanoic acid (C ₃ H ₆ O ₂)	Ethancarboxylic acid		1.20 (99%) ^b 11.68 (>99.5%) ^c [79-09-4]
(2 <i>R</i> ,3 <i>R</i> ,4 <i>S</i>)-Pentane- 1,2,3,4,5-pentol (C ₅ H ₁₂ O ₅)	1,2,3,4,5- Pentahydroxypentane or Xylitol		15.21 (>98.5%) ^a 18.52 (98.%) ^d [87-99-0]
Ethane-1,2-diol (C ₂ H ₆ O ₂)	Ethylene glycol		0.84 (99.9%) ^b 2.96 (99%) ^c [107-21-1]
Acetic acid (C ₂ H ₄ O ₂)	Ethanoic acid		0.70 (99.8%) ^b 27.49 (>99.7) [64-19-7]
Formic acid or Methanoic acid (CH ₂ O ₂)	Hydrogen carboxylic acid		0.64 (85%) ^b 2.76 (>96%) ^c [64-18-6]

IUPAC name	Other names (Molecular formula)	Chemical structure	Prices (\$/lb)(Purity (%)) (Sunivo, 2009 and Icis.com,2009) [CAS No.]
Oxiranylmethanol (C ₃ H ₆ O ₂)	2,3-Epoxy-1- propanol or Glycidol		233.24 (>95%) ^a [556-52-5]

Note:

^a Natural grade

^b Industrial grade

^c Reagent grade

^d No report grade

^e Food grade

ศูนย์วิทยทรัพยากร
จุฬาลงกรณ์มหาวิทยาลัย

APPENDIX D

GENERAL REACTION OF GLYCEROL REFORMING

D.1 Glycerol reforming in acid solution without applied electricity

In acid solution, the 1°- or 2°- alcohol group of glycerol reacts with H⁺ and dehydrates to form two types of intermediates, 2,3-dihydroxypropene and 1,3-propenediol or 3-hydroxypropanal which rapidly rearrange to 1-hydroxyl-2-propanone (acetol) and acrylaldehyde (acrolein), respectively. Acrolein is very reactive carbonyl compound which can be further dehydrated to propene to propene as shown in Figure D.1.

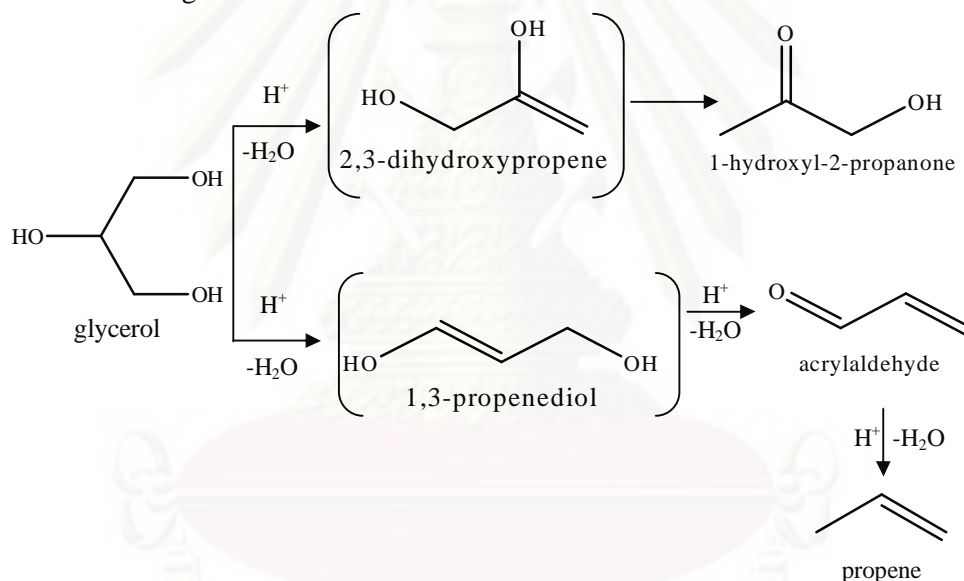
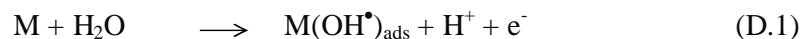


Figure D.1. Glycerol reforming to 1-hydroxyl-2-propanone (acetol), acrylaldehyde (acrolein) and propene in acid solution.

D.2 Glycerol reforming in acid solution within applied electricity

When the electricity is applied, OH[•] radicals are produced from the oxidation reaction of H₂O on the Pt electrode (Reaction D.1). The OH[•] radicals can extract the H atom of the C₁ or C₂ of the glycerol molecule and rapidly rearrange to acrylaldehyde and 1-hydroxyl-2-propanone, respectively.



The acrylaldehyde product is directly and easily produced from the reaction of radical mechanism of glycerol compared with 1-hydroxyl-2-propanone but it can be reformed to other compounds.

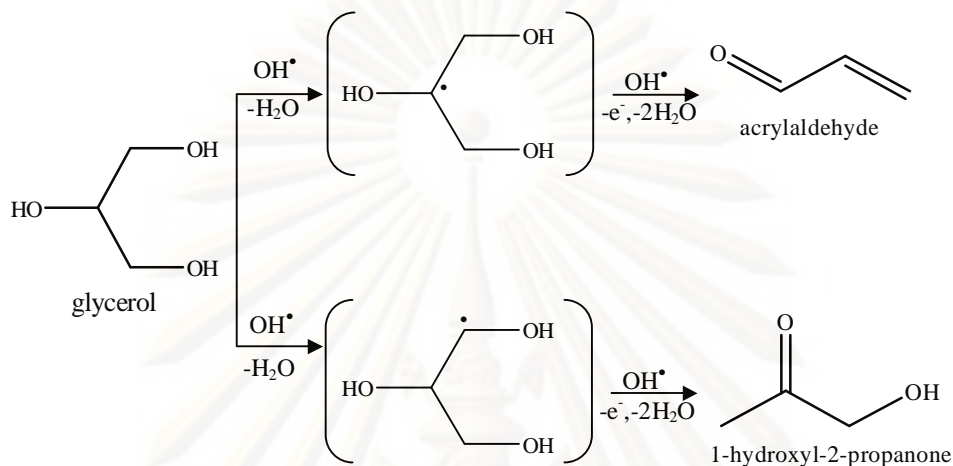


Figure D.2. Glycerol reforming to 1-hydroxyl-2- propanone and acrylaldehyde in acid solution within applied electricity.

Regarding the reactions with radicals, the C₁-C₂ bond of glycerol is proposed to be cleaved by the oxidation reaction to form a C₁ alcohol free radical. It is then dehydrated to formaldehyde and acetaldehyde and ethylene glycol.

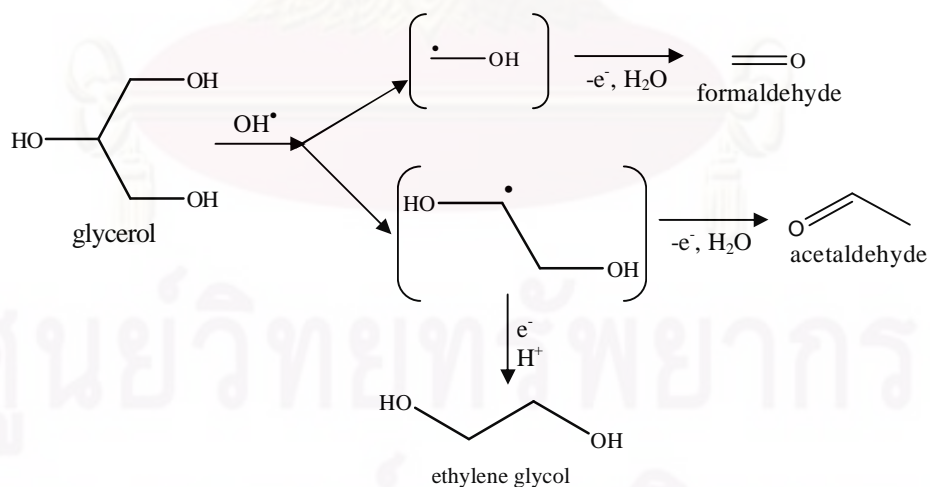


Figure D.3. Glycerol reforming to formaldehyde, acetaldehyde and ethylene glycol in acid solution within applied electricity.

The OH-atom of glycerol was reacted with OH free radical and was dehydrated to 2,3-dihydroxyl-propanal

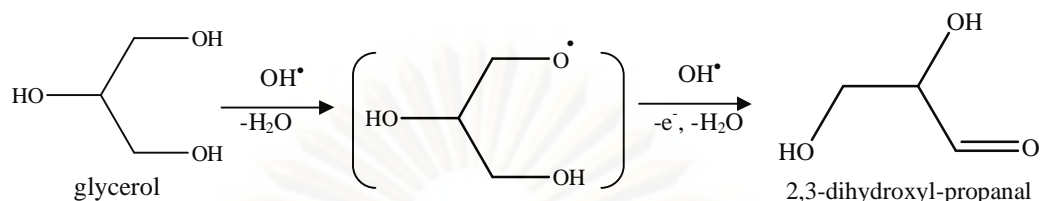


Figure D.4. Glycerol reforming to 2,3-dihydroxyl-propanal in acid solution within applied electricity.

The C₁-C₂ bond of glycerol is proposed to be cleaved by the oxidation reaction to form a C₁ alcohol free radical. It is then dehydrated to enol-form as 2-propenol and propanal. C₂ alcohol free radical can also be produced from glycerol which can be reduced to 2-propenol.

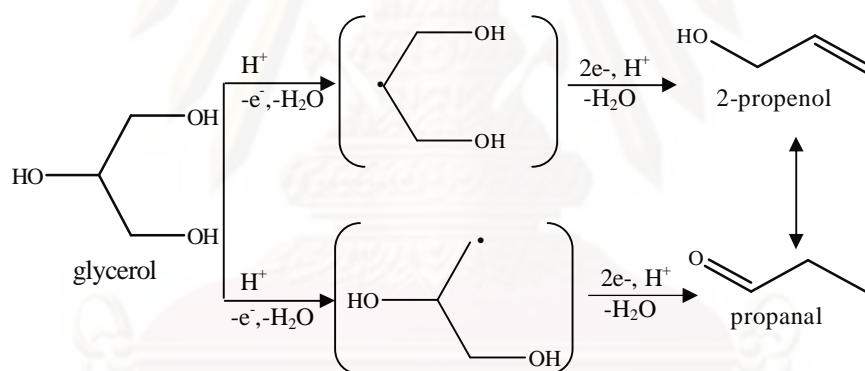


Figure D.5. Glycerol reforming to propanal and 2-propenol (allyl alcohol) in acid solution within applied electricity.

D.3 The other reforming reaction of glycerol or other compounds in acid solution within applied electricity

1-hydroxyl-2-propanone (acetol) is believed to be produced by dehydration of glycerol and the electrochemical reforming of glycerol in acid solution. It can be dehydrated to aldol compound and then reacted with glycerol to 2-ethyl-4-methanol-1,3-dioxolane, and isomerized to 2-methyl-1,3-dioxane,. It can also be protonated by the excess protons in solution leading to 1,2-propanediol.

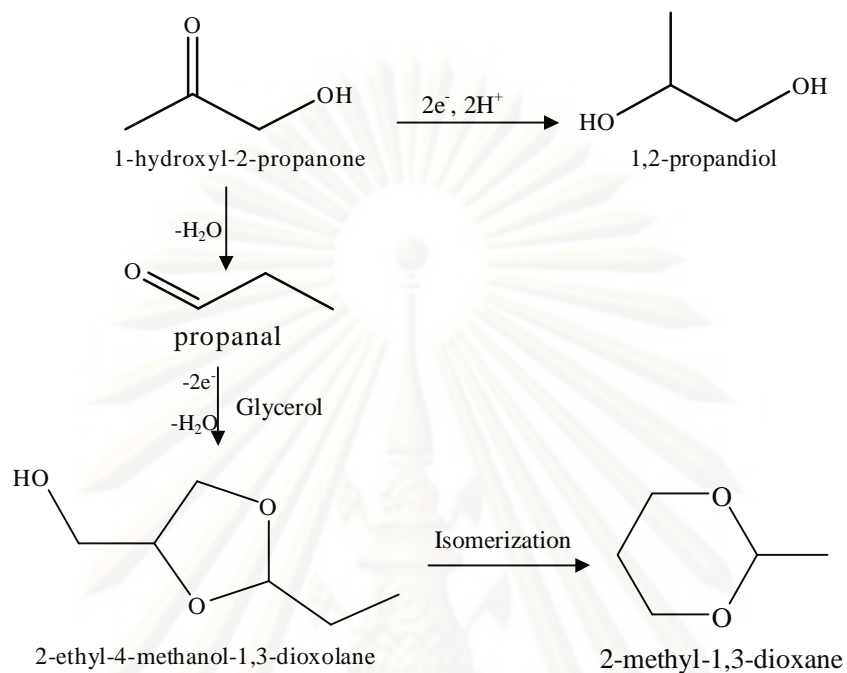


Figure D.6. 1-hydroxy-2-propanone reform to 1,2-propanediol and 2-ethyl-4-methanol-1,3-dioxolane in acid solution within applied electricity.

1-hydroxy-2-propanone can be rearranged to propanoic acid or can cleave the C_2 free radical, which can further reduce or react with OH^\bullet to form acetaldehyde and acetic acid, respectively.

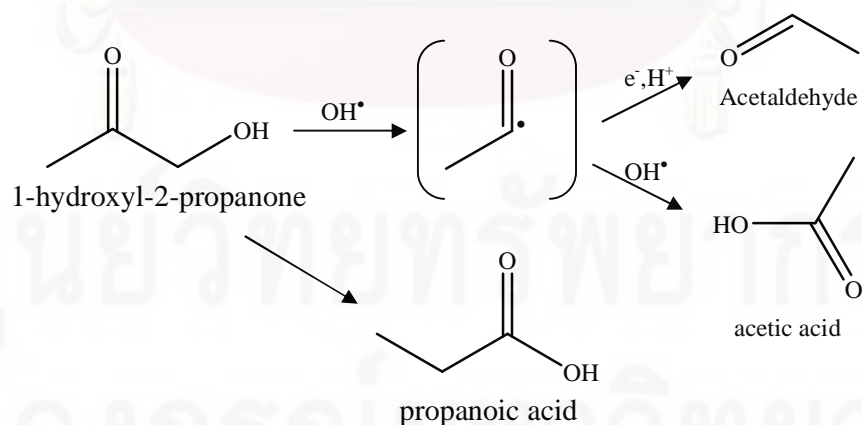


Figure D.7. 1-hydroxy-2-propanone reforming to acetaldehyde and acetic acid and propanoic acid in acid solution within applied electricity.

Acrylaldehyde is believed to be produced by dehydration of glycerol and the electrochemical reforming of glycerol in acid solution. It can be dehydrated further to propene or hydrolyzed/protonated/reduced to 1,3-propanediol

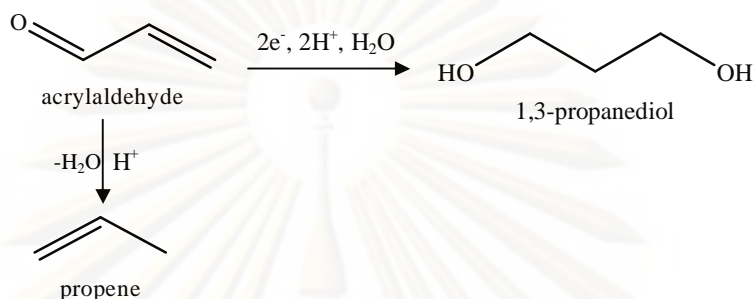


Figure D.8. Acrylaldehyde reforming to propene and 1,3-propanediol in acid solution within applied electricity.

Formaldehyde can be reacted with glycerol molecule and dehydrated to 5-hydroxy-1,3-dioxolane in acid solution within applied electricity.

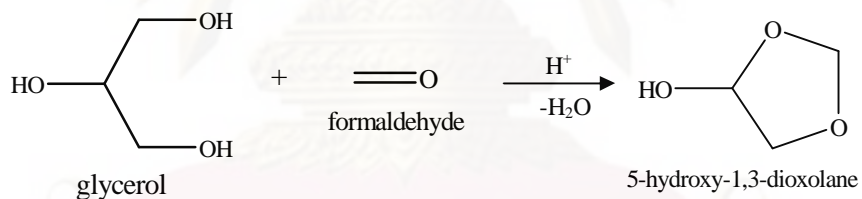


Figure D.9. Glycerol reforming with formaldehyde to 5-hydroxy-1,3-dioxolane in acid solution within applied electricity.

Glycerol is protonated at the secondary OH-group and the secondary carbonium ion is formed by water elimination and it can be further reacted to new product as glycidol.

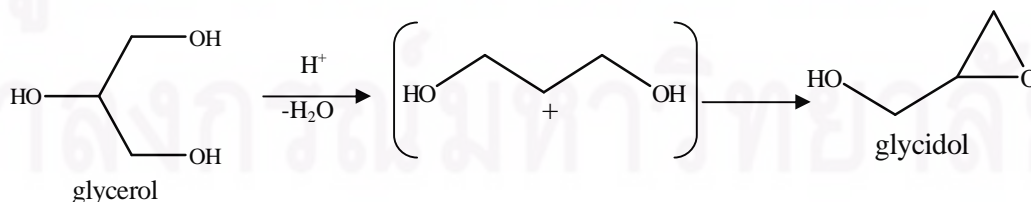


Figure D.10. Glycerol reforming to glycidol in acid solution within applied electricity.

BIOGRAPHY

Mr. Sangkorn Kongjao was born on December 24th 1979 in Nakhon Si Thammarat province, Thailand and graduated from Ramkhamhaeng University, Faculty of Science in 2000 with a Bachelor's of Science in Chemistry. Then, he became a Medicine of Science at Natural Products Research, Research Division, National Cancer Institute, Ministry of Public Health, Bangkok, Thailand. He resumed studying in 2002 and got a Master's Degree of Science in Chemical Technology, Faculty of Science, Chulalongkorn University in 2005. In 2006, he has studied in a Doctoral degree at the same department.



ศูนย์วิทยทรัพยากร
จุฬาลงกรณ์มหาวิทยาลัย